A Thermal-fluid Analysis of Piping Dead-legs in High Purity Water Systems

By

Daniel C. Coyle (B.Eng. MIMechE MIEI)

Thesis presented at Dublin City University in fulfilment of the requirements for the degree of Master of Engineering

Under the supervision of
Dr. Brian Corcoran

School of Mechanical & Manufacturing Engineering,
Dublin City University,
Ireland.

January 2007

Declaration

I hereby certify that this material, which I now submit for assessment on the programme of study leading to the award of Degree of Master of Engineering is entirely my own work and has not been taken from others save and to extent that such work has been cited and acknowledged within the text of my work.

Signed: Daniel C. Ogle ID No: 51366912

Date 06/02/07

Acknowledgements

I wish to acknowledge the following people for their advice and support during this research;

- My mother and father Without your unending support and encouragement I would never have achieved my academic goals. Sincere gratitude to you both.

- My sisters, for their many words of encouragement and uncanny ability to take my mind of my work

- Dr. Brian Corcoran for his project guidance. Your shared enthusiasm for the topic made the whole experience enjoyable Cheers!

- Many thanks to all the technical staff in School of Mechanical and Manufacturing Engineering

- Thanks to all my fellow peers for those extended lunchtime chats and endless coffee breaks!

Abstract

A Thermal-fluid Analysis of Piping Dead-legs in High Purity Water Systems
By

Daniel C. Coyle (B Eng MIMechE MIEI)

Purified water forms an integral part of pharmaceutical production The consistency of water quality produced by purification processes and distributed to points-of-use is of utmost importance Tee-sections installed in distribution loops are commonly used to divert fluid flow at take-off points However fluid flow restriction at tee-section branches can cause piping dead-legs.

Dead-legs consist of regions of stagnant fluid where harmful organisms can proliferate unaffected by the scouring effects of distribution loop flow. This thesis presents a thermo-fluid analysis focusing upon the fluid dynamics and heat transfer mechanisms occurring within dead-leg branches A literature review of high purity water system design details sanitization methods currently employed in industry with reference to the detrimental effects of dead-legs.

Experimentation was performed using a single-loop fluid rig complete with capped 90° tee-section representing a piping dead-leg. Analysis of the thermal conditions for various dead-leg configurations was performed including variations of branch length and diameter. The effect of varying loop velocity was also investigated. The application of non-intrusive analysis techniques was considered. Infrared thermography and surface-mounted thermocouples were used to map surface temperature distribution across a dead-leg branch

Increased temperatures were noted at the base of the dead-leg branch for increasing loop velocities. Comparison of reduced and equal diameter dead-legs for varying branch lengths suggested dead-leg temperature is strongly related to inlet loop velocity. Acceptable thermal responses were noted in 4d dead-legs for loop velocity > 0.94m/s, 2d reduced diameter dead-legs at 1 50m/s and in 2d equal diameter dead-legs throughout the examined velocity range.

Although all dead-leg configurations used in analysis adhered to industry recommendations; unsatisfactory thermo-fluid conditions recorded for remaining dead-legs suggests revision of accepted regulations. Non-intrusive analyses illustrated greater temperatures at branch mid-point compared with base measurements. However the application of techniques was deemed limited due to pipe wall conduction effects.

Table of Contents

Chapter 1 Introduction **Page 1 - 45**

List of Figures

Chapter 1 Introduction **Page 1 - 45**

Chapter 2 Materials and Methods **Page 46 - 58**

List of Tables

Chapter 1 Introduction **Page 1 - 45**

Chapter 2 Materials and Methods **Page 46 - 58**

Chapter 3 Results and Discussion **Page 59 - 112**

Nomenclature

D	main pipe diameter
d	branch diameter
l	dead-leg length
°C	Degrees Celsius
mg	milligram
mJ	milliJoules
ms	millisecond
µm	micrometer
mA	milliamp
V	Volts
µV	microvolt
A	cross-sectional area
CL	centerline
t	time
δ	differential switching point
Re	Reynolds Number
Q	volumetric flowrate (L/min)
q	volumetric flowrate (m^3/s)
µ	dynamic viscosity
ρ	fluid density
U_b	bulk loop fluid velocity
T_L	loop temperature
T_d	dead-leg temperature at base
$T_{d6, 4, 2}$	temperatures at base of 6d, 4d, 2d dead-legs
ID	internal diameter of main pipe
OD	outside diameter of main pipe
id	internal branch diameter
od	outside branch diameter
ΔT	temperature difference
cfu	colony (bacteria) forming units
Ra	Roughness Average
L_h	hydrodynamic entry length for turbulent flow

Abbreviations

HPWS	High Purity Water Systems
FDA	Food and Drugs Administration
ASME	American Society of Mechanical Engineers
WFI	Water for Injection
RO	Reverse Osmosis
CCC	Calcium Carbonate Concentrate
AC	Activated Chlorine
UV	Ultraviolet
EDI	Electro De-Ionizing
WHO	World Health Organization
PID	Piping and Instrument Diagram
SS	Stainless steel
PVDF	Polyvinylidene Fluoride
PVC	Polyvinyl Chloride
PTFE	Polytetrafluoroethylene
CIP	Clean-In-Place
SIP	Steam-In-Place
RTD	Resistance Temperature Devices
LDA	Laser Doppler Anemometry
CLR	Cycle Log Reduction
CFD	Computational Fluid Dynamics
LDV	Laser Doppler Velocimetry
PIV	Particle Image Velocimetry
TIG	Tungsten Inert Gas
ASTM	American Society of Testing Materials
BSP	British Standard Pipe
IR	Infrared

Chapter 1 Introduction

Purified water forms the core of every pharmaceutical manufacturing plant Every pharmaceutical facility requires purified water, and its quality is critical to all production processes [1] The consistency of water quality achieved is as important as the quality of water The expense and high technology involved in water purification is negated if the distribution system cannot maintain the required water quality [2] A reduction in water quality may result in the suspension of pharmaceutical processes. Production downtime suffered during cleaning and rectification can have significant detriment upon manufacturing output and company revenue

For flow conversion, fluid isolation and take-off points in a sterile process pipework system, the installation of a tee-section piece is the most commonly used method [3] However the installation of tee-sections in high purity water systems (HPWS) has the potential to compromise water quality By restricting flow in the tee-section branch; dead-legs can occur The stagnant water in a tee-section dead-leg promotes the growth of biofilm [4] When dead-leg water is released, it has the potential to contaminate entire production

1.1 The 6d-Rule

In an inspections guide [5] issued for review the Food and Drugs Administration (FDA) stated that "no pipe should have an unused portion greater in length than 6 diameters of the unused pipe measured from the axis of the pipe in use". This statement became known as the 6d-rule within industry A representation of the 6d-rule is shown in figure 1 1

The FDA stressed that the regulation applied to hot water systems only (75-80°C) They considered any unused portion of pipe in an ambient or cold circulating system as a dead-leg, having the potential for biofilm formation The FDA recommended ambient water systems have a self-sanitizing procedure in place for dead-legs or eliminate them entirely

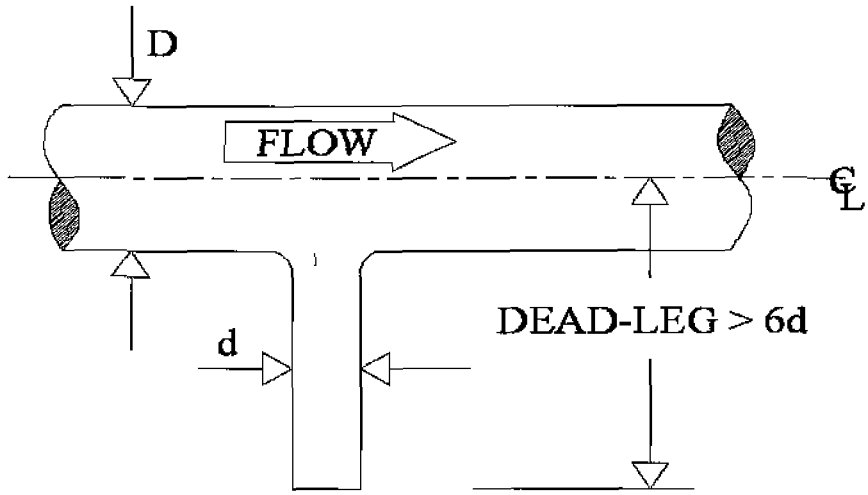

Figure 1.1 - Classic 6d dead-leg configuration

Although the 6d-rule became an industry standard for suitable dead-leg length, it is not truly representative of what dead-leg characteristics are critical to designing a cleanable process piping system [6]. The American Society of Mechanical Engineers (ASME) suggested that dead-legs within HPWS be designed to achieve a dead-leg length of 2 or less, where the length of the dead-leg extension is measured from the inside diameter wall. The ASME states that this is merely a target, not an absolute requirement and that the system designer must attempt to eliminate system dead-legs and identify where exceptions exist [7].

Compared to the ASME, the FDA recommendation is poorly worded The ASME recommendation measures from the true beginning of the dead-leg whilst the 6d-rule measures the length of the dead-leg from the centreline of the main branch. The 6d-rule becomes questionable when designing systems with smaller diameter branches located off larger diameter main pipelines Figure 1.2 displays dead-leg configurations with varying branch diameters. Shown are loop to branch diameter ratios of 1:1, 2:1 and 4:1. Take the example of a designer placing a 12 5mm valve off a 50mm diameter main section of pipeline; a 2d length already exists at the pipe wall. Should the main pipe have a 150mm pipe diameter, the 6d-rule is already compromised

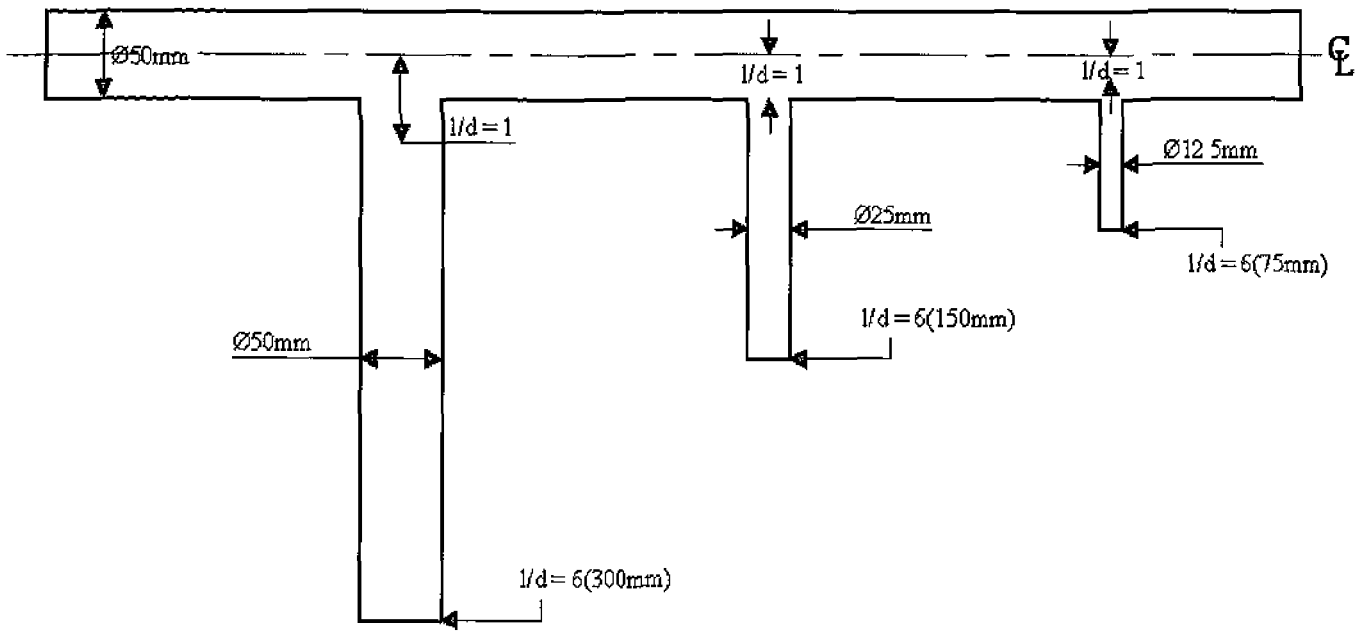

Figure 1 2 - Application of the 6d-rule with varying branch diameter

Definite confusion exists concerning the application of the FDA 6d-rule. Research has shown that various industry experts [2, 8 & 9] have their own recommendations of suitable dead-leg lengths. These can range from 1d - 5d lengths, however all accept that the 6d-rule is flawed.

In a recent paper [10] the validity of the 6d-rule is questioned;

"There are many guidelines currently in use that "assist" the industry (pharmaceutical) in engineering equipment and systems Some of the guidelines are used simply because they are considered to be "standards" Often, what is not considered is the actual applicability of a given guideline to a particular system or piece of equipment "

Pharmaceutical companies expend significant expense to adhere their system to the FDA 6d-rule, however little is known of actual suitable lengths for dead-legs The rule itself is ambiguous, ultimately leading to confusion among HPWS designers, which must be avoided in such a delicate manufacturing sector.

1.2 Pharmaceutical Waters

In order to understand the sanitary issues associated with piping dead-legs, one must first consider the systems they can compromise Considerable expense is incurred in the purchase, installation and validation of central purification equipment in HPWS [2]. These systems are essentially designed with a desired water quality in mind Various standards of product water are used in the pharmaceutical industry depending upon the end-use of the manufactured product.

Four standards of production water exist each discernable by their level of purity These include;

- Source Water
- Potable Water
- Purified Water
- Water for Injection

1.2.1 Source Water

Source water is water in its rawest untreated state It comprises of water in reservoirs, lakes, rivers and streams prior to being withdrawn for treatment and distribution as potable water supply. Geological factors contribute to the quality of such waters Having had contact with its surroundings, source water cannot be assumed pure. Dissolved minerals, salts from earth and rocks will have leached into the water Water, falling as rain will have also scrubbed various gases from the atmosphere [4]. Natural waters serve to nurture organisms such as bacteria and other viruses.

Therefore, water approached as a source supply by a facility is not entirely water, but contains a multitude of aqueous solutions and substances [4] The standard of source waters will vary by location, however some of the impurities that can exist in source water supplies include:

- Ionic and Organic Contaminants
- Bicarbonate and Scaling
- Suspended Matter
- Silica and Dissolved Gases

Source waters will inevitably require cleansing to remove such contaminants and achieve higher purity.

1.2.2 Potable Water

Potable water or 'city water' as it is sometimes termed acts as feed water for facility production. The recommended microbial limit for potable drinking water specified by the FDA is 500*cfu*/ml [5]

The purification of source water to potable standards typically begins with the treatment of water with an oxidant to remove tastes and odours. Following this, water is clarified by removing large suspended matter using alum treatment Filtration is performed to remove smaller organisms before finally chlorine is added to protect against after-contamination

Additional attention must be paid to the quality of source water as it can be subject to environmental changes. For example, new construction or fires can deplete water stores and cause an influx of heavily contaminated water from storage [4]

1.2.3 Purified Water

Purified water is used in the manufacturing of topical and oral medications in the pharmaceutical industry. Purified water consists of potable water having undergone a series of purification methods to further remove damaging bacterial elements The FDA recommends an upper bacterial limit of 100*cfu*/ml for high purity water [5]

1.2.4 Water for Injection

Water for Injection (WFI) as the name suggests is used in the pharmaceutical industry for manufacturing drugs intravenously administered to patients Distribution systems carrying high quality WFI are assumed essentially sterile However, sampling of the water takes place in non-sterile environments therefore some microbial counts are assumed FDA recommended microbial limits are shown in table 1.1 [5].

Upper bacterial limit	10*cfu*/100 ml
Upper endotoxin limit	0 25 units per ml

Table 1.1 - FDA microbial limits for WFI

An endotoxin is a toxic substance bound to the bacterial cell wall released when the bacterium ruptures or disintegrates. The above limits do not refer to pass or fail standards, only action limits. When the supply exceeds the above limits then process engineering must investigate the problem, reduce the microbial presence and analyze the impact that heightened limits may have had upon production.

1.3 Pre-treatment Processes

The preparation of waters for application in the pharmaceutical, semi-conductor or power-industries can involve three main stages: pre-treatment, principal purification methods and point-of-use treatment [4] Principal purification typically involves one or more of distillation, ion exchange or reverse osmosis (RO) processes. However, to ensure principal purification treatments produce the high quality waters they must, pre-treatment methods must first be performed. Additionally in the interest of costs, pre-treatment methods can extent the service life of valuable principal equipment

Figure 1 3 illustrates the stages necessary to increase the purity of potable water to the high standard required of Water for Injection

Facilities that use source water as opposed to a potable supply must perform initial purification methods. Yet potable water has limited direct application in pharmaceutical manufacturing processes because it contains variable amounts of dissolved substances, and added chlorine for microbial control [4] Facility water is separated from 'city water' by a check-valve to prevent back flow, which may contact and contaminate production equipment One of the initial pre-treatment processes in a high purity loop is filtration with multi-media filter

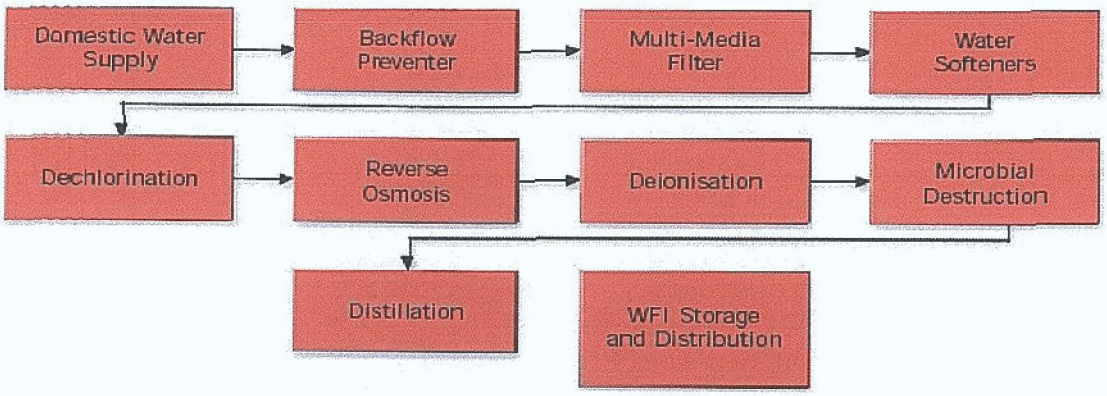

Figure 1.3 - Functional block diagram of WFI system [11]

1.3.1 Deep Bed Filtration

The function of a deep-bed filter is to prevent the passage of suspended matter, accommodate a reasonable volume of suspended material and hold retained solids loosely to aid easy cleaning by backwashing [4].

A deep-bed filter consists of a multi-media bed, with levels of varying media such as charcoals, manganese greensand, garnet or anthracite with a final support layer of gravel. Beneath the gravel support layer a distributor tank collects the water. Considering figure 1.4, the treated water is removed from the holding tank via a system outlet pipe. Silica sand is the typical medium used in deep-bed filter construction, aiding the removal of bulky substrate in the water. However deep-bed filters may themselves become havens for organisms to flourish [4]. Accordingly chloride is added prior to the water passing through.

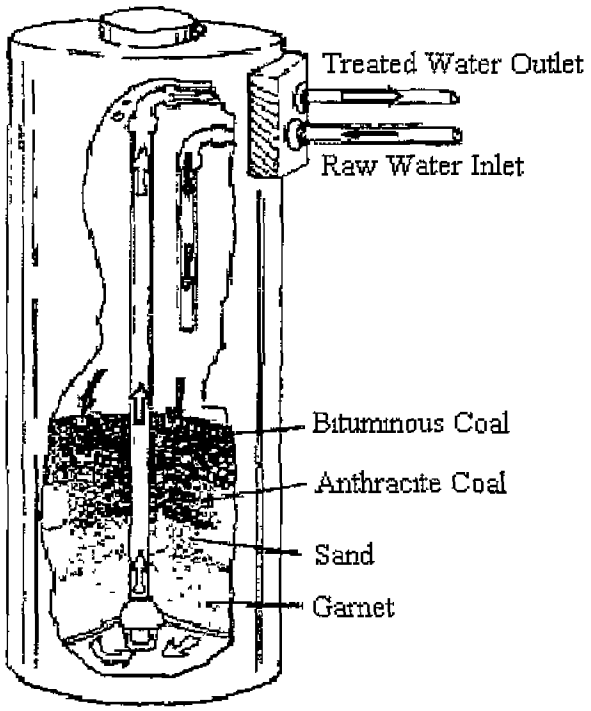

Figure 1.4 - Multi-media filter illustrating various media [13]

1.3.2 Water-softening

Water softening techniques typically follow media filtration. Water varies in hardness from soft to very hard depending upon mineral content. Table 1 2 displays the hardness levels of water in terms of calcium carbonate concentrate (CCC).

Figure 1.5 illustrates the water softening process Using ion-exchange, hardening ions such as calcium and magnesium are removed from the water and replaced with non-hardness ions (sodium). Sodium ions are supplied via dissolved sodium chloride salt or brine. Backwashing up through filter beds removes foreign particulate. Salt/ brine solution is passed through the bed, removing magnesium (Mg) and calcium (Ca) ions Loosely attached sodium ions are released in their place, effectively charging the bed with substitute ions. Finally the bed is rinsed to remove excess sodium/brine solution

Level	CCC (mg/l)
Soft	0-60
Medium Hard	60-120
Hard	120-180
Very Hard	> 180

Table 1.2 - Water hardness levels [14]

Water softening does not remove bacteria, silt or sand, lead, nitrate, pesticides, and any other organic and inorganic compounds [15] However, water softening does remove alkaline [19]. Alkaline reduction protects from scale formation on RO membranes and within distillation stills downstream, thereby improving operating lifetimes of expensive principal purification equipment. However application of water softening techniques can allow for the invasion of the water-processing system by organisms [4] To counteract such effect, chlorine is added to the system.

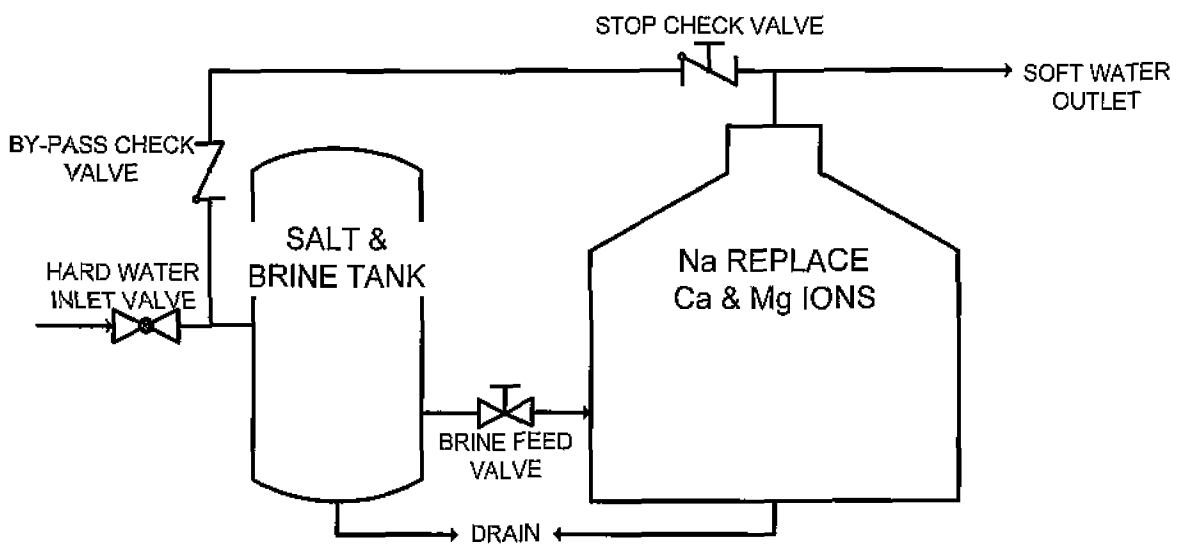

Figure 1 5 - The water softening process

1.3.3 De-chlorination

Chlorine destroys bacteria and prevents biofilm development on wetted pipe interiors [16]. De-chlorination introduces chlorine into the water using activated chlorine (AC) or direct chlorine injection. Chlorine injection does not foster microbial-growth as opposed to AC beds and is favored within industry [17] The chlorine injection technique is shown in figure 1 6.

When chlorine is injected into the water, it oxidizes into sulphate. Free chlorine in the system reacts with the sulphate and forms chlorine ions. Both sulphate and chlorine ion by-products are easily removed by RO treatment down-stream [17]. It is worth noting the presence of chlorine residual in water is prolonged for as long as possible as it undergoes treatment to act as a safety precaution against the ever-present threat of microbial recontamination.

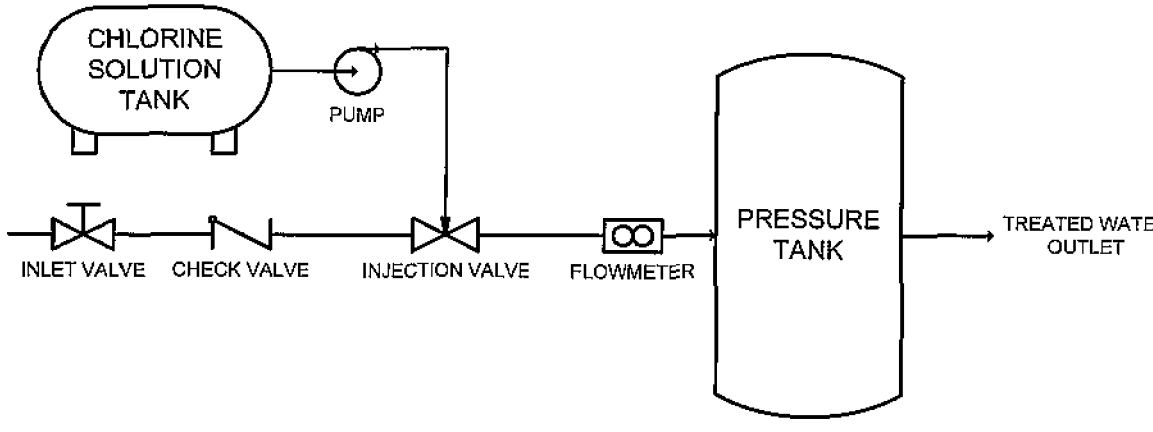

Figure 1 6 - De-chlorination injection system

1.3.4 Reverse Osmosis

Osmosis refers to the natural movement of pure or distilled water through a membrane to a concentrated water solution containing salts and other impurities [18]. With the application of sufficient pressure to the concentrated solution, the osmosis process can be altered. Forcing a concentrated water solution of salts and other impurities on one side of a semi-permeable membrane through to an empty holding tank is known as reverse osmosis [18]. The technique is shown in figure 1.7 Pure water seeps through the membrane to a holding tank leaving behind impurities trapped in the membrane Impurities such as bacteria are removed from the membrane by a sieving action.

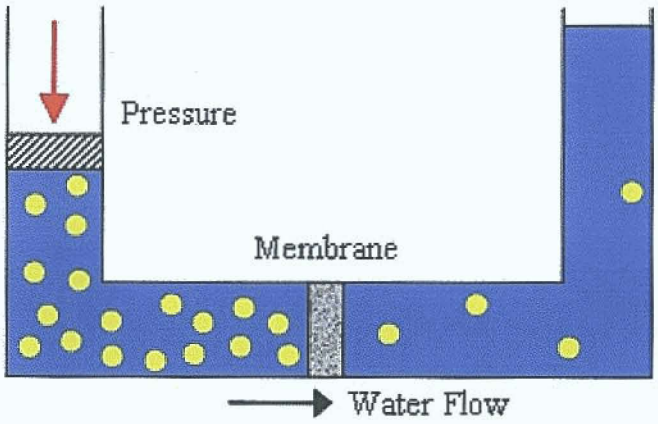

Figure 1.7 - The reverse osmosis process [18]

Membrane pores are minute in size (approx. 0.005μm), with the smallest typical bacteria around 0.2μm. In fact, some membranes can reject 99.0% of sodium chloride [17]. Should continuous pressure be applied to the water to separate impurities through the membrane, dissolved impurities would become so concentrated they would precipitate the solution and foul the membrane [18]. Accordingly, a technique is employed to carry away the impurities forming around the membrane. This is performed by 'reject water' which is flushed from the process in sacrifice of pure or 'product water' [18].

The amount of 'product water' separated from total water (reject and product) is known as the process 'recovery'. The amount of 'recovery' depends upon the performance of the process equipment and the standard of water feeding the process.

The reverse osmosis process removes the following impurities;

- Particulate matters – scale, rust, sediment, sands
- Colloidal matter – particulate that is continuously suspended, never settles
- Dissolved sodium
- Bacteria
- Pyrogens – bacterial by-products
- Organic molecules – sugars, protein, dyes

Pre-treatment of feed water is recommended by manufacturers of distillation equipment and is particularly advised for RO units [5] Although RO offers a substantial purification of water it does suffer one draw back. Substances such as alcohols, phenols, formaldehyde and other dissolved gases cannot be removed using RO. Therefore, the process is viewed merely as a bacterial reduction mechanism as opposed to a complete sanitization method [4].

RO product water is typically de-ionized and passes through a microbial reduction process, such as filtration or high intensity ultraviolet (UV) light [11]. Electro De-Ionizing (EDI) is often used in industry in conjunction with RO, RO waters serving as desirable permeate for the EDI process

1.3.5 Electro de-Ionizing

Electro de-Ionizing consists of selective membranes that isolate ions from their counter-ions [18]. Anions are negatively charged ions; their resins permit only other anions to pass. Equally a cation is a positively charged ion that can only pass through a similarly charged resin By spacing alternating layers of anion and cation resins, a series of diluting and concentrating compartments are created, all under the influence of a DC current [18]. A basic EDI system is shown in figure 1 8

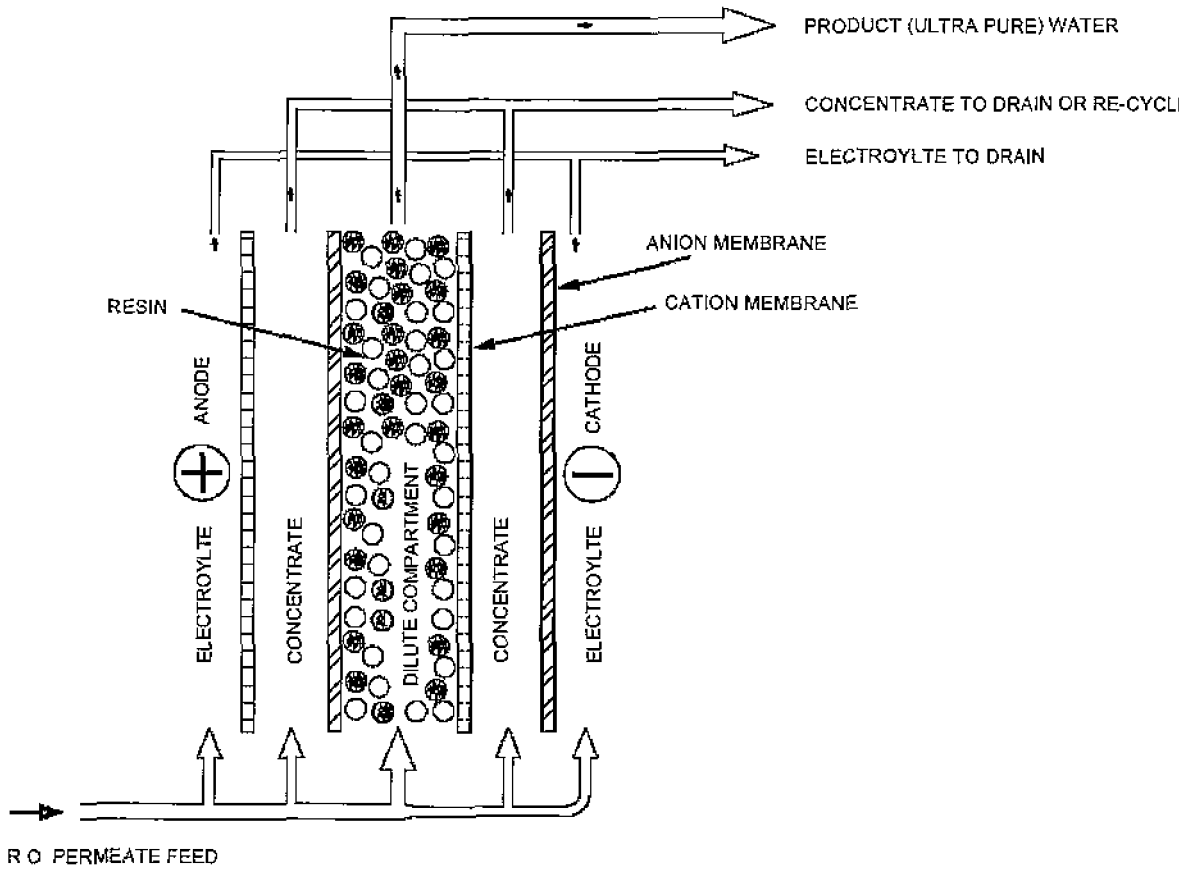

Figure 1 8 - Electro de-Ionizing system [18]

Water is channelled between three compartments, dilute, concentrate and anode/cathode (electrolyte) streams. Membranes do not allow water to permeate through them, acting as barriers to fluid flow. Therefore feed water is channelled into the concentrate and dilute compartments. As the water passes through the dilute compartment, sodium and chlorine ions are exchanged for favourable ions on the resin surface

Electrical current drives ions away from the resin through the membrane into the concentrating compartments. Negative ions in the product stream are then attracted towards the anode These ions pass through the anion permeable membrane into the adjacent concentrating stream where they are repelled by cation permeable membrane and become trapped.

As water moves through the flow compartments, ions in the dilute stream will deplete and become concentrated in the adjacent concentrating stream The resulting water is flushed from the system.

1.3.6 Distillation

Distillation is used to remove volatile impurities such as low-molecular-weight organics, carbon dioxide and oxygen from water. The purification process uses the volatilization of water as a means of separating it from its non-volatile impurities; and the condensation of the volatilized water (steam) to isolate it from its more volatile impurities [4].

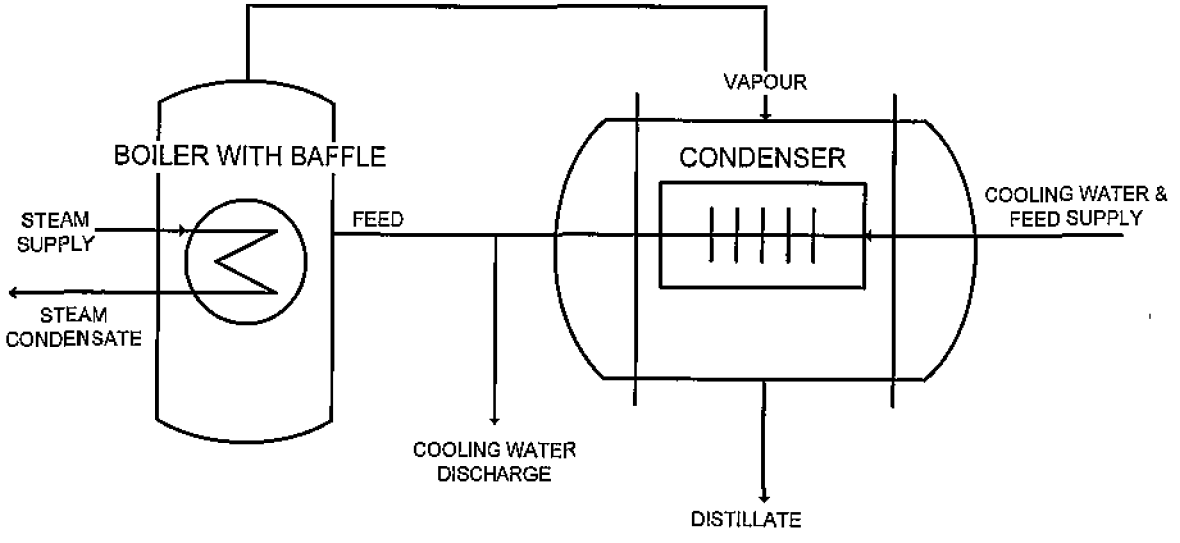

Figure 1 9 - Single-still distillation system

An example of basic distillation equipment is a one-stage still shown in figure 1 9 One-stage stills consist of a boiler to vaporize the water, a dis-entrainment device and a condenser to convert the water back to its liquid state. Liquid particles can become trapped within vapour in the form of mist particles The entrainment of water particles (mist) must be reduced to avoid the carryover of non-volatiles. Devices such as baffles help prevent such carryover

Any water vapour is condensed into its liquid form by encountering cooling surfaces within the condenser Condensation heat that must be removed to re-liquidize the water is extracted by cooling water flowing within coils that condensate the water upon contact Cooling must be adequate but minimal as higher degrees of cooling encourage the condensation of volatiles also [4].

Distillation is not an absolute process [4] The quality of the distilled water is proportionate to the quality of the feed water entering the system.

Bacterial Limits (*cfu*/ml)			
Sampling Location	**Target**	**Alert**	**Action**
Raw Water	200	300	500
Post multi-media filter	100	300	500
Post softener	100	300	500
Post activated Carbon filter	50	300	500
Feed to RO	20	200	500
RO permeate	10	50	100
Points of Use (post EDI)	1	10	100

Table 1 3 - World Health Organisation microbial limits [19]

Additional point-of-use treatments such as polishing ensure high purity water maintains bacteria free after principal purification until time of use Polishing brings water to its highest point of purity prior to entry into production Table 1 3 displays microbial stipulations per process recommended by the World Health Organization (WHO).

1.4 High Purity Water System Design - Sanitary Considerations

The design of high purity water systems is tailored to meet the requirements of the process yet maintain optimum economy [2]. The purified water distribution system forms the integral link between pre-treatment and point-of-use instances. The distribution system must be above all capable of maintaining the required water quality.

Crucial design parameters for HPWS design include maintaining continuous water recirculation at an adequate velocity, continuous or periodic sanitization/ sterilization and the absence of stagnant areas [2] Failure to achieve any of these parameters may lead to a non-sterile system of contaminated product water

1.4.1 Main Distribution Loop Size

Distribution loop size is a factor of user requirements. HPWS designers consider distribution loop size based upon circulation velocities and circulation quantity assuming maximum simultaneous system draw-off Standard distribution system sizes include,

- Single pipe loop
- Double pipe, flow and return loop
- Double pipe, flow/reverse return loop

We will consider single pipe distribution loops, the remaining loop sizes are beyond the scope of this discussion. Table 1.4 lists the characteristics of a single pipe distribution loop.

Advantages	Disadvantages
- least amount of pipework - equal flow rate/velocity around loop	- possibility of high system pressures - flow balancing devices required - flow balancing is complex

Table 1 4 - Characteristics of a single pipe loop

A piping and instrument diagram (PID) of a typical single pipe distribution loop is shown in figure 1 10 A PID displays the distribution system including flow regulation devices, circulation pumps and the operator control systems with key components such as storage vessels and heat exchangers Where sterile point-of-use requires increased water temperature a sub-loop incorporating a heat exchanger is installed. However the added cost of such sub-loops can be negated by designers using separate cold and warm distribution loops [2].

Single pipe loop systems are the natural choice for cold or ambient distribution requirements They are most suited to situations where the main requirement is for loop temperature outlets with a small number of variable temperature outlets [2] Single pipe loops offer equal flowrate throughout the line along with the least amount of pipework thereby reducing costs and installation space [2]

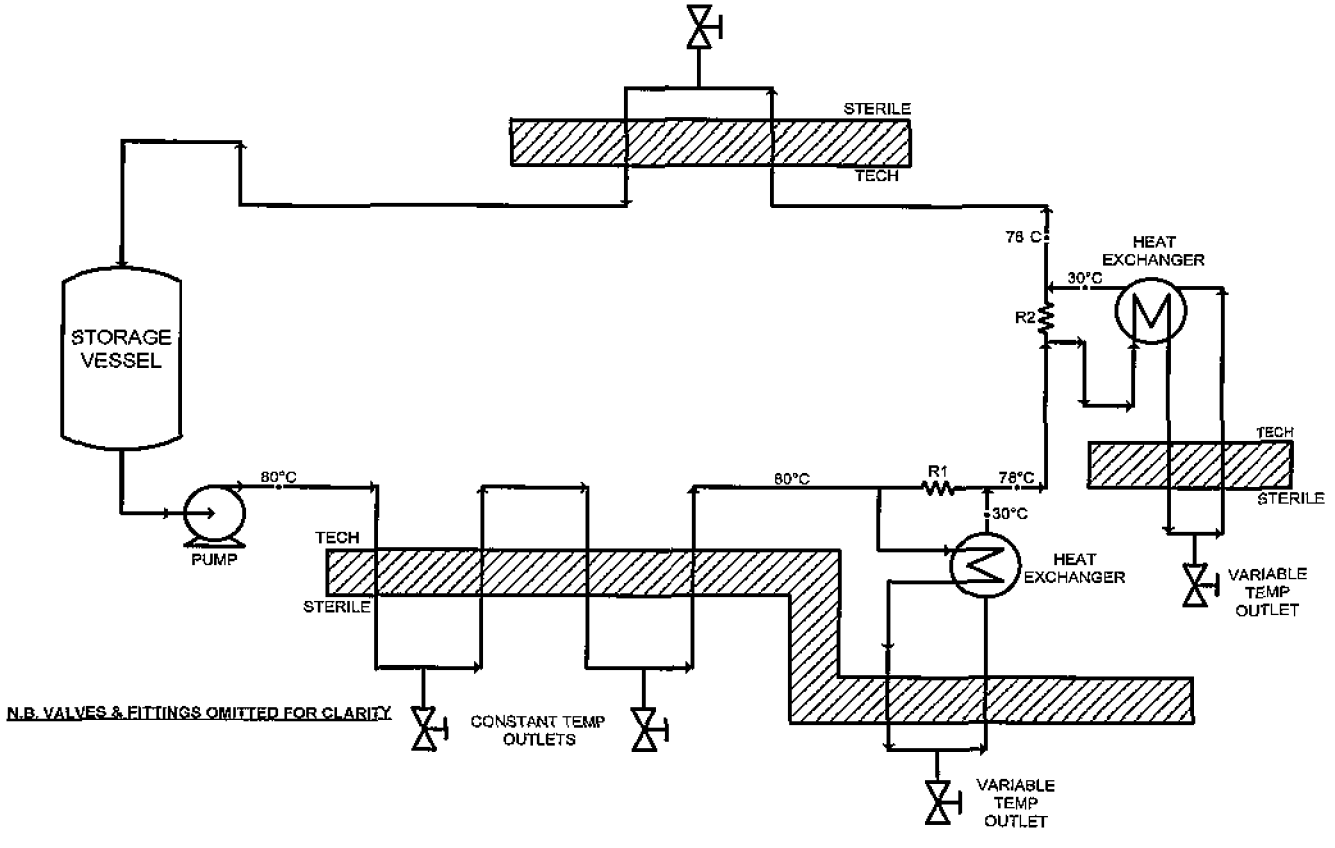

Figure 1 10 - Single pipe distribution loop

Yet system pressures are a concern in such systems. Maximum recommended system pressure is 10bar, with a potential pressure drop across a heat exchanger of 0.3bar [2] Heat exchangers have an accumulative pressure effect and can therefore present a significant portion of system pressure alone. As such single pipe loops are suitable for a small number of heat exchangers only [4]

1.4.2 Circulation Temperature

The circulation temperature of the distribution system is determined by the required microbial limits and/or point-of-use temperatures For a microbial limit of less than 10*cfu*/100ml a minimum continuous temperature of at least 80°C is required to ensure self sanitization occurs [2]. However for less stringent microbial specifications, a hot system (≥80°C) may not be necessary

1.4.3 Circulation Velocity

Recirculating systems are essential if microbiological limits are to be maintained [2] Low velocity or stagnant regions within the distribution loop have the ability to promote the growth of bacteria Non-recirculation is acceptable for purified water systems should the water be continually consumed and flush procedures are in place during non-use.

The accepted minimum circulation velocity range for HPWS is 1 5 - 2.0 m/s [2]. This range is concerned with preventing the adhesion of biofilm to inner pipe walls However recent research [20] indicates required velocities for biofilm control are less than half of current industry recommendations In fact required velocities to ensure biofilm control can vary for hot and ambient distribution systems

1.4.4 Pipework and Assembly

Distribution pipework must remain inert to the purified water it carries and not leach any components into the water Additionally it must withstand sterilizing agents used during cleaning procedures. 316L Stainless Steel (SS) is the preferred pipework material for valves and pipework distribution systems [3] Polyvinylidene fluoride

(PVDF) and Polyvinyl chloride (PVC) plastic pipes are used in systems with liquid temperatures less than 50°C [21].

316L SS has a low-carbon content (0.03%) minimising carbide precipitation during welding which can lead to reduced corrosion resistance in the steel. SS offers smooth surface finish, dimensional consistencies and ease of cleaning. The typical biopharmaceutical finish is approximately 15 *Ra* (Roughness Average) or 0.38 μm for electropolished 316L SS [22] Electropolishing serves to smooth pipe inner surface and reduce differentials between microscopic peaks and valleys.

Pipework assemblies with threaded or flanged connections are avoided as contaminants can accumulate in spaces between threads [22]. As a result system pipework is typically welded together. Figure 1.11 illustrates a threaded connection compromising system waters. With respect to cleaning procedures pipework return lines require suitable slope to encourage gravity drainage and avoid potential air pockets which prevent cleaning solution from reaching inner surfaces [22]

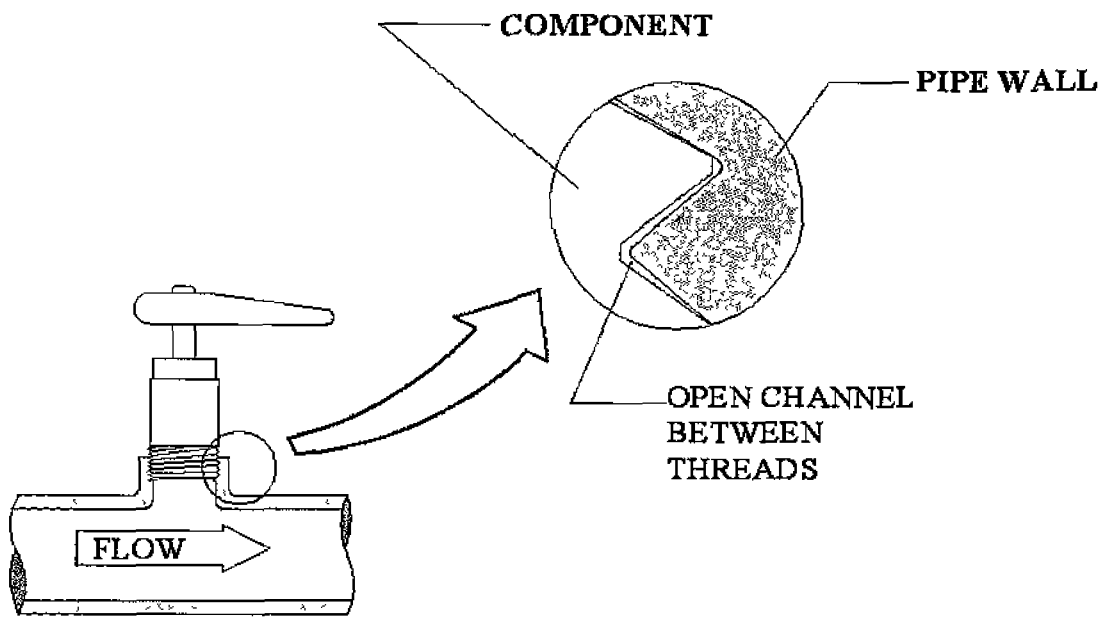

Figure 1.11 - Contamination via threaded sections

1.4.5 Valves

Valves installed within distribution loops have the potential to contribute to the proliferation of contaminants It is recommended that all parts of a valve in contact with product waters be crevice-free and accessible to steam sterilisation [3]. Figure 1.12 displays the types of valves available to HPWS designers

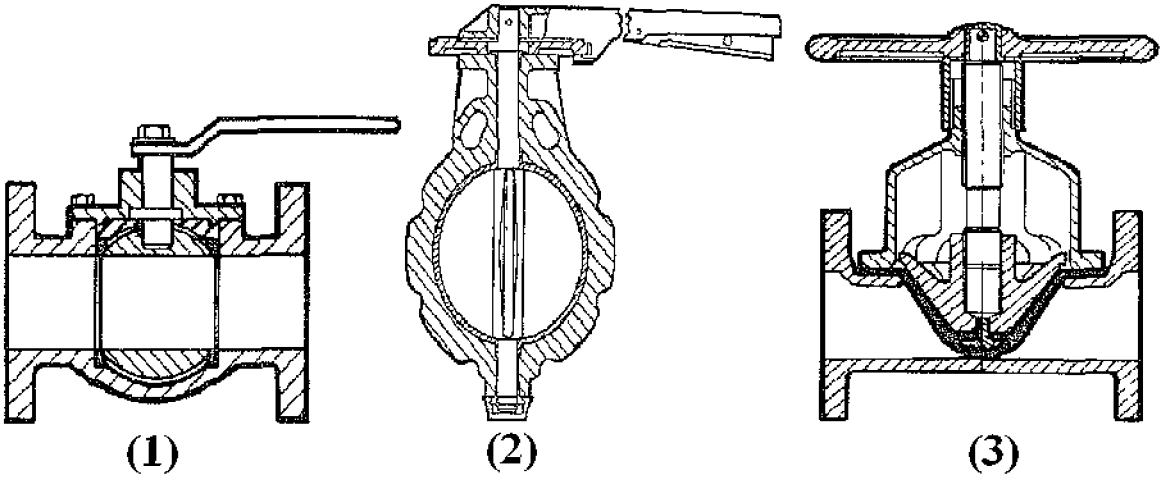

Figure 1 12 - Selection of valves, (1) Ball (2) Butterfly and (3) Diaphragm [23]

Ball and Butterfly-type valves are considered non-sterile as they can harbour steam and water in air-tight crevices effectively creating stagnant pools that encourage bacterial formation. The spacing between the elastic diaphragm sections and valve housing of diaphragm valves can also serve as potential contaminant crevices

Self-drainage is an important attribute of valve design [3];

- making high quality cleaning possible by reducing soil deposition
- allowing free-drainage of condensate during steam sterilisation
- minimising fluid retention, important during small batches or the manufacture of high quality product.

As with pipework it is necessary to construct valve components chemically inert to process fluid. As such SS is the material of choice for most valve housings Seals, gaskets and other flexible diaphragm materials in contact with process fluids are

typically manufactured of Polytetrafluoroethylene (PTFE) providing the designer with excellent chemical resistance [3]

All valves can pose a sterilisability risk for designers Selection must be based upon minimising possible system contamination along with incorporating necessary sanitizing techniques to limit bacterial proliferation

1.4.6 Pumps

Fluid pumps are required to manipulate purified water through the system at required velocities. Both constant and variable speed pumps are used in industry. Constant speed pumps involve less initial capital expense and maintenance compared to variable units However, both flow and pressure output of a constant speed pump varies with changing water usage. Therefore pump efficiency and performance is dependent upon the demand for water

Multistage centrifugal pumps are commonly used in pharmaceutical production as they offer a low rate of wear at common operating levels Pump wear is an important sanitary consideration for designers Particles are generated from the wear of rotors, seals and other internal parts Therefore pumps should be installed sufficiently upstream of pre-treatment units to ensure particle removal via filtration.

Additional pump units are incorporated into system design to compensate for main unit failure However the FDA identify waters present in any additional pipework used to connect stand-by units to main distribution loops as stagnant and possible areas of bacterial proliferation [5].

1.4.7 Storage Vessels

Facilities often use high purity water to rinse pipework and process equipment following batch production The high volume of water necessary during rinsing requires an adequate system storage capacity during such periods of maximum demand. Storage vessels act as reservoirs storing purified waters for periods of high 'draw-off'

However storage vessels have the potential to generate bacteria growth due to low velocities of waters within. Vessels also have the propensity to promote bacterial growth on internal surface walls when not completely filled [4]. Therefore vessel capacity should be selected to ensure system recirculation flowrate results in storage volume being replenished approximately every 6 hours [2] Additionally vessels installed in re-circulatory systems dispense return waters along tank walls via wall-mounted spray balls to minimise bacteria growth.

1.4.8 Heat Exchangers

A heat exchanger is a device which provides for transfer of thermal energy between fluids at different temperatures [24] They are typically employed as part of sub-loops in HPWS used to manipulate fluids to required point-of-use temperatures. Heat is transferred between fluids via conduction through a heat transfer surface.

Figure 1 13 shows a single pass shell-and-tube type exchanger commonly used in industry Shell-and-tube exchangers consist of circular tubes mounted within a cylindrical shell with tube axis parallel to that of the shell. Fluid of set temperature flows along and across the exterior of the tubing heated by a fluid at elevated temperature within the tubes

Heat exchangers are susceptible to bio-fouling. A minimum velocity of 1m/s is recommended for tubular heat-exchangers to reduce the incidence of biofilm formation [25]

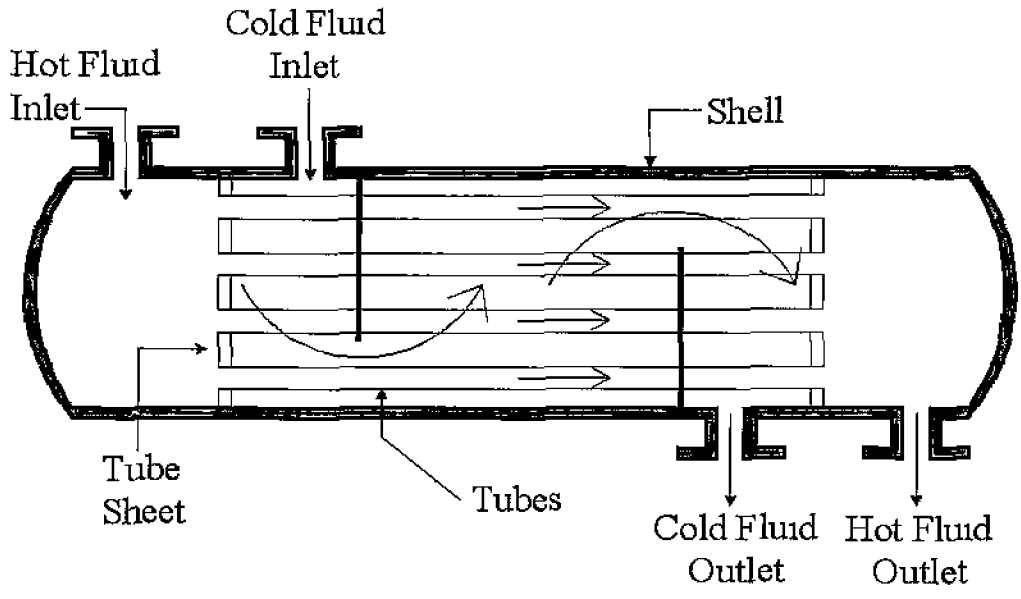

Figure 1.13 - Single pass shell-and-tube type heat exchanger [24]

1.5 Sanitization - Bacterial Control of Pharmaceutical Water Systems

Recently the cleaning of pharmaceutical facilities and production equipment has become one of the most important issues in the pharmaceutical industry [10]. Sanitization is the process of cleansing each component that contributes to the process of water purification. Sanitization is necessary in the reduction of harmful bacteria in process waters that can compromise the quality of manufactured product

Sanitization is however not considered an absolute phenomenon, only serving to partially remove organisms Free-floating bacterial population is eliminated, yet surface attached biofilm can remain on equipment walls [4] Hence cleaning validation is required to ensure the desired contaminants have in fact been removed, and that all process equipment has been sanitized to an appropriate level. Validation of sanitization has now become a primary focus of both regulatory agencies and the industry as a whole [10]. Various methods of sanitizing water systems within industry are employed Their application and frequency is dependent upon the manufacturer's desired water quality.

The main methods [26] used for microbiological control in industry include;

- Maintenance of piping at elevated temperatures
- Use of chemical disinfecting agents
- Use of sterilizing radiation (UV)
- Clean-In-Place (CIP) which renders piping chemically clean
- Steam-In-Place (SIP) followed by the use of sterile barriers

Biopharmaceutical operations are typically based upon 24 hour per day, seven days a week production. Pharmaceutical facilities may utilize some or all of the cleaning methods mentioned above to ensure a sterile system For example in a 24/7 operation, CIP may only be part of a typical 8-hours turn-around (dirty to clean) cycle which also includes SIP and the associated heat-up, cool down, and integrity testing [22].

1.5.1 Sterilization

Pharmaceutical water systems may operate at ambient temperatures or contain water at elevated temperatures. High temperature systems (≥80°C) are termed self-sanitizing as water temperature is considered sufficient to naturally kill bacteria [4] Ambient systems require the water to be heated to 80°C for a fixed period of time before cooling the system back to distribution temperatures in order to kill harmful bacteria.

The effectiveness of sterilization in bacterial control is accomplished by a combination of exposure to contaminated surfaces and temperature [28] However maintaining distribution temperatures above 80°C will only limit bacterial proliferation [2] Sterilization should not be assumed a complete phenomenon but be incorporated as part of flushing techniques and/or CIP or SIP procedures

1.5.1.1 Bacterial Kill Rates

Temperature is one of the key parameters influencing growth, propagation and survival of all waterborne organisms [29] Although temperature ranges where organisms exhibit their greatest or least growth exist, it is widely accepted that increasing temperatures above a particular point will destroy microbes affecting a

sterilizing consequence Optimal temperatures for growth tend to occur near the upper limits with lethal temperatures occurring only a little above optimal

During sanitization, bacteria subjected to heat are killed at a rate dependent upon temperature of exposure and the time required at this temperature to accomplish the desired destruction rate. The D-value of an organism is a measure of its heat resistance. It is given as the time required destroying 90% of organism population at a given temperature Z-value reflects the temperature dependence of a reaction. The Z-value is defined as the temperature change required altering the D-value by a factor of 10

Pseudomonas aeruginosa is a gram-negative organism typically found in aqueous biofilm Gram-negative organisms are known to shed endotoxins which can cause sickness when injected into humans [4] *Pseudomonas* microbes find adequate nutrition even in waters of extremely low nitrogen and carbon content (purified waters). The FDA stated that the presence of *Pseudomonas* in WFI would be cause for its rejection [4].

The optimal growth of *Pseudomonas aeruginosa* ranges from 28-38°C [30]. *Pseudomonas aeruginosa* do not survive temperatures of 60°C or higher for any extended periods of time, although the contact time required to kill them is longer at 60°C than at 80°C Reported D-values [31] of *Pseudomonas aeruginosa* in water are shown in table 1.5.

Temperature (°C)	**Time, t (mins)**
50-58	< 5
60	2.6
70	1.3

Table 1 5 - D-values of *Pseudomonas aeruginosa*

Figure 1 14 represents the D-value for *Pseudomonas aeruginosa* at a temperature of 70°C

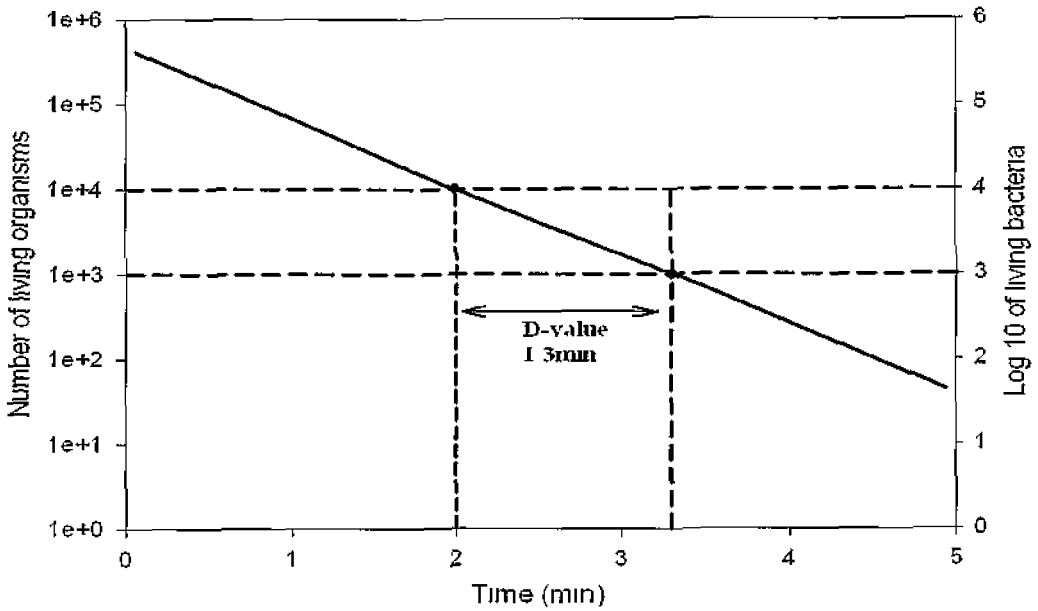

Figure 1.14 - *Pseudomonas aeruginosa* D-value at 70°C

1.5.2 Ultraviolet Radiation

Radiant energy from ultraviolet (UV) light induces a photochemical reaction in micro-organisms inhibiting their growth [4] In higher doses UV radiation can kill such micro-organisms. UV radiation methods are used both during the pre-treatment stages of water purification as well as during polishing prior to point-of-use application UV is generated via discharge lamps consisting of glass/quartz tubing containing an inert gas and metal. Mercury/Aragon lamps are favoured for high efficiencies and performance [4].

The bacterial destructiveness of UV radiation is wavelength dependent. Organisms exhibit different sensitivities to different parts of the UV spectrum [4]. However organism destruction is not only dependent upon UV wavelength but also radiation intensity, duration of exposure as well as the medium through which the light is transmitted Suspended particles in the medium have the potential to absorb UV radiation destined for undesired bacteria As such, this media must be removed

upstream prior to UV disinfection processes. Additionally care must be taken to ensure UV lamps are dirt-free

UV dosage is a function of both radiation intensity as well as exposure time. The minimum recommended dosage for high-purity water treatment is 100mJ/cm^2 [4] (area refers to lamp geometry) Radiation exposure is also based upon water flow velocity and the geometry of the radiation chamber Should the suspended media travel at excessive velocities through the chamber minimum required absorption may not occur.

1.5.3 Clean-In-Place

Clean-In-Place refers to the process of cleaning systems and equipment without major disassembly of process components [22]. CIP involves the introduction of chemical cleaning agents into the existing water distribution system. Chemical solutions of alkali, acid and sodium hypochlorite are used to aid the removal of contaminants. Sufficient but not excessive chemical concentrations, temperature and force are applied to the internal surfaces being cleansed. CIP allows the cleaning solution to be brought into contact with all soiled surfaces of the process equipment by a sequence of draining, rinsing, washing and rinsing [32].

The cleaning sequence involves a series of preset manual and automated operations Manual cleaning is considered unsafe and the standard of cleaning is typically much less effective and consistent compared to a fully automated CIP procedure [21]. Additionally automation reduces system maintenance costs, production down-time and improves operator safety [22]

CIP utilises high pressure pumps, spray nozzles and spray balls permanently or temporarily installed in the system to ensure chemical solution contacts all necessary surfaces. Certain equipment such as ball valves, globe valves and gate valves are considered not suitable for HPWS as parts of their surfaces may not be exposed to the sterilizing agent during CIP.

Once the CIP process has finished and the final rinse has been performed, it is necessary to ensure the complete removal of all cleaning agent residue All sections of pipe must have an adequate slope to encourage the flow of material under gravity out of points such as elbows, valves or specially installed openings for drainage A slope of at least 1:100 for all pipework is recommended to guarantee self-draining [2].

Once CIP is complete, testing is performed to ensure desired contaminants are removed from the system and it has now been sterilized to an appropriate level to return to production Microscopic counts, filtration tests along with other contaminant counts are performed as verification

1.5.4 Steam-In-Place

Sterilization by steam or Steam-In-Place involves draining the system, pressurization by steam, venting and refilling The sterilization of WFI systems should not be attempted with industrial steam as it may contain chemical additives and will not be free of pyrogens [2]. Although steam-sterilization is considered energy wasteful, it is probably the most widely used sanitization method within industry [2].

CIP operations are often used in conjunction with SIP. In fact CIP performed prior to SIP procedures can aid steam-sterilization. CIP serves to remove chlorides that may cause stress corrosion when heated, along with proteins that can become 'baked' onto equipment surfaces by steam [22] A system designed for CIP can be readily adapted to perform SIP operations. Additional hardware such as steam traps, vent valves and resistance temperature devices (RTD) are necessary to control and withstand the steam sterilization cycle [32].

Entrapped air is recognised as the greatest impediment to the effectiveness of steam-sterilization because it retards heat and moisture penetration [28] As such vents and bleed valves within the system allow advancing steam to displace entrapped air During the SIP cycle it is accepted that steam temperature will decrease during heat transfer Condensate steam water (<100°C) must be removed by drainage as this will reduce sterilization temperatures Self-draining capabilities are important for systems

incorporating SIP sterilisation as the required sanitizing temperature of 121°C could not be guaranteed in parts of the system where residual water is present [2]

1.6 Dead-legs - Formation in a High Purity Water System

Dead-legs have the potential to jeopardize the manufacture, cleaning, sanitization as well as sterilization of HPWS. Regardless of the pretreatments and costs expended to secure the desired microbial level of production water, dead-legs can critically compromise water quality.

A dead-leg is an unused section of piping that contains originally sterile product waters. They represent a weak point in systems as transport into them is not directly affected by recirculation [26] Dead-legs are effectively stagnant havens where organisms can attach themselves to surfaces, flourish and develop into a biofilm undisturbed by scouring water flowrates [4]. The limited or stagnant flow within such sections promotes the growth of biofilm within the dead-leg, which can expel organisms into the main stream of fluid.

Figure 1 15 shows an example of a tee-section dead-leg. Static waters remain trapped once the operator closes the branch valve. The length of the dead-leg is calculated from the centre of the main loop to the end of the branch-leg (length A+B+C)

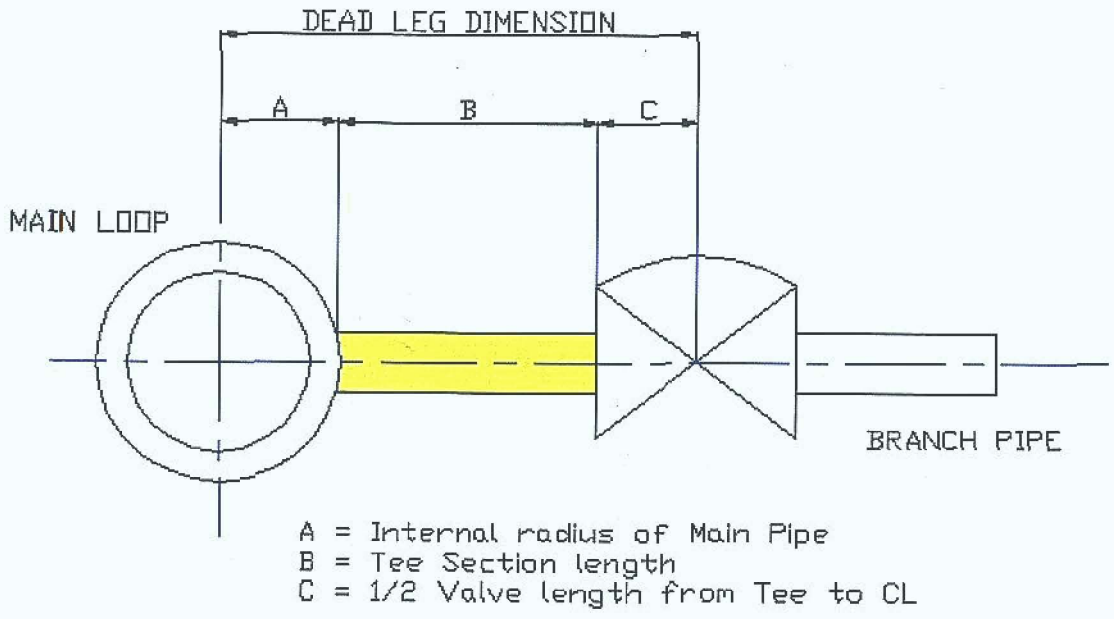

Figure 1.15 - Dead-leg dimension

However the formation of dead-legs is not restricted to tee-section configurations. In distribution networks, dead-legs can form where process equipment connects to the water system. When the equipment is not required and connecting valves are closed, water stagnates. Consider the equipment attachment in figure 1.16. Should process operators open the main isolation valve before the point-of-use valve then the main stream will contaminate with dirty water. Methods such as regular line flushing or slow constant flow from point-of-use can alleviate such problems

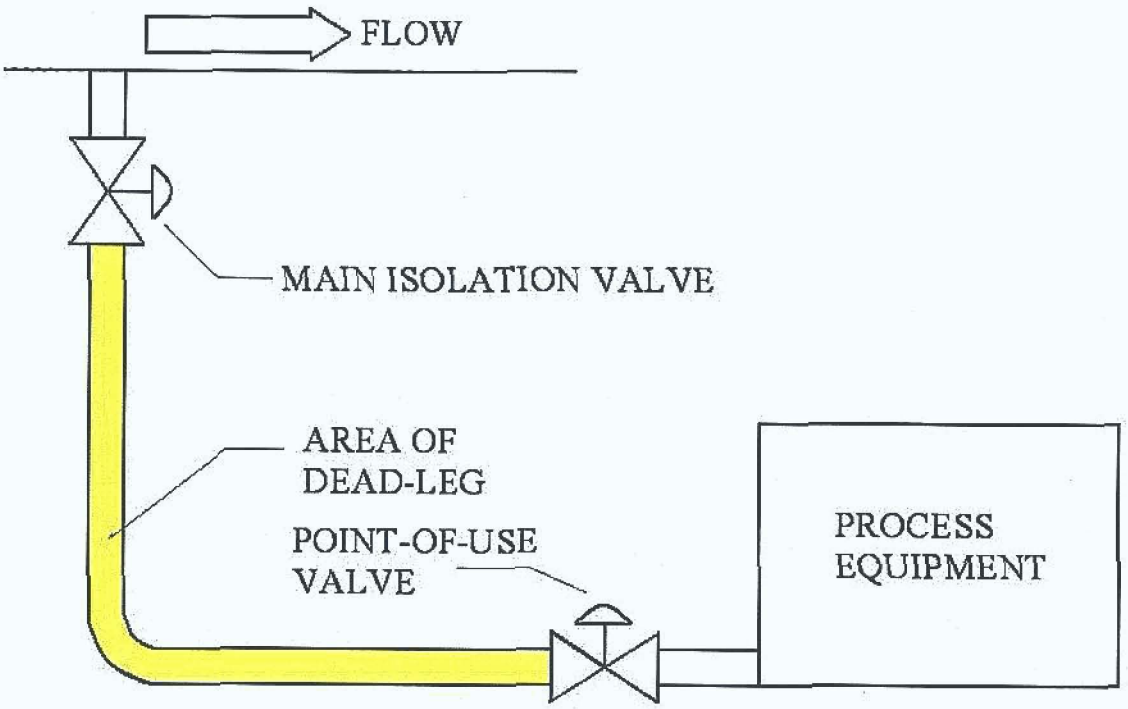

Figure 1.16 - Dead-leg at equipment attachment points

Consider the example of dead-leg formation in the ball valve shown in figure 1.17. Closing the ball valve across traps fluid, which remains stagnant until the valve is re-opened. Upon doing so, the main stream is exposed to contaminated waters and downstream flow may be compromised. The FDA state that such valves are not considered sanitary valves since the center of the value can contain water when closed [5]. This is a stagnant pool of water than can harbor microorganisms.

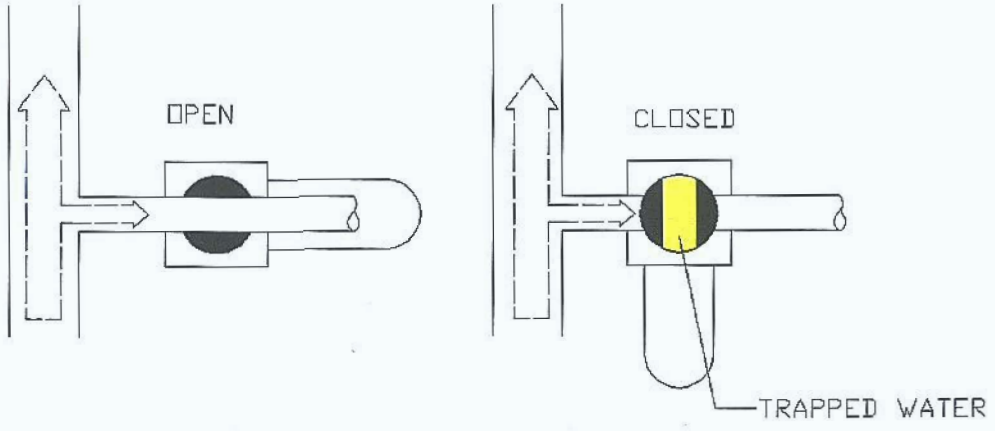

Figure 1.17 - Dead-legs in ball valves

Pumps have been known to fail and for this reason some systems have been installed with run or stand-by units. However the incorporation of an additional pump can lead to significant dead-legs in the system due to stagnant waters in the unused pump or piping. A risk also exists that should a section of process equipment be removed post-installation, a dead-leg can form from the overlooked section of piping that remains [2].

In an effort to eradicate dead-legs from process systems equipment manufacturers have developed specialized attachments. Specialty take-off valves, similar to figure 1.18 create minimal or 'zero dead-legs' at instances within the main loop.

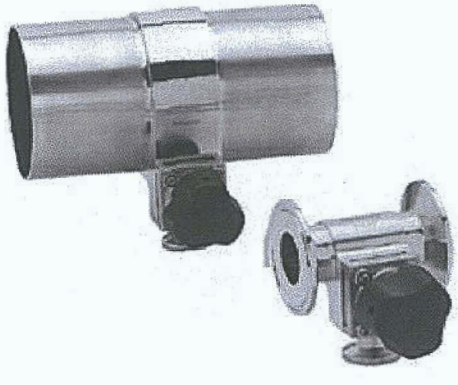

Figure 1.18 – 'Zero dead-leg' take-off valves [39]

'Zero static' tees are designed to reduce inherent dead-legs and areas of possible product entrapment. As illustrated in figure 1 19, these tees consist of a section of pipe routed to point-of-use complete with take-off valve minimizing static fluid flow.

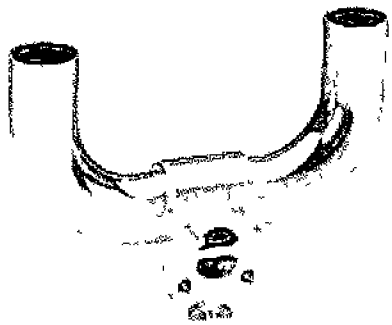

Figure 1.19 – 'Zero static' tee [39]

Such specialized valves ensure conformance to the 6d-rule yet some areas remain where bacteria can proliferate under stagnant flow conditions The presence of clamped connections to reduce dead-legs may not justify the presence of gaskets or threaded areas [40].

1.7 Biofilm - The link with Dead-legs

Biofilm is the accumulation of micro-organisms and their excretions onto surfaces of a water treatment system [33] A bacterial matrix or covering known as glycocalyx forms on surfaces and acts as a barrier that traps organisms away from the water source generating biofilm growth. The adhesion of organisms to the surface of pipe walls encourages the formation of additional organisms to system surfaces Figure 1.20 illustrates the mechanism of biofilm attachment to surfaces.

Biofilm detachment is a determining factor for biofilm formation, because it is the primary process that balances growth [34] Self-replicating biofilm can compromise the microbial integrity of liquid with shed organisms Therefore WFI and Purified waters in contact with biofilm could be sufficiently contaminated with undesirables

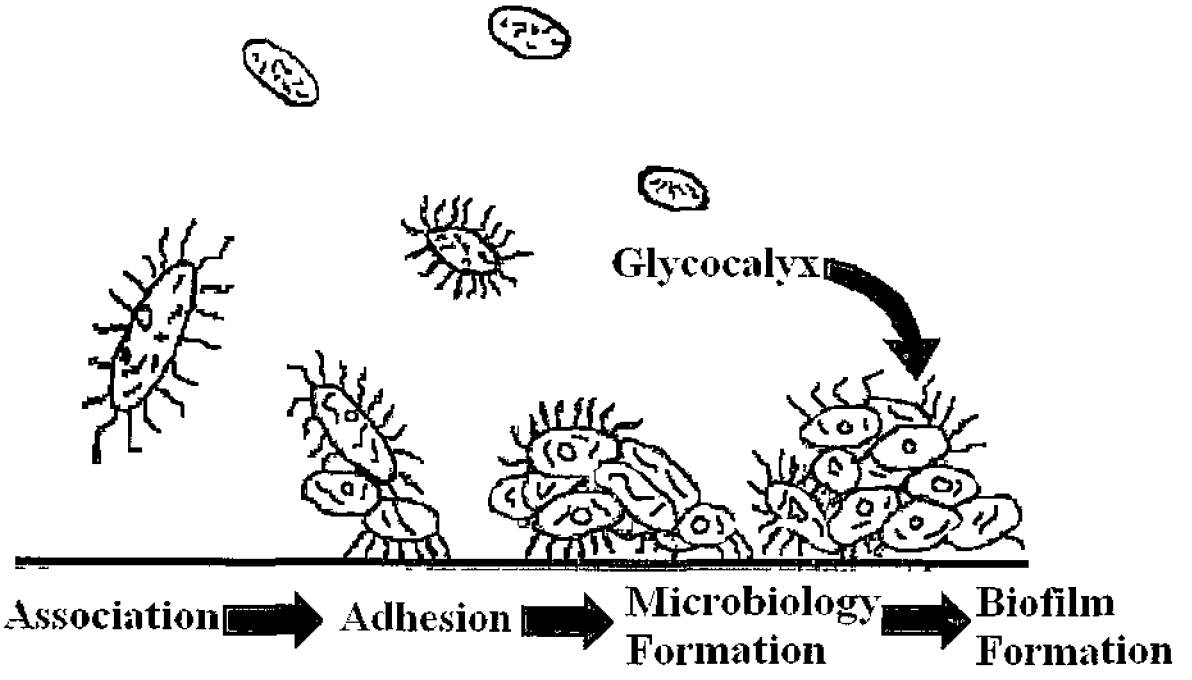

Figure 1 20 - Stages of biofilm formation [33]

Tests are performed in industry to monitor the amount of suspended organisms in an aqueous medium which represent plankton population Worryingly organisms that attach themselves to plant pipe walls will not flow freely within the body of liquid and would not feature in plankton samples Accordingly satisfactory plankton levels may not indicate the true magnitude of biofilm formation within the system In fact in environmental and industrial flow systems the majority of bacteria are attached to surfaces [12]

1.7.1 Surface Finish Characteristics

Regardless of the quality of valves and pipes biofouling can be expected. However smooth surface finishes are considered slower at permitting biofilm formation than rougher surfaces [12].

Purity water devoid of ions is often referred to as 'hungry water' [12]. Minerals that would otherwise have deposited a protective coating on materials upon contact are removed by de-ionizing or other water softening processes making waters highly

corrosive. SS pipework offers desirable corrosive resistance to 'hungry water' Internal variations (peaks and valleys) however in SS pipes with heights as little as 4μm can successfully house bacteria and permit biofilm formation [3].

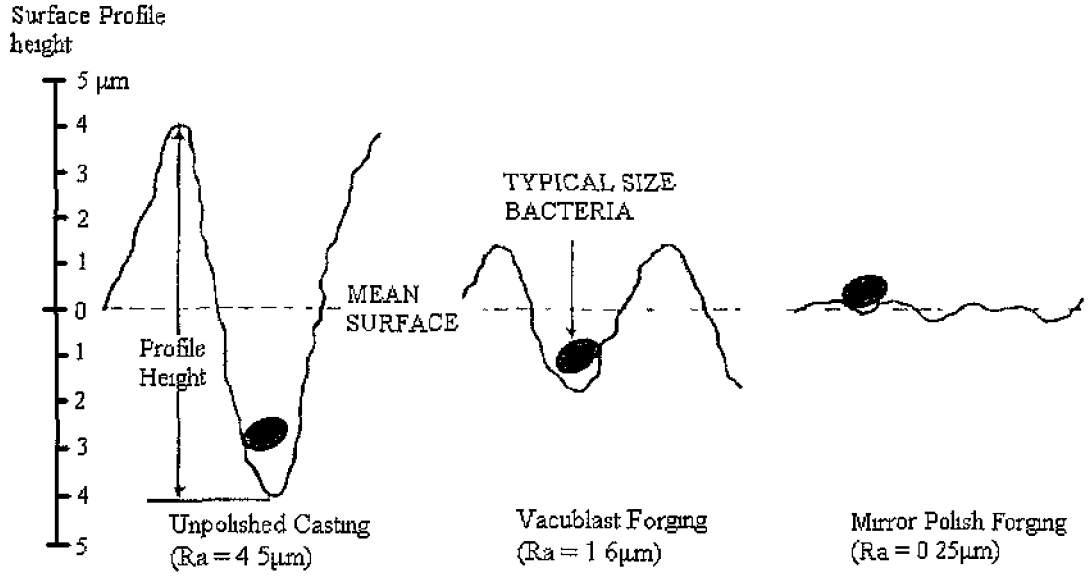

Figure 1 21 - Bacterial movement due to surface roughness [3]

The surface profile of an unpolished SS pipe is shown in figure 1.21 Polishing techniques are employed to reduce surface roughness. A polished SS surface with *Ra* < 0.2μm permits contaminating bacteria to be swept away during cleaning [3] Electropolishing can achieve a high standard of surface finish (up to 0 25μm) provided the part is pre-polished mechanically [35] Therefore since biofilm is a surface phenomenon – the rougher the surface the higher the possible presence.

1.7.2 Flow Velocity and Recirculation

Dead-legs and regions of low velocity flow can signify areas of particular biofilm presence The magnitude, structure and induction time of biofilm formation is influenced by fluid velocity [36]. Research [37] has shown induction times for biofilm formation at high velocities were over three times greater than that of low velocity induction times Reduced induction times at low velocities are owing to the

limited shear forces acting at pipe walls Minimal shear forces permit bacterial elements to attach to pipe walls

Planktonic samples do suggest that bacteria presence is higher in stagnant flow conditions. However as mentioned previous such samples primarily record free floating organisms. As velocity is increased these free floating organisms migrate to container walls where they form as biofilm [4]. Subsequently free floating planktonic counts are reduced indicating an overall improved microbial situation Yet an increased quantity of biofilm may have in fact occurred.

Limited recirculation of fluids in dead-legs results in reduced mixing occurring within the section branch. Circulating flow magnitude within dead-end pipes observed as inner pipe surface shear strength is considered the major contributory cleaning force [10] Lack of turbulent flow results in lower wall shear stresses which effectively leads to reduced cleaning actions. Recent research [20] confirms wall shear strength as the controlling parameter of biofilm growth as opposed to specific distribution loop velocities

Cleaning solution recirculation and temperature are essential to maintain efficient CIP procedures [9]. Maintaining system temperatures above 80°C is shown to aid the reduction in the presence of biofilm [38] Although high temperature sanitization serves to eliminate free-floating bacteria, sessile or surface attached biofilm remains protected by the surrounding glycocalyx film In relation to dead-legs and biofilm content thereof, it is difficult to explain why dead-legs should be conducive to organism growth except where heat is involved; turbulence makes for good heat transference [4]

1.8 Dead-legs - Sanitization Difficulties

The threat dead-legs can pose to distribution loop cleaning procedures are of particular concern Dead-legs have the ability to compromise the overall effectiveness of automated cleaning procedures ultimately leading to contaminated product waters.

1.8.1 Sterilization Issues

The lack of re-circulation at the base of the dead-leg contributes to lower temperatures in the branch As such water contained within the branch tends to be cooler, having been passed less frequently through a heat exchanger The inability to reach required sterilization temperatures contributes to a reduction in the destruction of micro-organisms Higher loop velocities can increase eddy diffusion down the dead-leg branch [40]. The increased presence of eddies may contribute to improved heat transfer generating greater fluid temperature within the branch

The possible detriment a dead-leg can have upon sanitization can be determined by the length of the dead-leg The overall cleanability of a dead-leg pipe within a distribution loop is considered a function of both fluid velocity and the branch length/diameter (l/d) ratio of the dead-leg itself [41] However the industrially accepted design guideline of $l/d = 6$ is generally not considered sufficient to sanitize dead-legs, with industry experts recommending $l/d \leq 4$ [2, 9, 26]

1.8.2 Clean-In-Place Issues

Dead-legs can retain contaminants making full removal of soiled waters difficult during CIP procedures In an effort to remove these waters increased cleaning cycle times are required This leads to increased plant effluent and usage of valuable high quality waters The most expensive stage of the CIP process is the final rinse due to the large volume of WFI or Purified water required flushing chemicals from the system [41]

Dead-legs also pose difficulties during the cleaning stage of CIP procedures Cleaning chemicals may not diffuse down the entire length of vertically orientated dead-legs. This can result in regions of inner pipe surface remaining unexposed to cleaning solution concentration for an acceptable length of time or temperature [40].

Should the dead-leg end with a valve, pulsing the valve open several times during each cleaning step ensures that the entire length of the dead-leg sees fresh chemicals and also cleans the valve seat. A dead-leg cleaned in this manner may not require

strict adherence to the 6d-rule and the use of conventional sanitary fittings is sufficient as opposed to 'zero static' valves

Optimum cleaning occurs within piping when flow rate yields a Reynolds Number in the turbulent regime [41]. Turbulent flow will increase fluid movement towards pipe surfaces where the solvent can mix and react with protein or other contaminants, assisting in moving the resultant mixture away from the internal surface [22]. Diffusion and convection are the controlling elements of cleaning kinetics in dead-legs [41] Alternatively limiting branch length may allow inner pipe walls to be susceptible to recirculation cleaning at normal velocities [9].

1.8.3 Steam-In-Place Issues

During SIP procedures importance is placed upon achieving the required sterilization temperature of 121°C at every point within the distribution loop equipment Failure to maintain set-point temperature results in partial system sterilization [8]. Trapped liquid and air within system pipework serve as potential thermal resistors The temperature of steam is effectively lowered at such instances, thereby reducing sterilizing effects. Unless 'zero dead-leg' valves are incorporated into system design, all air vents have the potential to yield dead-legs [2].

Failure to adequately remove particle deposits during sterilization and CIP procedures leads to further difficulties during SIP. Biofilm for example remaining on pipe inner walls can cause less efficient heat transfer and lower wall temperatures, thereby reducing the sterilizing effects of steam upon those surfaces [8].

Dead-end geometries represent a severe challenge for the removal of air [28]. The physical orientation of dead-legs is an important issue concerning systems incorporating SIP procedures Research [28] has shown that dead-legs orientated vertically upward reached steam sterilization temperatures over a shorter length of time compared to horizontally mounted pipes Dead-legs mounted vertically struggle to achieve sterilization temperatures, filling with condensate protecting the dead-leg from the full steam temperature

Branch diameter also has a significant effect upon SIP procedures. The time taken to achieve sterilization temperatures decreases with respect to increased pipe diameter [27] Increased pipe diameter can negate the effects of negative dead-leg orientation As such distribution loop designers must strike a balance between the optimum dead-leg orientations for steam (vertically upward) and for clean (horizontal) operations

1.9 Research of Piping Dead-legs

In the ever expanding pharmaceutical industry with increasingly stringent regulations, the elimination of design flaws such as piping dead-legs has become ever critical.

Contamination issues associated with piping dead-legs and the dangers they pose to the sanitary consistency of HPWS has prompted extensive research into the fluid dynamics associated with such phenomenon

Research has attempted to describe the physical parameters affecting dead-legs and how the manipulation of these can reduce or at best eliminate associated contamination risks

Early research by Bates et al [42] identified flow characteristics in an equal diameter 90° tee-section for branch and straight flow scenarios Using Laser Doppler Anemometry (LDA) to describe flow conditions, a flow induced cavity with swirling motion was identified within the branch section

In research by Sierra-Espinosa [43] the author argues that the majority of previous research had assumed symmetrical fluid motion in tee-sections Static pressure analysis across the branch exit indicated however the presence of asymmetric pressure conditions. Such asymmetry the author claimed was a result of dynamic three-dimensional swirl flow in the branch as opposed to a mere recirculating region

LDA measurements along the branch exit indicated high velocity flow along the downstream wall with lower, negative magnitudes occurring along the upstream wall. Changes in boundary layer behaviour at the entrance of the branch were also

noted. Boundary layers change from separated-recirculating flow along upstream branch wall to thin jet-like layers along the downstream wall position

Recent work by Nakamori et al [44] identified issues surrounding dead-legs in piping lines within nuclear power facilities The author highlighted the occurrence of thermal stratification and thermal cycling effects in vertically orientated reduced diameter dead-end pipes

By placing thermocouples along the outer wall of branch pipes, cavity flow penetration depths were determined from outer wall temperature distribution.

An increase in cavity flow penetration length with respect to increased main loop velocity was noted It was determined that reduced penetration depth occurred for non-isothermal conditions due to density differences between warm and cool fluids within the branch. A mathematical expression between cavity flow penetration depth and main loop velocity was developed and experimental results compared well with numerical analysis.

The issues associated with piping dead-legs during sanitization operations are of particular concern Dead-legs can retain contaminants thus requiring additional flushing They are also prone to limiting the adequate diffusion of chemicals into the branch thereby reducing the effect of cleaning solution

Earlier work by Noble [26] analysed the transport of thermal and ozone disinfectant during sterilizing treatments with respect to piping dead-legs Research focused upon methods in which fluid is transported into dead-legs, turbulence from attached convective stream, natural convection in thermal systems and diffusion. Using a mathematical expression, regions of dead-leg flow were separated into turbulent, free convection and diffusive transport zones of dominance.

It was argued that beyond the turbulent zone in vertically downward dead-legs, thermal transport is accomplished via diffusion effects Based upon mathematical methods Noble predicted that substantial temperature drop occurred within this diffusional zone.

Noble alluded to the presence of heat conduction in the walls and its significant role in heat transport, assisting the transport of energy within a dead-leg branch An equation was developed for diffusional thermal response time with applications to CIP sanitizations

Recent research conducted by Haga et al [10] studied relationships between dead-leg length and fluid flowrate and the effect these parameters had upon cleaning temperatures and times during CIP operations

By placing a fixed amount of contaminant at the base of a dead-leg branch and passing cleaning solution through a main loop, the effect loop velocity and branch length had upon dead-leg cleanability was monitored. Analysis was performed using an equal branch diameter tee-section of 23mm. Results indicated for l/d = 6, loop velocity <2m/s was required to immediately remove residue. However lower main loop velocity of 0 5m/s was sufficient to remove residue for l/d = 2 8

Coupled with experimental results, computational simulation was used to investigate cleaning mechanisms Results confirmed increased main loop velocities (>2 0m/s) generated larger regions of recirculating flow in the dead-leg branch The author suggested that circulating flow magnitude was associated with wall surface shear strength which contributed to internal cleaning. The author concluded the cleanability of dead-end sections must be considered in terms of both l/d ratio and main loop velocity

Entrapped air in dead-leg geometries can severely impede the effectiveness of steam sterilization as it retards heat and moisture penetration Work performed by Young et al [28] provided insight into parameters affecting heat and mass transfer during SIP operations in various dead-leg branch diameters SIP sterilization was governed by heat and mass transfer which were dependent upon equipment geometry and size. Steam temperature was monitored using thermocouples secured to a nylon string positioned along the centreline of an operational branch.

Cycle Log Reduction (CLR) times (time taken to reduce bacterial population by 1 log) were compared with D-values of *Bacillus stearothermophilus* in stainless-steel tubes 0 4 - 1 7cm ID and 9.4cm in length.

It was discovered that dead-ended tubes orientated at 5° to the horizontal resulted in temperature decrease as distance up the tube increased. At similar branch positions greater temperature decreases were evident in vertically upward tubes compared with 5° horizontal dead-ends 12-log reduction in spore population took 50mins in vertically orientated 1.7cm tubes whereas 167mins was required for 1 0cm tubes.

In relation to mass transfer the author concludes that retarding viscous forces increase with tube diameter resulting in higher transport of steam up the tube and removal of air from the top of the tube

Increased computer processing power and the advent of Computational Fluid Dynamics (CFD) afforded researchers the opportunity to investigate fully turbulent conditions occurring within tee-sections. Although beyond the scope of this research, CFD analysis has provided insight into flow behaviour in dead-ended branches

Recent research by Corcoran et al [45] identified flow characteristics in equal diameter branches under both divided and dead-leg flow scenarios The author highlights flow scenarios in a 50mm diameter 90° tee-section using a numerical model based upon earlier Laser Doppler Velocimetry (LDV) data [43].

Using CFD models, regions of low turbulence were identified within the dead-leg branch Branch wall analysis provided areas of low velocity and low wall shear stress; conditions the author argues are conjugative of biofilm development.

Flow visualization provided by a two-dimensional flow plate collaborated well with CFD findings, identifying a slow moving vortex circulating fluid into the branch along the downstream walls Dye injected into the base of the two-dimensional flow plate branch revealed stagnant flow conditions.

Negative effects of piping dead-legs are not limited to pharmaceutical applications In the oil and gas industry dead-leg corrosion presents the highest percentage of internal damage to pipelines [46].

Research conducted by Habib et al [46] analyzed the effect dead-legs had upon pipe corrosion in piping systems transporting crude oil and water solution. Using computational fluid modelling in conjunction with Laser Particle Image Velocimetry (PIV), the author described flow field geometry and orientation in reduced diameter dead-leg branches Analysis included horizontal and vertical branch orientations using fixed inlet velocities with l/d ratios ranging 1-9.

Flow visualization studies correlated well with computational analysis It was concluded that no stagnant zones exist for $l/d < 3$ for vertical orientations For ratios $l/d > 3$, regions close to main loop flow are characterized by vertical fluid circulation. The remainder of the branch was shown to remain stagnant

Research by El-Shaboury [47] investigated forced convection in equal and reduced area ducts using computational modelling It was determined that branch flow parameters were strongly influenced by branch-to-inlet ratio. Reduction in ratio resulted in decreased vortex magnitude within the branch The size of the re-circulation zone was also shown to decrease with Reynolds Number

The author also suggested that for a reduced branch size which constitutes less area compared with an equal area branch size, heat flux will increase as the fluid has less area within which to transfer

A review of research to date has indicated that flow behaviour within capped tee-sections is complex in nature. The presence of recirculating vortices is highlighted in dead-leg branches, the magnitudes of which can vary with inlet velocity Branch flow dynamics in general are shown to change with respect to branch depth and position.

Certain key parameters affecting re-circulating flow magnitude in dead-legs are highlighted With respect to CIP procedures in distribution systems with dead-legs

present; loop velocity along with branch length and diameter are recognised as the crucial factors affecting cleanability The manipulation of such parameters therefore may contribute to dead-legs of acceptable configurations.

However the general consensus of dead-leg researchers is that the 6d-rule is in fact flawed. Fluid dynamic studies continually describe the presence of stagnant zones in dead-leg configurations $\leq$ 6d. This could lead to the construction of possibly contaminating system dead-legs which are deemed acceptable based upon 6d-regulation.

1.10 Objectives of Thesis

This research aims to investigate the sanitization and cleaning abilities of piping dead-legs considered within the limits of industry recommendations Analysis offers the opportunity of identifying the thermo-fluid characteristics of dead-legs with respect to varying branch configurations and loop operating velocities Consideration of any findings with particular application to the 6d-rule will be explored in terms of the destruction and removal of contaminants under flow conditions

Experimental discussion will focus upon,

- Evaluation of dead-leg thermal profiles detailing maximum temperature and profile patterns

- The fluid dynamics contributing to, if any, regions of cooler stagnant waters within dead-legs as well as factors contributing to the scale of fluid mixing

- Comparison of branch temperature and fluid dynamics with respect to fixed dead-leg geometry ratios

- Determination of the heat transfer mechanisms occurring in dead-leg branches

- The effect of loop inlet velocity upon dead-leg temperatures.

- The application of non-intrusive techniques to determine methods of calculating dead-leg temperature based upon surface temperature measurements.

Chapter 2 Materials and Methods

Experiments were performed using capped 90° tee-sections fixed to a single pipe distribution loop A schematic of the distribution loop is shown in figure 2.1. All pipework and component fittings were supplied by Leslie Reynolds & Company Pipework and fittings were manufactured from 316L SS with 50mm outer diameters.

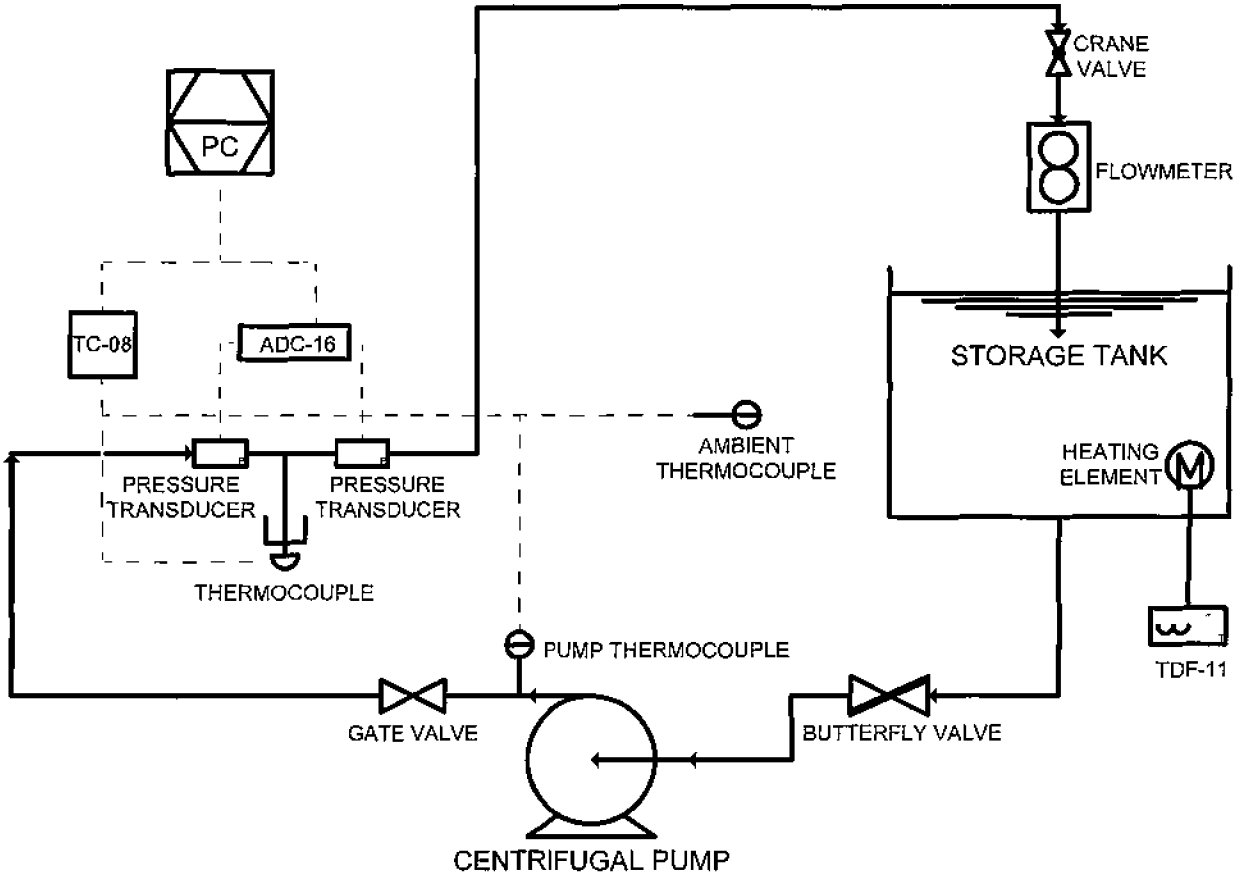

Figure 2.1 - Schematic of single loop fluid rig

All pipework was insulated with 15mm thick insulation supplied by Marr Insulation Ltd. to reduce heat loss via wall conduction Sections of piping were machined to required lengths and all fittings were butt welded using a Tungsten Inert Gas (TIG) welder. Gas purging was performed on internal pipe surfaces to ensure welds were flush with internal pipe walls Sections of pipework were wall-mounted using wall brackets manufactured by DCU engineering workshop Manufactured from aluminium, they provided adjustable fixing to ensure accurate levelling and sloping of pipework where necessary

To ensure fully developed bulk fluid velocities and sufficient turbulence intensity profiles approaching the tee-section, a straight length of pipework was installed Calculations for suitable hydrodynamic entry length were based upon the equation {1} for turbulent flow at the maximum operational loop velocity [48]

$$L_h \approx 4\ 4D\ (Re)^{1/6} \qquad \{1\}$$

Exit and entry lengths of 1 5m and 3m respectively where as those used in similar experimentation procedures [42].

2.1 Pump

A constant speed multi-stage Grundfos CHI 12-10 centrifugal pump supplied by Grundfos Ireland Ltd was installed to generate required water velocities Shown in figure 2.2, the pump (1) is similar to those used in single loop systems within industry [4] Pump housing and impeller were manufactured from SS with carbon seals, capable of pumping thin non-explosive fluids between -15°C and +100°C The CHI 12-10 model has a rated flow of $10m^3/h$ with rated head of 15m

A 3-phase motor is controlled via an isolation switch (4) mounted on the pump housing. The pump is complete with 1 ½" (38.1mm) BSP female axial suction and radial discharge ports connected to supply (2) and feed lines (3) respectively The unit is complete with pressure gauge (5) and gate valve (6) supplied by Radionics Ltd. used to regulate flow into the unit for manual control during pump priming All pipework was attached to ports using tri-clamp brackets.

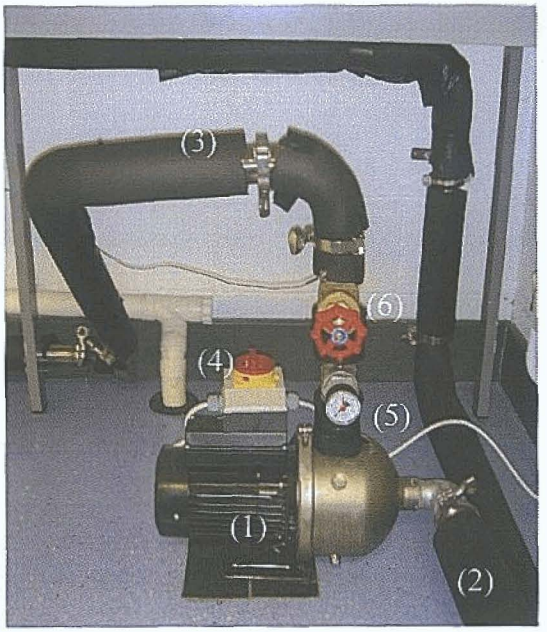

Figure 2.2 - Centrifugal pump assembly

2.2 Flow Regulation

A D931 Crane valve supplied by BSS Ireland Ltd. was installed to regulate system flowrate. Shown in figure 2.3, the valve (1) is complete with 1 ½" (38.1mm) BSP female connections attached to pipework via in-house altered tri-ferrule fittings, thereby minimising total process welds.

Flow is controlled using a valve-mounted microset hand wheel with diaphragm seal. The accuracy of flow measurement is +/- 5% across the wheel settings. The valve is mounted vertically within the system using 50mm galvanised wall brackets supplied by BSS Ireland Ltd.. The position of the valve at the highest point possible in the distribution loop ensures pipework remained flooded and flow could be regulated accurately.

Figure 2.3 - Flow regulation showing (1) Crane valve and (2) Flowtrak dial indicator

A variable area flowmeter (2) supplied by Manotherm Ltd. was installed in the system vertically below the Crane valve to determine the setting of volumetric flowrate. As water passed through an orifice within the flowmeter, a float assumed a position where the forces created by flow were balanced by the weight of the float. A magnet in the float is then sensed by a Flowtrak dial indicator providing a direct reading of volumetric flowrate.

The wetted areas of the variable area flowmeter were manufactured from 316L SS. The device has an operating temperature range between -40°C and +200°C and is suitable for monitoring the flowrate of liquids or gases in industrial process lines. Accuracy is given as +/- 2% of full scale reading.

Pipework lengths of 10 and 5 internal pipe diameters were placed upstream and downstream of the flowmeter respectively. As per manufacturer recommendations, the placement of bends and other such fittings in close proximity to the flowmeter were avoided as such fittings may disrupt flow and compromise steady movement of the internal float device. Additionally the flowmeter was installed to ensure it was

not in proximity to areas of high magnetic field or magnetic materials which may alter movement of the dial recorder.

2.3 Storage Vessel

The storage vessel provided the volume of water necessary for adequate flowrates within the loop pipework The storage vessel consists of an open tank 600mm in diameter and 1500mm in height manufactured by DCU engineering workshop Tank volume is 150L Storage vessel complete with insulated lid (1) is shown in figure 2.4

A cover was placed onto the tank to reduce heat loss to atmosphere Further heat loss was reduced by insulating both tank and lid with foam insulation supplied by Marr Insulation Ltd Lid and tank exterior were insulated with 13mm and 15mm thick insulation respectively. The tank was placed upon SS supports to reduce heat conduction to earth.

A butterfly valve (2) installed at the exit line of the tank enables tank isolation during maintenance and system drainage The feed line to the pump (3) is sloped to avoid air bubbles proliferating into the pipework The pipe exit line (4) is positioned within the storage tank to ensure that it is fully submerged when the tank is approximately ¾ full This ensured that the water flowed from the pipe exit line into the storage vessel in a uniform manner as opposed to draining from the section under gravity

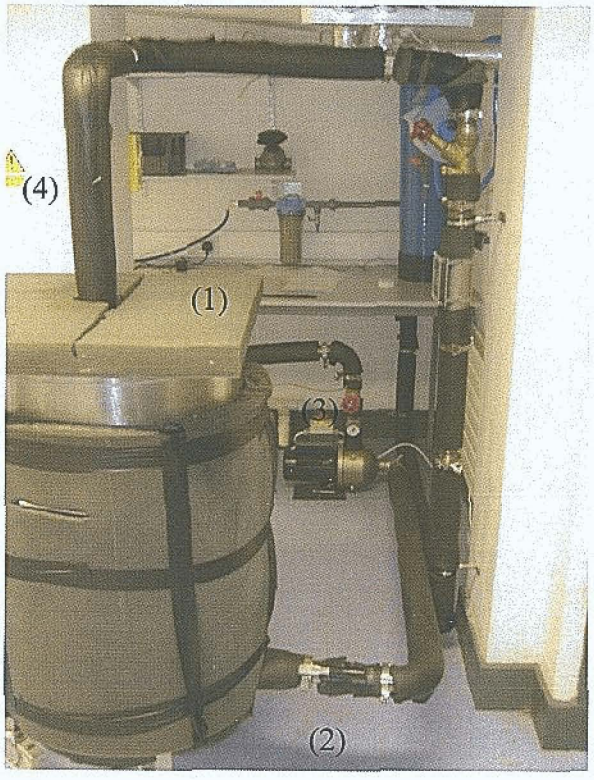

Figure 2.4 - Insulated storage vessel and related components

2.4 Heating Element and Temperature Control

Electrical components relating to the heater element and temperature controllers were housed in a galvanised box (shown in figure 2.5) supplied by John Denis Contracting Ltd. mounted to the laboratory wall. Each component was fused within the box to protect against electrical overload.

A 9kW 3-phase SS immersion heater supplied by Ideal Ltd. was mounted to the base of the storage tank. The heating element increased water in the storage vessel to required temperatures based upon operator input via a Technologic TDF 11 temperature controller. Both heating element and controller were supplied by Ideal Ltd.. Water temperature was monitored via a wall-mounted T-type thermocouple within the tank. Temperature data was returned to the controller and a contactor switch was used to reactivate heating to maintain user specified temperatures. Figure 2.5 displays the TDF 11 control unit (1) with wall-mounted master switch (2).

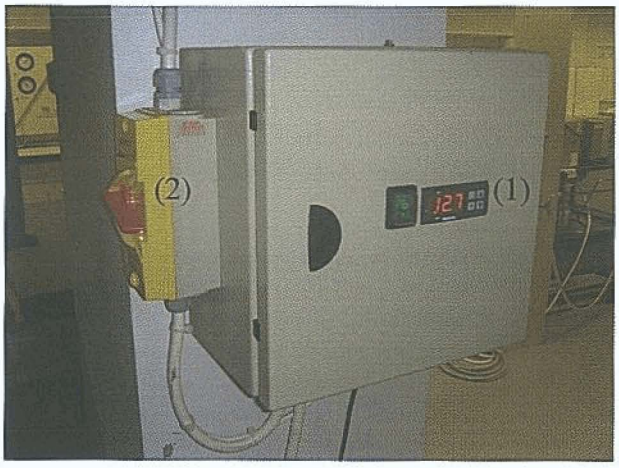

Figure 2.5 - Galvanised box containing TDF 11 unit and controls

2.5 Tee-section Test Pieces

All tee-sections were supplied by PetroChem Ltd. and manufactured by Stainless Fittings Ltd. as part of the Biobore® range. Test pieces (see also Appendix A) were manufactured from 316L SS as part of active American Society of Testing Materials (ASTM) A270 T316L standards. Tee-sections were manufactured with sateen polish surface finishes of 0.8–0.9 μm externally with a maximum internal finish of 0.5 μm.

Figure 2.6 displays equal diameter branch tee-sections consisting of (1) 6d, (2) 4d and (3) 2d branch leg lengths. Each section has 50mm outer diameter with branch lengths measuring 300mm (6 x 50mm), 200mm (4 x 50mm) and 100mm (2 x 50mm) from the centreline the straight section.

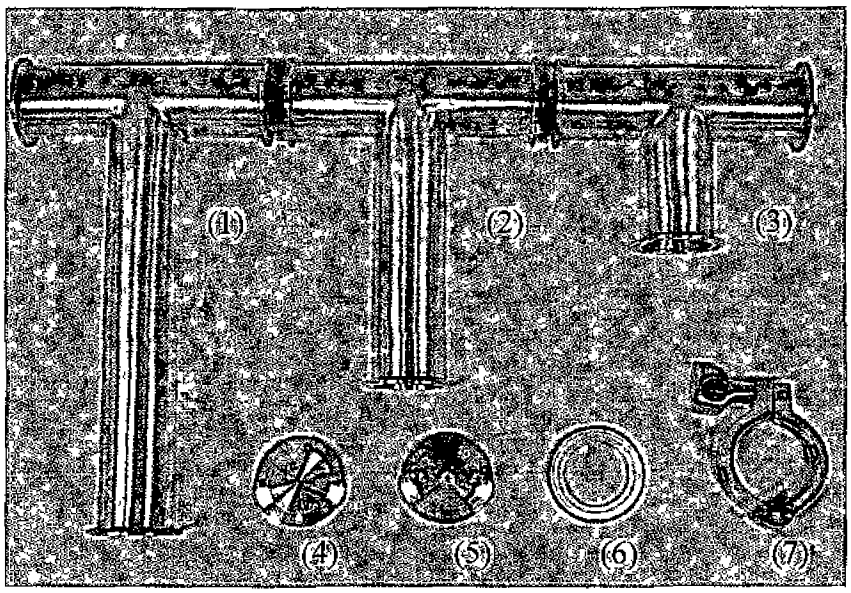

Figure 2.6 - Equal diameter tee-sections with accompanying attachments

The branch leg of test sections was capped-off using a base-cap (4) with PTFE o-ring seal (6) and tri-clamp assembly (7) to recreate a dead-leg flow scenario A base-cap machined by DCU engineering workshop incorporated compression fittings (5) complete with internal seals for thermocouple sheaths. Compression fittings allowed the manipulation of thermocouple depth and secured probe position during experiment

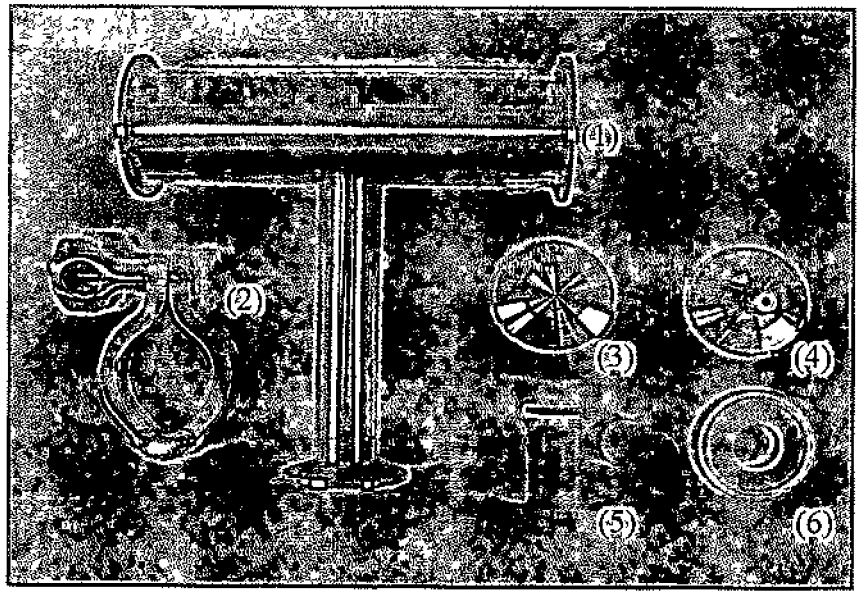

Figure 2 7 - Reduced diameter tee-section with accompanying attachments

Displayed in figure 2.7 the 6d reduced branch tee-section (1) consisted of a 50mm outer diameter reducing to a 25mm outer diameter branch, 150mm (6 x 25mm) in length measured from the centreline of the straight section. Nylon inserts (5) manufactured by DCU engineering workshop complete with PTFE seals were placed within the tee-section branch to restrict internal branch length to 50 and 100mm to reflect 2d and 4d section flow respectively (see Appendix A). The base of the reduced diameter branch was capped-off using a base-cap (3) with PTFE o-ring seal (6) and tri-clamp assembly (2). Also shown is a base-cap (4) machined by DCU engineering workshop to incorporate a thermocouple compression fitting

Figure 2.8 illustrates the dead-leg configuration with temperature measurement via a base-cap inserted sheath-type thermocouple. All sections where specified with ferrule ends to ensure ease of attachment to and removal from pipework assembly using PTFE seals and tri-clamp attachments. Test-sections were attached to the distribution loop with a clearly defined inlet and outlet and subsequent upstream and downstream branch walls.

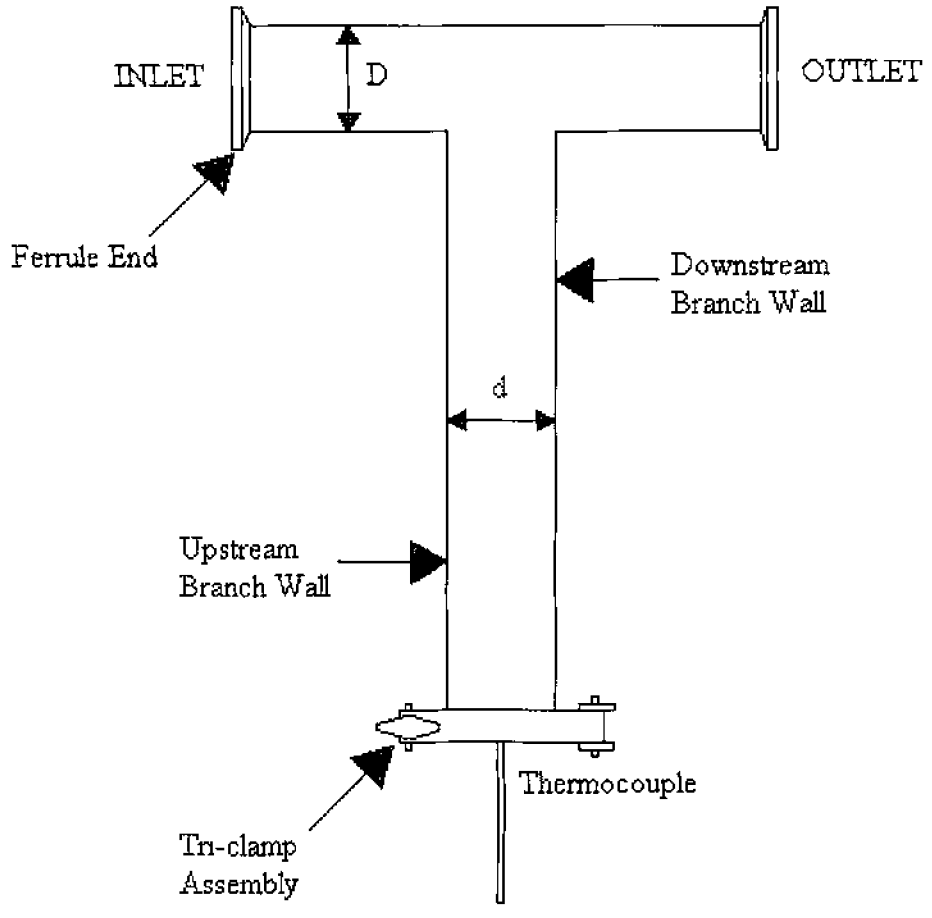

Figure 2 8 - Schematic of dead-leg test section

2.6 Data Acquisition

Temperature measurement was performed using a Pico TC-08 data-logger supplied by Pico Technology Ltd and attached T-type thermocouples. The data-logger (shown in figure 2 9) measured both loop fluid and ambient air temperatures The TC-08 unit provided for cold junction compensation as well as for thermocouple curve normalisation

Attached to a PC via serial port, the TC-08 acts as a converter transforming the measured parameter (voltage across the thermocouple) into the desired system output (temperature recording) T-type thermocouples measured temperature on the rig whereby the TC-08 amplified the signal, feeding it to a 16-bit analogue to digital (ADC) unit T-type thermocouples produced approximately 40μV voltage change per degree Celsius. Thermocouple tables relating voltage to temperature were stored

in the accompanying software Details of hardware specifications of the TC-08 unit are described in table 2.1

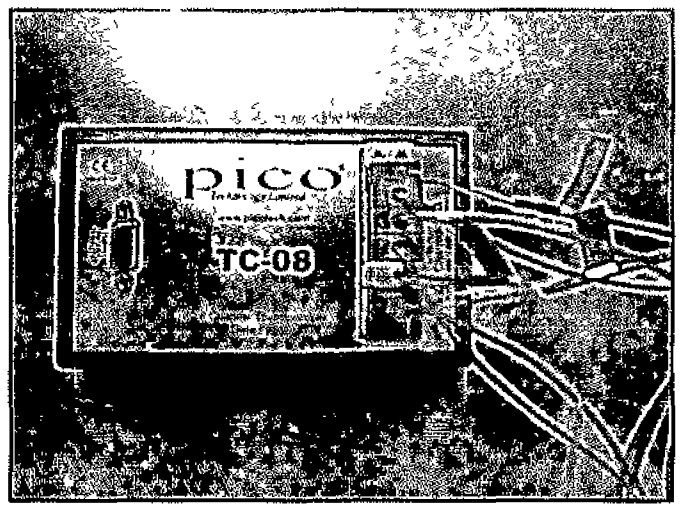

Figure 2 9 - TC-08 data-logger with attached thermocouples

Thermocouple types	B,E,J,K,N,R,S,T
Number of input channels	8
Conversion time per active channel	200ms
Standard accuracy	the sum of ±0 3% and ±0.5°C (cold-junction compensation)
Input connectors	Miniature thermocouple
Environmental conditions	0-50°C/ 0- 95% humidity

Table 2.1 - TC-08 data-logger hardware specifications

T-type thermocouples consisting of SS sheathed and bead-types were supplied by Instrument Technology Ltd.. The thermocouples consisting of Copper and Constantan (CuNi) wires joined at both ends produced a measured current between ends when heated. Accuracy of the T-type thermocouples is detailed in table 2.2.

Overall Resolution (°C)	0.1°C Resolution (°C)	0.025°C Resolution (°C)
-270 to 400	-230 to 400	-20 to 400

Table 2.2 - T-type thermocouple resolutions

Flowrate pressure was monitored upstream and downstream of the tee-section test piece using two submersible Gems pressure transducers supplied by Manotherm Ltd.. The transducers manufactured from 316L SS have a pressure range of 0-2.5 Bar. Transducer output range of between 4-20mA was converted via the ADC-16 unit and recorded. The ADC-16 unit (shown in figure 2.9) is a high resolution 16-bit converter offering 8 analogue input channels capable of detecting signal changes as small as 40μV. The hardware specifications of the ADC-16 unit are displayed in table 2.3.

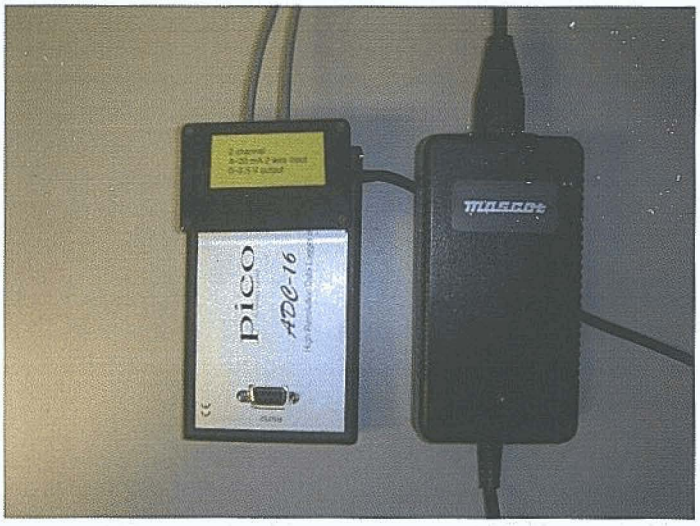

Figure 2.10 - ADC-16 converter with power supply

The pressure transducers were positioned 100mm upstream and downstream to measure potential pressure drop across the test-section during experiment. Changes in loop flowrate would result in variations in system pressure. Transducers were used as means of validating flowrate changes indicated by the Flowtrak dial were local

disturbances only, ensuring the desired system flowrate was maintained for the duration of the experiment.

Resolution	16 bits + sign
Input range	±2.5 V
Sampling rate	1.5 samples per second
Accuracy	0 2%
Input connector	D25 female
Outputs	2 (fixed ±5 V references)

Table 2 3 - ADC-16 converter hardware specifications

2.7 Pico-log Software

The accompanying Pico-log software was installed onto the PC connected to the TC-08 and ADC-16 units. The software continuously monitored readings from the active thermocouple channels and pressure transducers Software was complete with Pico-recorder and Pico-player applications

Pico-recorder was used to record data while Pico-player allowed the user to scroll quickly through stored files to compare previous results Pico-recorder monitored data in real-time modes providing continuous recording over long periods of experiment Pico-log allowed the user to record as many samples as possible or a single sample across a recording interval By recording as many samples as possible, Pico-log saved an average of readings across the interval thereby providing accurate results of a system that in this case was dynamically changing.

Chapter 3 Results and Discussion

3.1 Introduction to Analysis

Results are presented for a thermal analysis of pharmaceutical dead-legs Results include dead-leg temperature profiles recorded over time for varied dead-leg lengths and branch diameters across a range of loop distribution velocities

Preliminary results are presented detailing initial difficulties encountered with experimental techniques The resolutions of these initial problems are discussed.

Final results are presented for a thermal analysis of 6d, 4d and 2d equal and reduced branch diameter tee configurations Results include;

- Evaluation of the effect of main loop velocity and branch diameter upon dead-leg end temperature
- Evaluation of thermal profiles with respect to temperature, time and profile pattern.
- Detailed discussion of suitable thermal dead-leg conditions with respect to branch diameter and length.
- Evaluation of comparable dead-leg fluid and branch surface temperatures in equal diameter dead-legs

A thermo-fluid analysis of pipe dead-legs is presented based upon experimental data retrieved from an experimental fluids rig.

Analysis of temperature limits with respect to dead-leg configuration is presented Recommendations regarding dead-leg sanitization based upon heating times and maximum achievable temperatures are set forth An investigation of the application of non-intrusive analysis within equal diameter dead-legs is performed

3.2 Preliminary Experimentation

All preliminary results are based upon data recorded during experimental runs performed using the fluid rig, testing and data acquisition techniques described in the Equipment & Materials section previous.

Dead-leg temperature T_d, represents fluid temperature recorded at the base of a dead-leg Figure 3 1 displays loop temperature T_L and dead-leg temperature profiles A and B recorded for separate experiment runs with respect to time Profiles represent data recorded over a 10800s (3 hour) sample period with temperature recorded in 1 second intervals Time zero signifies the instance heating was activated in the system with thermal profiles representing temperature recorded every 5 minutes

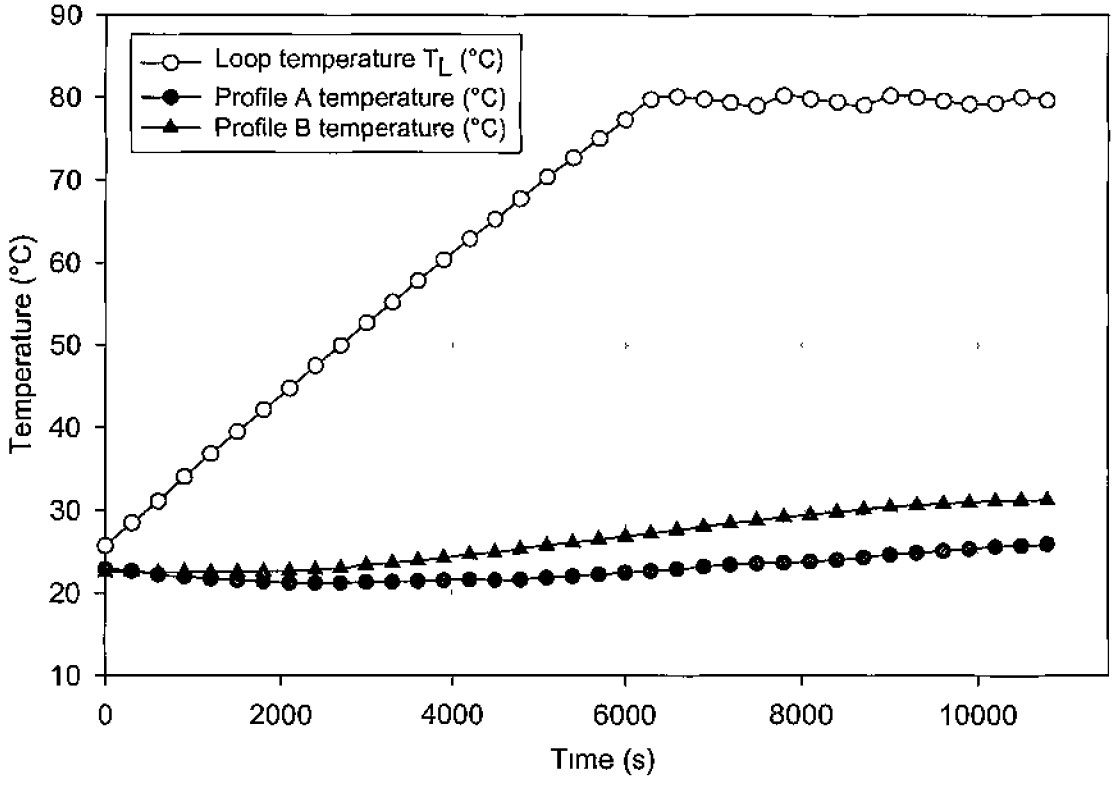

Figure 3 1 - Loop temperature profile and contrasting responses of T_d

The dead-leg temperature T_d recorded for both profiles at fixed time intervals during the experiment run are shown in table 3.1 Temperature is shown to vary between profiles with respect to time. Loop flowrate recorded for profile A decreased by 25%

over the duration of the experiment The required flowrate was maintained for profile B At this stage it was deemed necessary to remove all major flowrate loss from further experimentation to ensure both accuracy and continuity of results

Following investigation it was determined that trapped pockets of air escaping from loop pipework during system ramp-up to set-point temperature contributed to drops in volumetric flowrate. As such, prior to each experiment run a complete and thorough purging cycle was performed to remove all entrapped air from the system. The purge cycle consisted of slowly increasing system flowrate by set increments, along with visual inspection of the storage tank for evidence of air bubbles escaping from the pipe exit line Once the system had been fully purged of air, flowrate was adjusted to required levels and inspected periodically for change.

Time, t (s)	Dead-leg Temperature, T_d (°C)	
	Profile A	Profile B
1	22 92	22 52
1800	21 38	22 63
3600	21 45	23 95
5400	22.03	26 11
7200	23.43	28 43
9000	24.62	30 41
10800	25 89	31.26

Table 3.1 - Thermal data of contrasting profile responses of T_d

The profile of loop temperature T_L shown in figure 3 1 represents fluid temperature measured by a T-type thermocouple positioned on the outlet pipe of the centrifugal pump This thermocouple records temperature in the distribution loop post storage vessel where fluid is heated to required temperatures.

The TDF 11 unit controls system temperature based upon an ON/OFF heating mechanism. Heating occurs according to a fixed set-point (80°C), with a user specified negative differential switching point, $-\delta$ Figure 3.2 illustrates the ON/OFF heating mechanism and resultant temperature response The differential switching

point is defined as the decrease in temperature necessary to reactivate heating once system set-point temperature has been achieved.

This ON/OFF heating process is reflected in the periodic profile response of loop temperature represented in figure 3 1 once set-point temperature of 80°C is achieved This response was accepted as being inherent within the system and consideration was taken toward this profile response for all experiment results The differential value, δ, was shown to remain below 1.6°C for all experimentation.

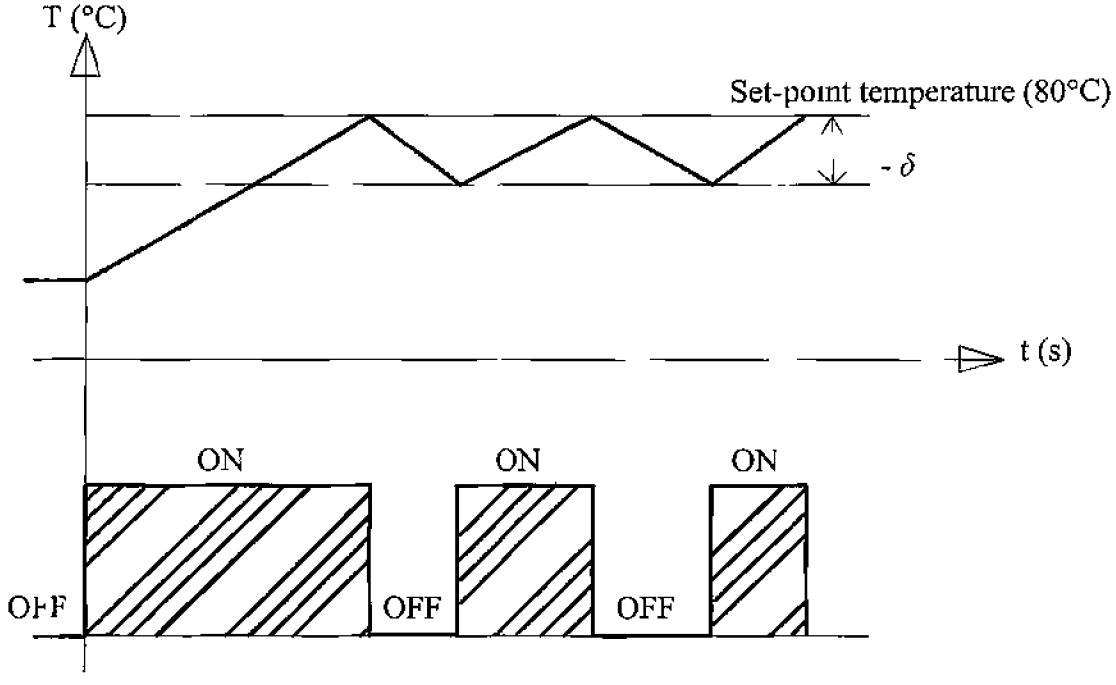

Figure 3 2 - Negative differential heating and temperature response

3.3 Final Experimental Analysis

Having resolved preliminary testing issues, final experimentation and analysis proceeded All experimentation was performed using the fluid rig, testing equipment and data acquisition techniques detailed in the Equipment & Material section previous Thermal data was recorded for equal and reduced branch diameter dead-legs of varying branch length across a range of distribution loop velocities

Distribution loop flowrate was converted to bulk loop velocity U_b based upon volumetric flowrate and internal pipe diameter Reynolds Number calculated for all velocities (see Appendix B) represented flow in the turbulent regime [48]. Bulk loop velocities and corresponding Reynolds Numbers are shown in table 3 2

Volumetric Flowrate, Q (L/min)	**Velocity, U_b (m/s)**	**Reynolds Number, *Re* (-)**
20	0 19	2.33×10^4
40	0 37	$4\ 65 \times 10^4$
60	0 56	$6\ 98 \times 10^4$
100	0 94	$1\ 16 \times 10^5$
120	1 12	1.39×10^5
160	1.50	$1\ 86 \times 10^5$

Table 3.2 - Conversion of flowrates to velocity and Reynolds Number

3.3.1 Temperature Profile Analysis

Results are presented of data recorded for experimental runs as per the recording conditions outlined for preliminary analysis Ambient air temperature was 21 ± 1°C for all experimental runs Heater control set-point was fixed at 80°C Results are presented as per branch configuration (see also Appendices C & D)

Part A: Equal Diameter Dead-leg Analysis

The geometries of dead-leg configurations used as part of this analysis are described in table 3 3.

Diameter	Branch Lengths
- D = d	- 6d (300mm)
- 50mm OD	- 4d (200mm)
- 47 5mm ID	- 2d (100mm)

Table 3 3 - Equal diameter dead-leg configurations

3.3.1.1 6d Equal Diameter Dead-leg

Figure 3.3 presents thermal profiles of loop temperature T_L and dead-leg temperature T_{d6} with respect to time for loop velocity 0.19m/s T_{d6} represents the temperature recorded at the base of the 6d dead-leg.

The profile of loop temperature follows two distinct phases. From ambient, fluid temperature increases or ramps in a controlled linear manner. Once set-point temperature is achieved, loop fluid maintains a steady-state temperature of 79 15 ± 1°C for the remainder of the run These characteristics of distribution loop temperature were shown to be similar for all loop velocities.

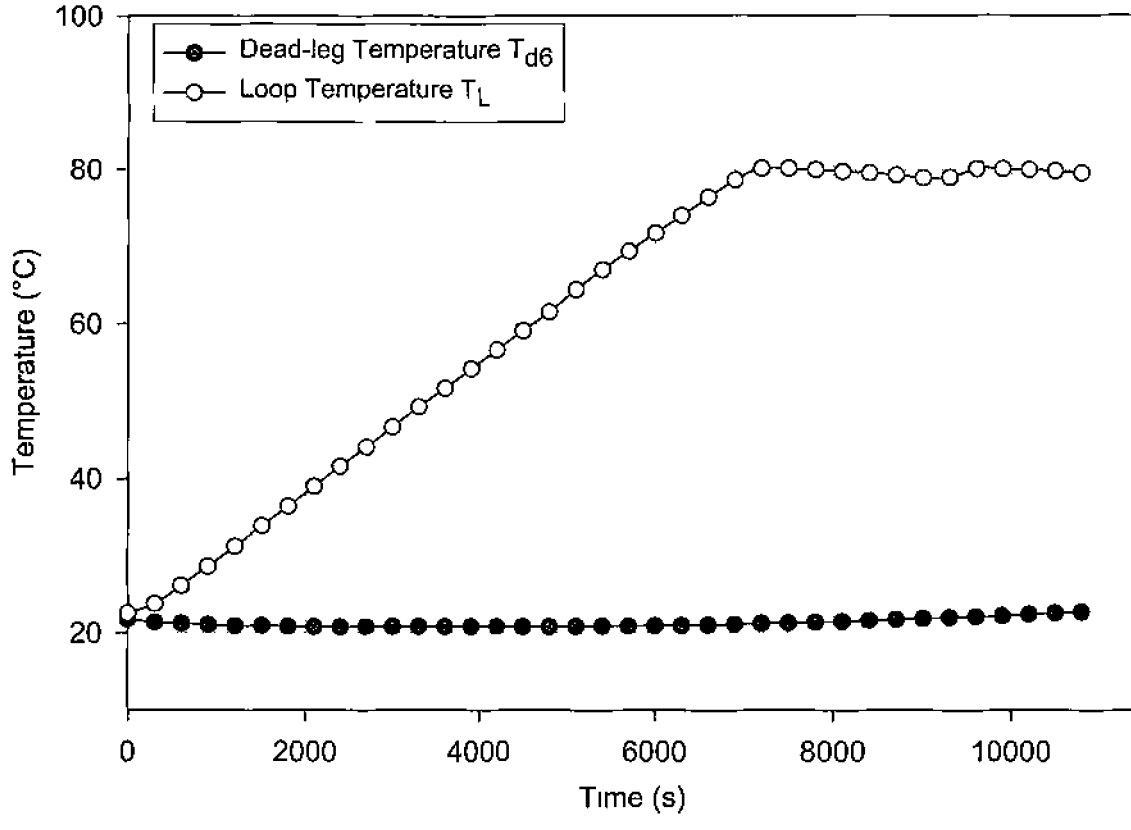

Figure 3 3 - Profile of T_{d6} for $U_b = 0$ 19m/s

T_{d6} shows minimal temperature increase for the duration of the experiment From initial temperature 21 74°C, fluid at base of the dead-leg achieves a minimum of 20 78°C after 2400s. T_{d6} increases overall by 0 98°C at constant loop velocity indicating a poor standard of mixing between loop fluid and fluid at the base of the dead-leg for this flowrate Lack of turbulent mixing contributes to a decrease from initial temperature during the course of the experiment

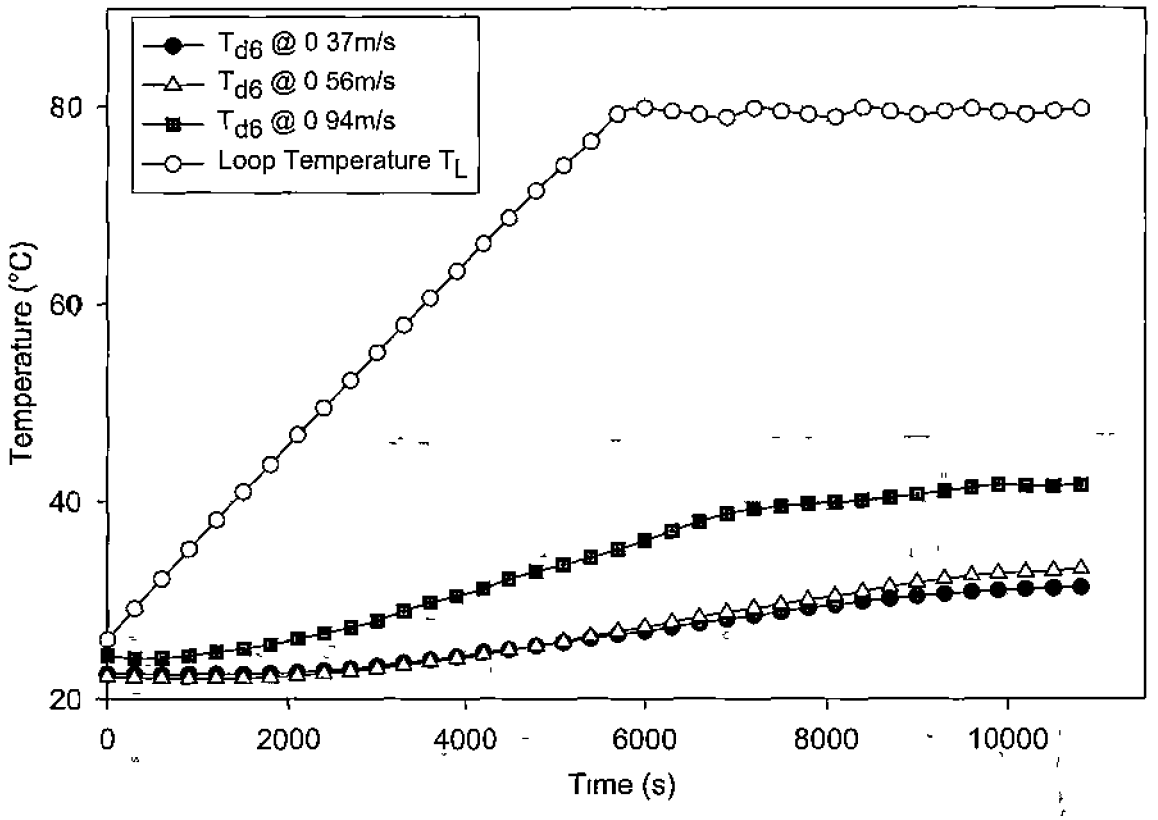

Figure 3 4 - Profiles of T_{d6} for U_b = 0.37, 0 56 and 0 94m/s

Profiles of dead-leg temperature for loop velocities 0 37, 0 56 and 0 94m/s are presented in figure 3.4 All profiles follow smooth increasing patterns From initial temperatures, T_{d6} shows increases of 8.74 and 10 83°C for loop velocities 0 37 and 0.56m/s respectively Improved dead-leg temperatures are evident for 0.94m/s velocity, T_{d6} increases by 17 21°C over the duration of the experiment

Increase in loop velocity from 0.37 to 0 56m/s does not result in significant increase in temperature at the base of the dead-leg. The steady manner of temperature increase over the experiment suggests constant diffusive transfer of loop fluid into the dead-leg branch at these velocities

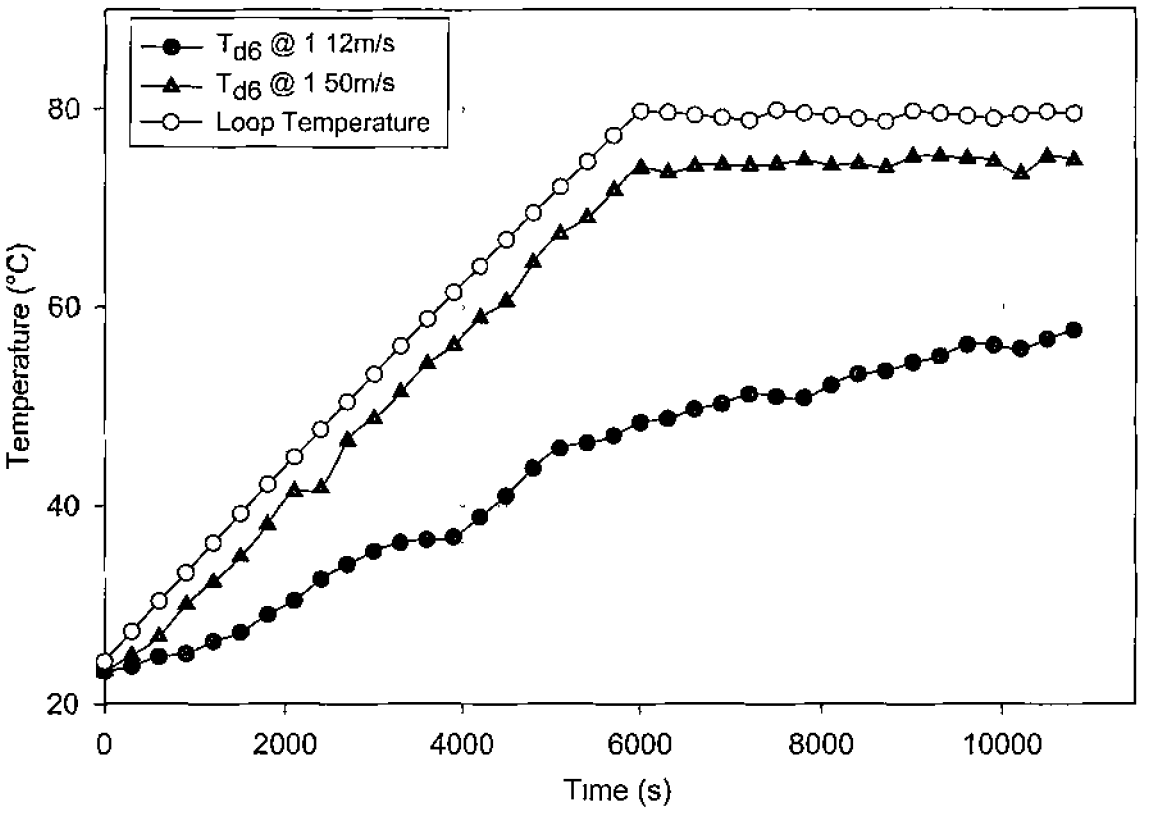

Figure 3 5 - Profiles of T_{d6} for U_b = 1 12 and 1 50m/s

Temperature profiles for loop velocities 1 12 and 1 50m/s are presented in figure 3.5. Both profiles exhibit non-linear heating patterns From ambient temperature, T_{d6} increases by 34 35°C across the experiment for fixed loop velocity 1.12m/s Fluctuations in T_{d6} are however evident Sudden decreases followed by subsequent increases in temperature are noted at 3900, 7800 and 10200s The dynamic mixing of warm and cooler fluids along the base of the dead-leg may have resulted in sudden changes in T_{d6}. Research has shown greater loop velocity contributes to the increased magnitude of recirculating fluid motion in the dead-leg branch [44]

The thermal profile of T_{d6} for loop velocity 1 50m/s shows an increase in temperature close to that of loop set-point T_{d6} exhibits approximately linear increase, reaching steady-state temperature close to loop set-point at 6000s. T_{d6} increases by 51 5°C over the duration of the experiment The temperature profile

indicates improved fluid transfer from main loop into the branch and along the base of dead-leg

However fluctuations in T_{d6} suggest non-uniform flow within the branch. Reductions in temperature are noted at 2400 and 10200s which indicate the rate of fluid flow at the base of the dead-leg varies and is velocity dependent Sudden decreases in temperature imply the disturbance of cooler fluid at the base of the branch.

Table 3 4 displays the maximum temperatures recorded at the base of the dead-leg per distribution loop velocity. Data indicates an increase in maximum temperature with respect to increased loop velocity The maximum dead-leg temperature recorded for the 6d equal diameter branch configuration was 75 14°C for loop velocity of 1 50m/s T_{d6} did not achieve distribution loop temperature 79 15 ± 1°C across the velocity range

Velocity, U_b (m/s)	Maximum T_{d6} (°C)
0 19	22 72
0.37	31.26
0.56	33 08
0 94	41 64
1 12	57 60
1 50	75 14

Table 3 4 - Maximum temperatures recorded for 6d equal diameter dead-leg

Temperature profiles for $U_b \leq 0.56$m/s suggest minimal fluid transfer into the base of the dead-leg branch. These profiles follow controlled increasing patterns indicating no turbulent fluid flow at 6d depths. Temperature increases for $U_b \leq 0.56$m/s are nominal; maximum temperatures remaining significantly lower than distribution loop temperatures Results indicate the primary mechanism of heat transfer into the dead-leg is diffusion at this velocity range

Improved fluid transfer within the branch is evident for $U_b \geq 1$ 12m/s Results indicate temperatures approaching loop set-point with respect to increased Reynolds Number Thermal profiles follow non-linear patterns with fluctuations in temperature

evident The primary mechanism of heat transfer at this velocity range is forced convection as higher velocity fluid from the loop carries warm fluid into the dead-leg branch However such fluid transfer is non-linear as demonstrated by fluctuations in the rate of temperature increase

Further insight into the standard of mixing occurring within the dead-leg branch is provided by examining in detail thermal profiles during system heating Figure 3 6 illustrates temperature profiles of T_{d6} for loop velocities 1 12 and 1 50m/s recorded from 4500s to 5500s

T_{d6} follows a fluctuating pattern for loop velocity 1.50m/s with an increase of 10 4°C across the 1000s sample period recorded. Applying moving average calculations temperature is shown to fluctuate by ± 1 6°C.

The temperature profile for loop velocity 1.12m/s shows contrasting flow characteristics T_{d6} shows only marginal increase of 5 42°C over the sample period Based upon a moving average, T_{d6} shows minimal temperature fluctuations of ± 0.47°C.

Significant temperature fluctuations at the base of the dead-leg at 1 50m/s indicate the presence of turbulent mixing The magnitude of turbulence is a result of high velocity fluids entering the branch from main loop Forced convection becomes the primary mechanism of heat transfer to the base of the branch. With respect to 1.12m/s, temperature increase occurs primarily via the diffusion of warmer fluids into the branch from main loop flow The linear temperature profile indicates steady non-turbulent fluid transfer along the base of the dead-leg at this loop velocity

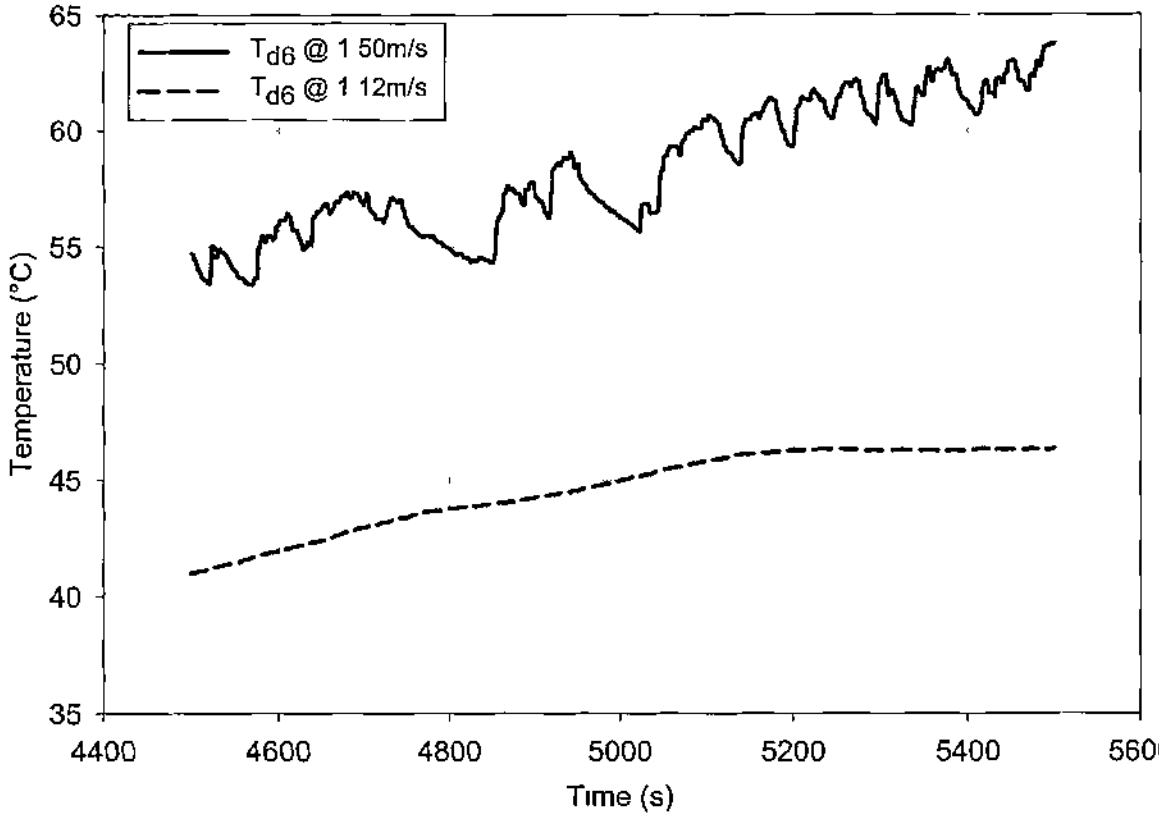

Figure 3.6 - Profiles of T_{d6} over reduced sample period for U_b = 1 12 and 1 50m/s

Results indicate the mechanism of heat transfer along the base of the branch contributes to the magnitude of heating taking place At lower flowrates diffusion is the main contributor to temperature increase compared with convection at higher flowrates Research has indicated that the depth of branch turbulence from loop fluid is directly proportional to the velocity at the inlet of the dead-leg [26] As demonstrated therefore (see table 3.4), increased temperatures are recorded with respect to increased loop velocity

3.3.1.2 4d Equal Diameter Dead-leg

Figure 3 7 presents the temperature profiles recorded for loop temperature T_L and dead-leg temperature T_{d4} at loop velocities 0 19 and 0 37m/s. T_{d4} represents the temperature recorded at the base of the 4d dead-leg

For loop velocity 0 19m/s, T_{d4} follows a smooth increasing profile Temperature at the base of the dead-leg increases by 17 95°C from ambient temperature The controlled manner of temperature increase indicates lack of turbulent mixing

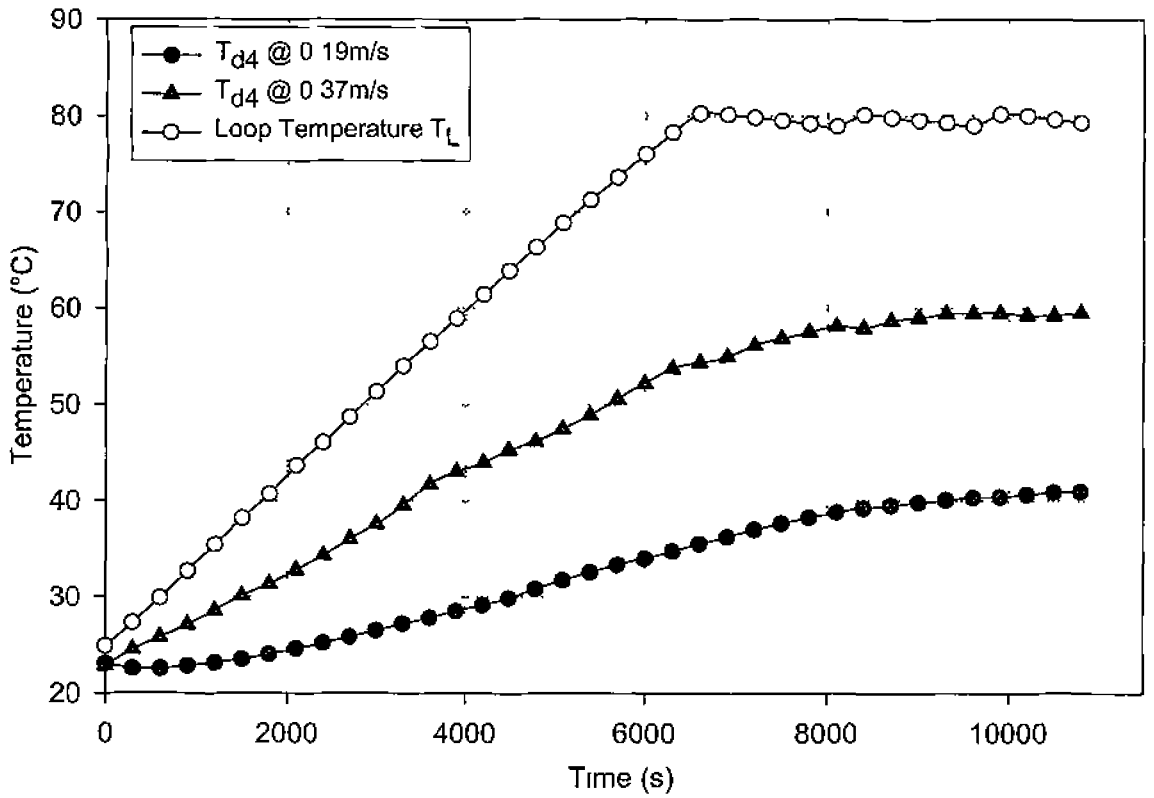

Figure 3.7 - Profiles of T_{d4} for $U_b = 0.19$ and 0.37m/s

Similar fluid transport mechanisms are evident for loop velocity 0.37m/s The profile of dead-leg temperature T_{d4} follows a controlled pattern, increasing by 36.74°C over the experiment Intermittent changes in temperature response are however evident. Decreases in T_{d4} are noted at 4200, 6600 and 8400s indicating dynamic fluid flow along the base of the 4d dead-leg. Such temperature changes may allude to the presence of pulsating fluid flow.

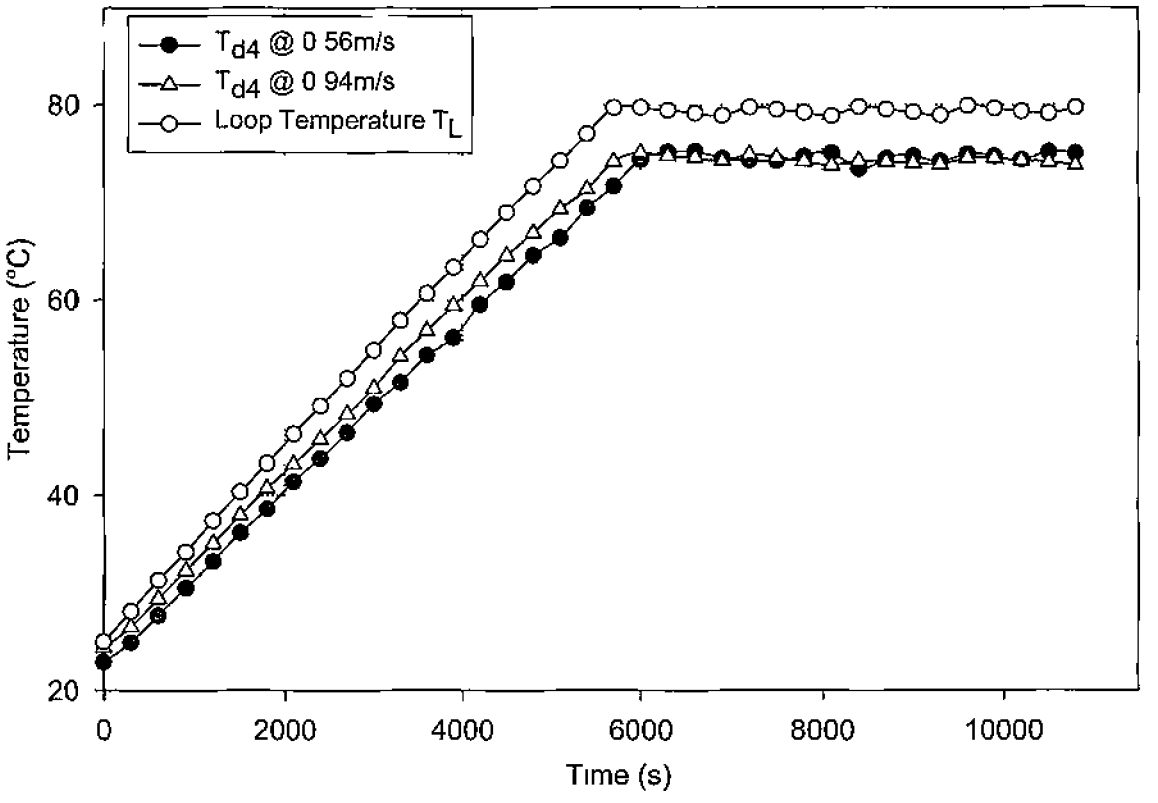

Figure 3 8 - Profiles of T_{d4} for U_b = 0 56 and 0 94m/s

Figure 3 8 presents temperature profiles for loop velocities 0 56 and 0 94m/s Both profiles follow similar patterns indicating comparable heating mechanisms. Profiles demonstrate linear heating ramp-up and steady-state temperature phases similar to the characteristic profile of the main loop

Similar maximum temperatures (see table 3.5) are recorded for both velocities yet differences exist between times taken to reach steady-state temperature. At loop velocity 0 56m/s, T_{d4} reaches steady-state temperature after 6000s compared to 6300s for loop velocity 0 94m/s Achieving steady-state temperature over a reduced time length would indicate comparably enhanced fluid transfer with respect to the increased loop velocity

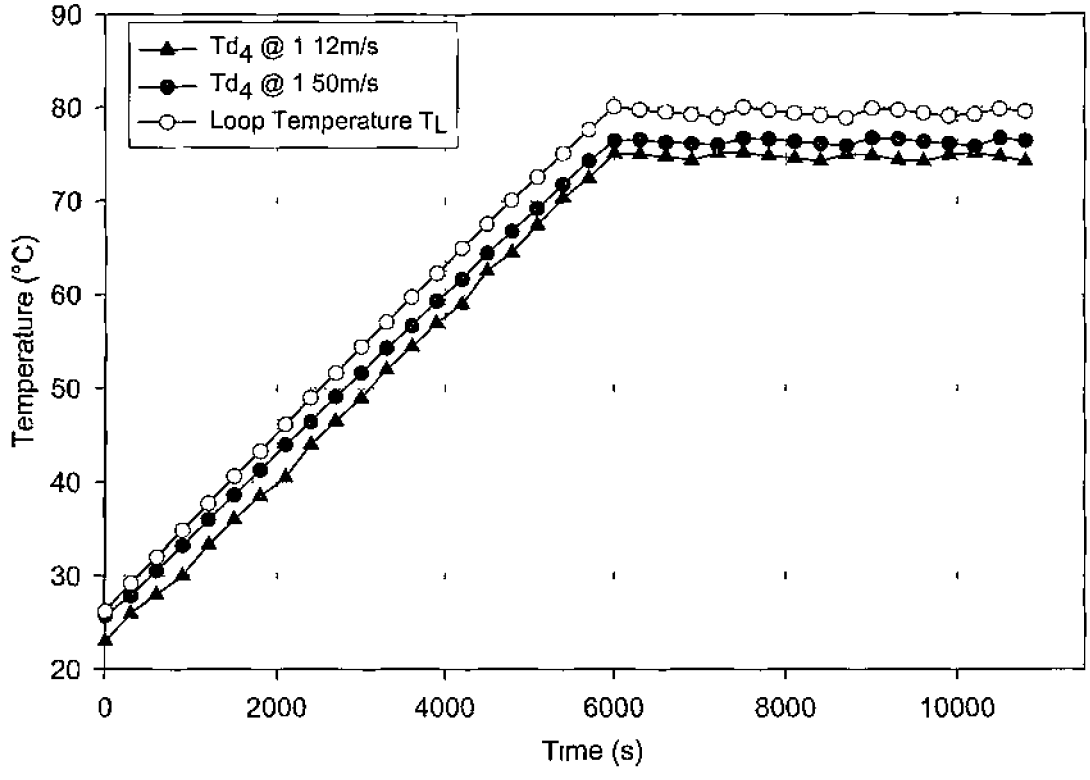

Figure 3.9 - Profiles of T_{d4} for U_b = 1.12 and 1.50m/s

Figure 3 9 illustrates temperature profiles for loop velocities 1 12 and 1 50m/s Profiles exhibit similar characteristics to main loop temperature indicating significant fluid transfer between the main loop and dead-leg branch T_{d4} reaches steady-state temperature at 6000s for both velocities.

Table 3.5 details maximum temperatures recorded at the base of the 4d equal diameter dead-leg per loop velocity Increases in maximum temperature at the base of the dead-leg are recorded with respect to increased loop velocity This confirms the relationship between loop velocity and dead-leg temperature shown for the 6d dead-leg configuration. The maximum recorded temperature in the equal diameter 4d dead-leg was 76 74°C for loop velocity 1.50m/s. Loop temperature set-point of 79.15 ± 1°C was not achieved across the distribution loop range

Velocity, U_b (m/s)	Maximum T_{d4} (°C)
0 19	40.98
0 37	59.55
0.56	75 22
0 94	75 08
1 12	75 22
1 50	76 74

Table 3.5 - Maximum temperatures recorded for 4d equal diameter dead-leg

Similar maximum temperatures are noted for $U_b \geq 0$ 56m/s This would suggest a thermal threshold is achieved with respect to increasing distribution loop velocity Further increases in loop velocity may not contribute to improved temperatures within the dead-leg

Figure 3.10 represents temperature profiles for T_{d4} recorded between 4500 and 5500s at loop velocities of 0.56 and 0 94m/s Temperature T_{d4} fluctuates significantly across the sample range with respect to loop velocity 0 56m/s, suggesting convective mixing of warmer and cooler fluid at the base of the dead-leg A temperature increase of 8 29°C is recorded across the sample range, with significant fluctuations of ± 1 3°C from a moving average noted

The temperature profile of T_{d4} for loop velocity 0.94m/s shows an increase of 7 96°C at the dead-leg base across the sample range. The profile of T_{d4} follows a quasi-linear pattern suggesting steady heat transfer Temperature at the dead-leg base fluctuates by ± 0 3°C for a moving average

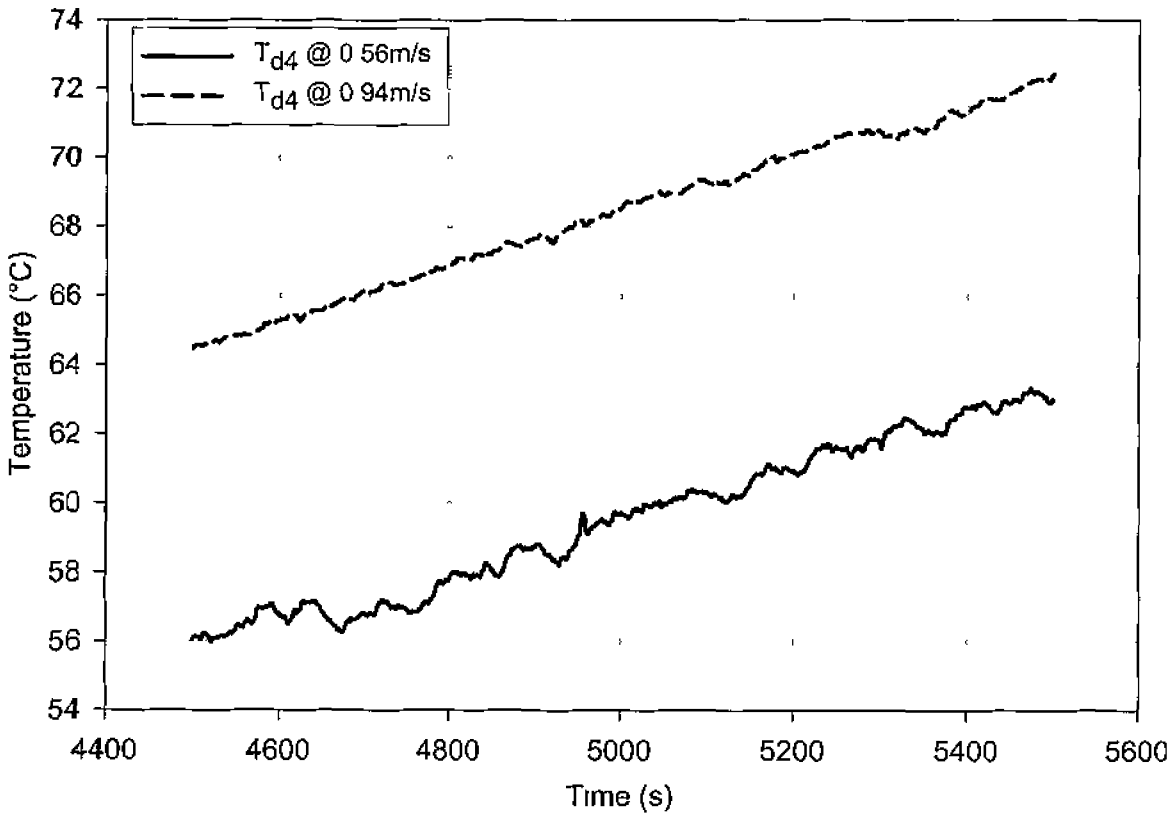

Figure 3 10 - Profiles of T_{d4} over reduced sample period for U_b = 0.56 and 0 94m/s

Results indicate similar magnitudes of heating with respect to velocities across the reduced sample range Yet profiles indicate a transition from fluctuating to linearly increasing temperatures with respect to increased loop velocity

This transition from dynamic to predominantly linear heat transfer is a result of improved mass transfer occurring with respect to increased branch inlet velocity. The turbulent mixing contributing to forced convective heat transfer for 0.56m/s is not sufficient to completely remove cooler stagnant fluid from the base of the branch Increased inlet velocity 0.94m/s does result in a sweeping action at the dead-end exacting a more rigorous re-circulation of warm loop fluids through the entire branch length

3.3.1.3 2d Equal Diameter Dead-leg

Temperature profiles of T_{d2} for loop velocities 0.19 and 1 50m/s are shown in figure 3 11. Profiles represent T_{d2}, the temperature at the base of the 2d dead-leg at high and low distribution loop velocities.

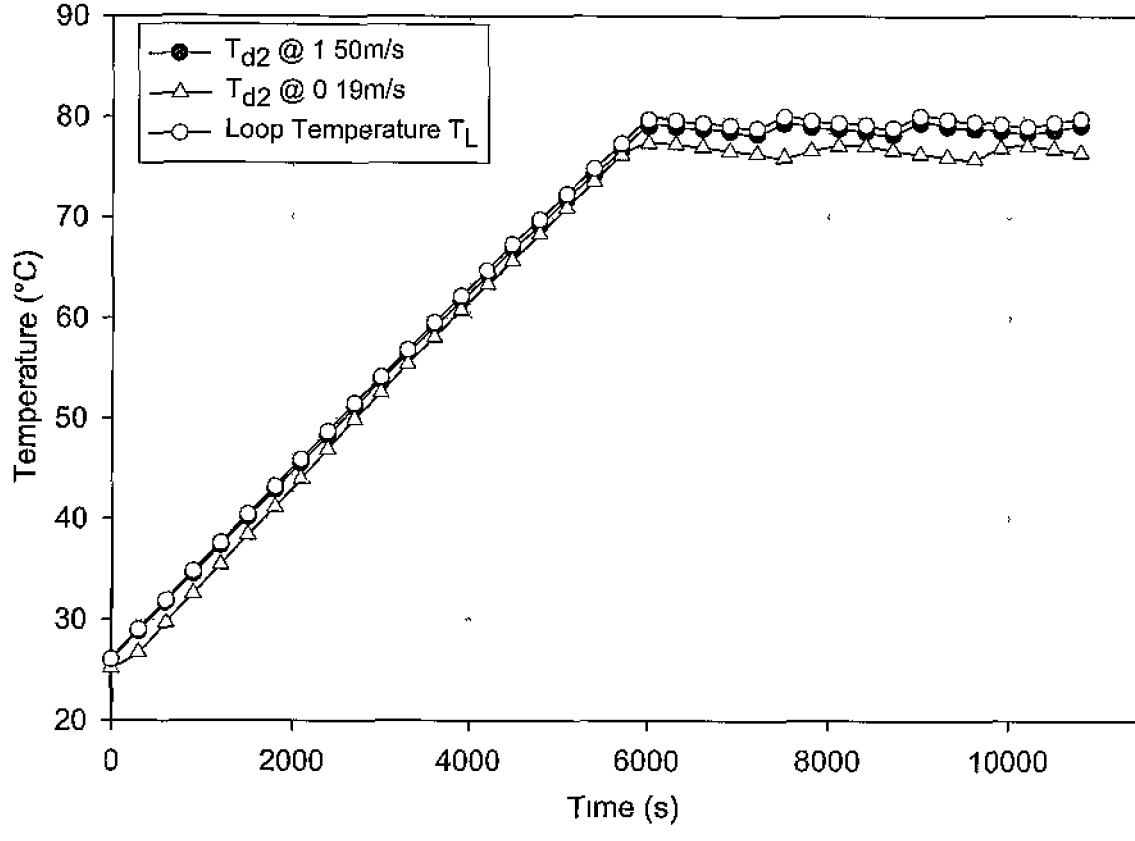

Figure 3.11 - Profiles of T_{d2} for U_b = 0.19 and 1.50m/s

Both profiles follow patterns consistent with the characteristic profile of loop temperature. This is indicative of a significant degree of mass transfer occurring between loop and branch fluid Table 3 6 details maximum temperatures recorded at the base of the 2d dead-leg with respect to loop velocity. T_{d2} is shown to increase with respect to loop velocity as with previous dead-leg configurations Loop temperature set-point 79.15 ± 1°C was achieved and maintained at the base of the 2d dead-leg for loop velocity 1 50m/s after 6000s

Both loop velocities contribute to fluid temperature at the base of the 2d dead-leg close to that of main loop flow. Fluid flow characteristics are comparable for both profiles as demonstrated by the time taken to reach steady-state temperature (6000s)

Velocity, U_b (m/s)	Maximum T_{d2} (°C)
0.19	77 40
1.50	79 45

Table 3 6 - Maximum temperatures recorded for 2d equal diameter dead-leg

The periodic response of loop temperature at steady-state initiates a similar thermal response at the base of the 2d dead-leg for both velocities T_{d2} for loop velocity 0 19m/s however displays a slower response to main loop temperature fluctuations, illustrated by the increased duration between temperature maximums in the loop and dead-leg Increased response lag with respect to reduced loop velocity indicates a slight reduction in the scale of fluid transfer into the dead-leg branch.

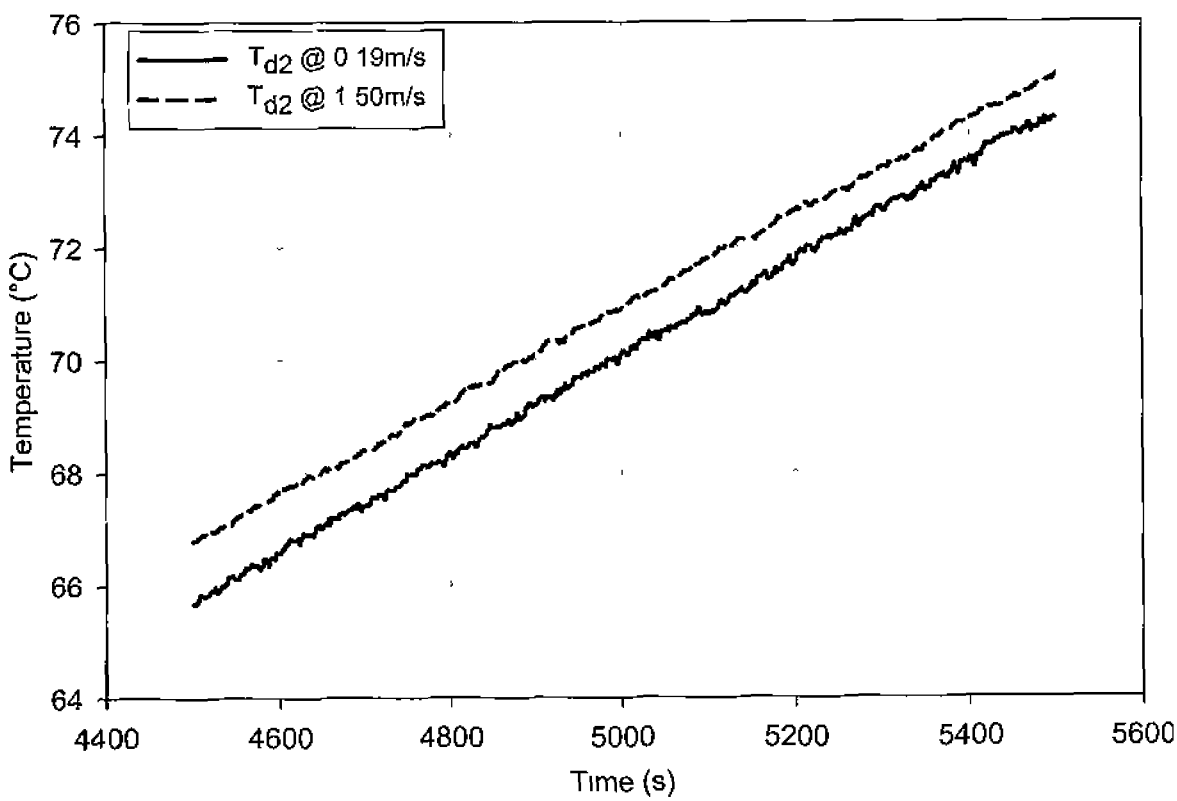

Figure 3 12 - Profiles of T_{d2} over reduced sample period for U_b = 0.19 and 1 50m/s

Figure 3 12 displays temperature profiles for selected velocities in the 2d dead-leg branch for 4500s to 5500s Both velocities exhibit linear heat transfer at the base of the branch with slight variances in temperature evident Fluid temperature increases by 8 62 and 8 27°C across the sample range at velocities 0 19 and 1.50m/s respectively. Based upon a moving average, temperatures fluctuations of ± 0 4°C and ± 0.5°C are recorded for loop velocities 1 50 and 0.19m/s respectively

Part B: Reduced Diameter Dead-leg Analysis

Reduced diameter tee-sections are installed in HPWS at point-of-use instances and for particular instrumentation connection Thermal profiles are presented for reduced branch diameter dead-legs, geometries as per table 3.7. Figure 3.13 illustrates the geometric transition from equal to reduced diameter dead-legs.

Diameter	Branch Length
- D ≠ d	- 6d (150mm)
- 50mm OD	- 4d (100mm)
- 47.5mm ID	- 2d (50mm)
- 25mm od	
- 22.5mm id	

Table 3.7 - Reduced diameter dead-leg configurations

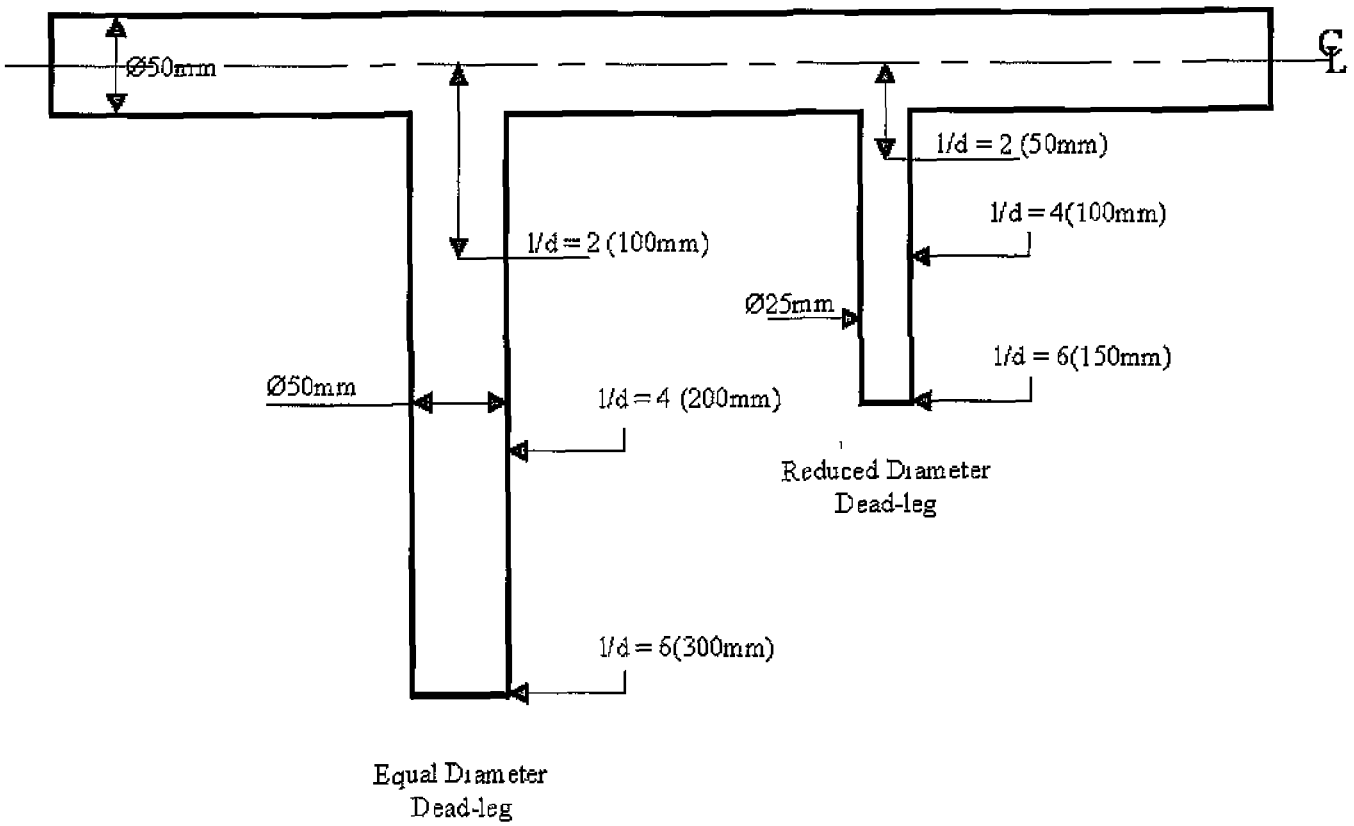

Figure 3 13 - Comparison of equal and reduced dead-leg geometries

3.3.1.4 6d Reduced Diameter Dead-leg

Figure 3.14 presents profiles of loop temperature T_L and dead-leg temperature T_{d6} with respect to time for loop velocity 0 19m/s. T_{d6} represents fluid temperature recorded at the base of the 6d dead-leg. The loop temperature profile follows the characteristic curve described previous with temperatures 79 15 ± 1°C maintained at steady-state for all experimental analysis

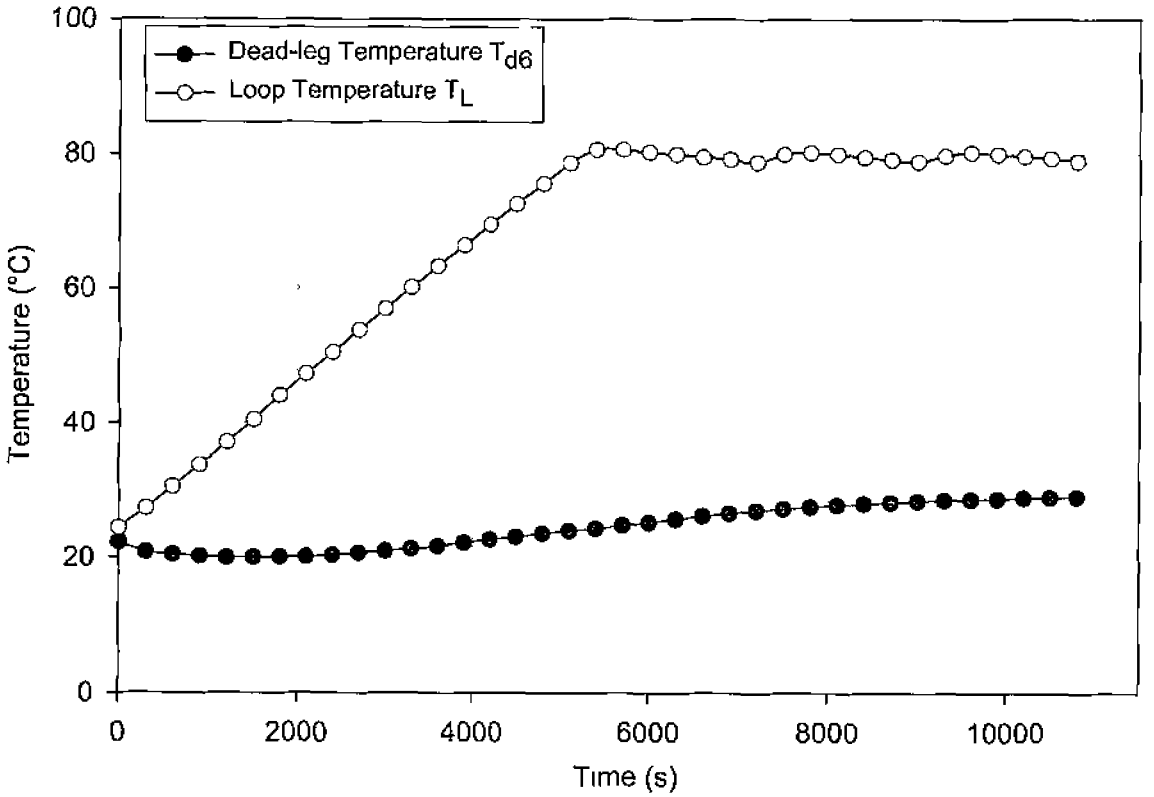

Figure 3 14 - Profile of T_{d6} for U_b = 0 19m/s

T_{d6} shows nominal increase over the duration of the experiment From initial temperature 22 27°C, fluid at the base reaches a minimum 20 04°C after 1500s T_{d6} shows only marginal increase of 6.81°C across the experiment suggesting negligible mixing between fluid within the distribution loop and that at the dead-leg base.

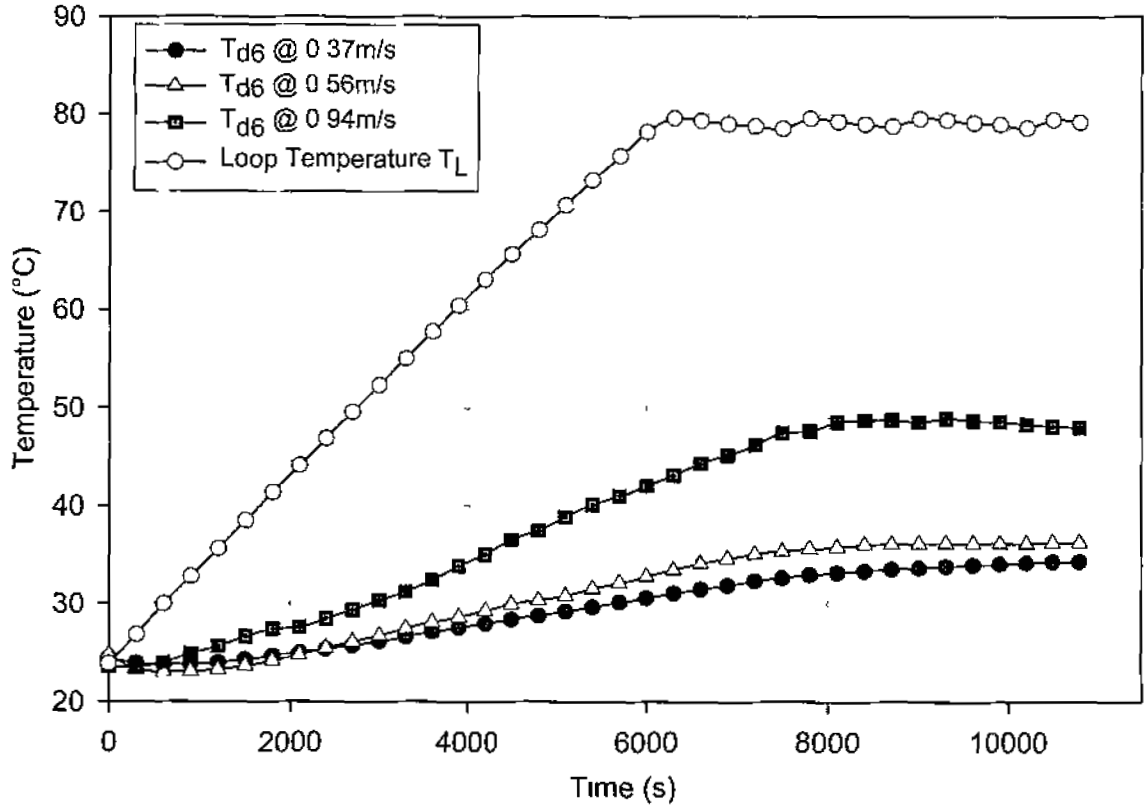

Figure 3 15 - Profiles of T_{d6} for U_b = 0.37, 0 56 and 0 94m/s

Figure 3.15 displays profiles of T_{d6} over increased loop velocities Thermal profiles demonstrate increased temperatures at the base of the dead-leg with respect to increased main loop velocity.

Similar temperatures are recorded for velocities 0 37 and 0 56m/s with increases in T_{d6} of 9.89 and 11 53°C recorded respectively over the experiment. The similarity of profile patterns suggest comparable standards of mixing within the branch for both velocities The steady transient increase illustrated by T_{d6} would indicate primarily diffusional heat transfer to the dead-leg base at these velocities

Improved mixing at the base of the dead-leg is evident with respect to increased loop velocity 0.94m/s T_{d6} increases by 24.37°C from initial temperature over the experiment Although the profile of T_{d6} follows a similar pattern to that of the previous velocities, temperature decrease post thermal maximum is noted This

indicates a reduction in the scale of fluid transfer to the base of the branch as a result of non-uniform fluid flow Previous results (see Part A) for equal diameter sections also suggested the occurrence of non-linear heat transfer within a dead-leg branch at fixed velocities.

As shown in figure 3.16 the profile of T_{d6} indicates improved mixing for $U_b \geq$ 1.12m/s The profile of T_{d6} at loop velocity 1 12m/s follows a non-linear pattern during ramp-up followed by considerable fluctuations once loop set-point temperature is achieved. The manner of fluid flow into the branch contributing to an increase in T_{d6} is non-uniform as suggested by the temperature decreases at 7800s and 9000s

The profile of T_{d6} for loop velocity 1 50m/s closely follows that of loop temperature indicating a strong transfer of fluid from loop to dead-leg base Although non-linear, the profile of T_{d6} clearly exhibits a ramp-up heating phase and quasi-steady state.

Further indication of non-uniform fluid flow within the dead-leg branch is evident with notable changes in the rate of temperature increase during ramp-up. The profile of T_{d6} exhibits increases and subsequent decreases in temperature at 2100s and 3000s respectively. Such thermal activity is conjugative to the presence of pulsating fluid flow at the base of the branch contributing to sudden temperature increase Pulsating fluid flow would contribute to the disturbance of cooler fluids along the base of the branch resulting in temperature fluctuation

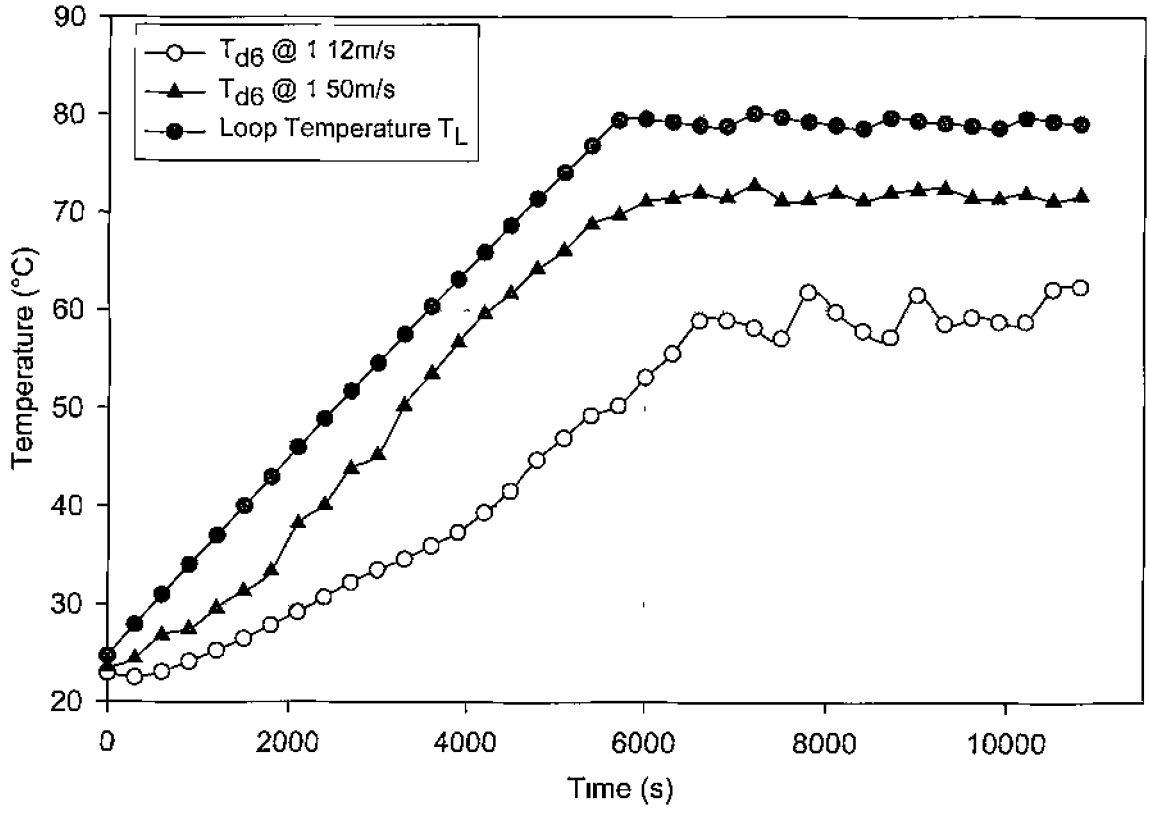

Figure 3 16 - Profiles of T_{d6} for U_b = 1 12 and 1 50m/s

Figure 3.17 displays the temperature response at the base of the 6d reduced diameter dead-leg with respect to a sample time of 4500 to 5500s at loop velocities 1.12 and 1.50m/s Loop velocities provide contrasting thermal responses at the base of the branch. T_{d6} follows a fluctuating pattern with respect to loop velocity 1.50m/s with temperature varying by + 3 2°C based upon moving average calculations. An overall temperature increase of 8 62°C is recorded across the sample range.

In comparison T_{d6} follows a controlled steady state pattern for loop velocity 1.12m/s with an increase of 8.23°C recorded across the sample range Temperature at the base of the branch varies by ± 0 7°C based upon a moving average However sudden increases in temperature are noted at 4710 and 5325s Such temperature increases are again indicative of the pulsating flow of warmer fluid down the branch as opposed to sustained turbulent flow recorded for loop velocity 1 50m/s.

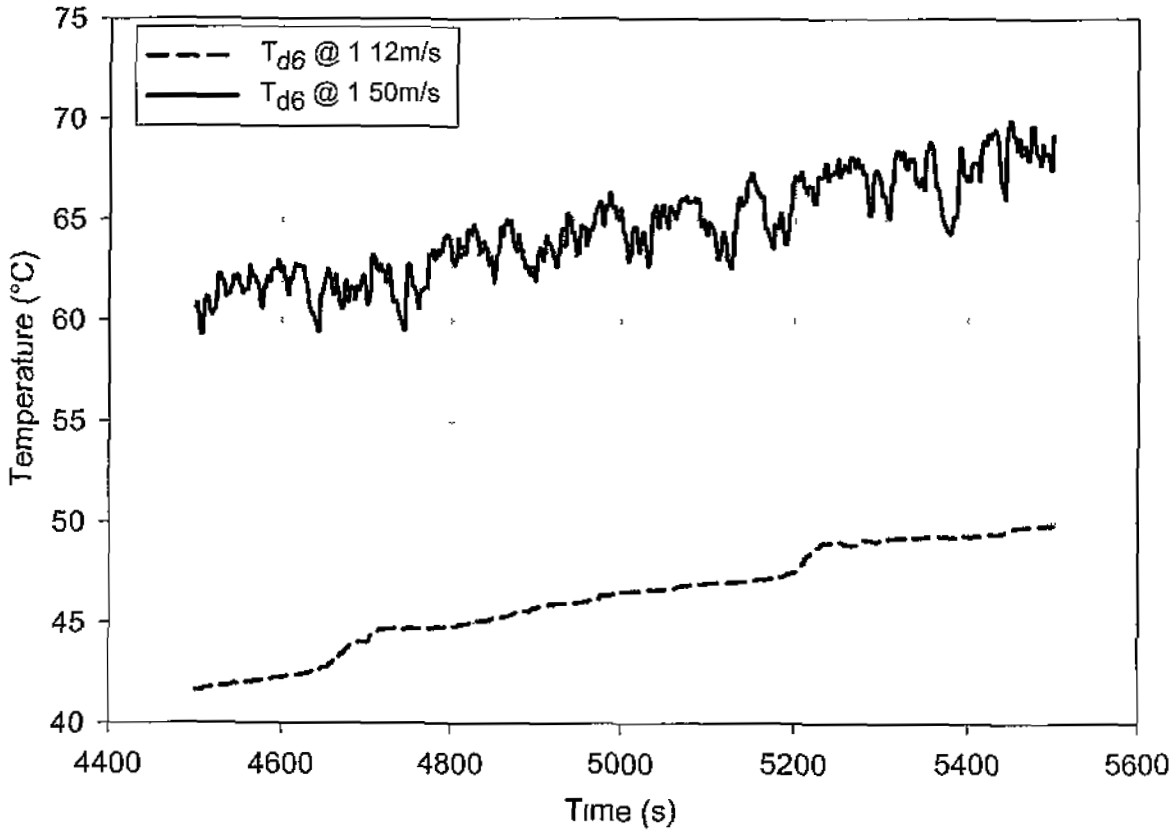

Figure 3.17 - Profiles of T_{d6} over reduced sample period for U_b = 1 12 and 1.50m/s

Neither loop velocity is capable of producing rigorous turbulent mixing at the base of the dead-leg branch The significant temperature fluctuations recorded for branch inlet velocity 1.50m/s suggest the inability of loop fluid to complete remove cooler fluid at the base of the branch

Table 3.8 displays maximum temperatures recorded at the base of the 6d reduced diameter dead-leg across the range of main loop bulk velocities

Velocity, U_b (m/s)	Maximum T_{d6} (°C)
0 19	29 08
0 37	34 33
0 56	36.28
0 94	48.97
1 12	62.46
1 50	72 77

Table 3 8 - Maximum temperatures recorded for 6d reduced diameter dead-leg

Data indicates a relationship between dead-leg temperature and increasing loop velocity Maximum temperatures at branch base improve with respect to increased Reynolds Number The highest temperature recorded in the 6d reduced diameter dead-leg is 72.77°C for loop velocity 1 50m/s. The desired temperature set-point of 79 15 ± 1°C was not achieved across the velocity range

3.3.1.5 4d Reduced Diameter Dead-leg

Figure 3.18 presents profiles recorded for loop temperature T_L and dead-leg temperature T_{d4} at loop velocities 0.19 and 0 37m/s. T_{d4} represents fluid temperature recorded at the base of the 4d dead-leg

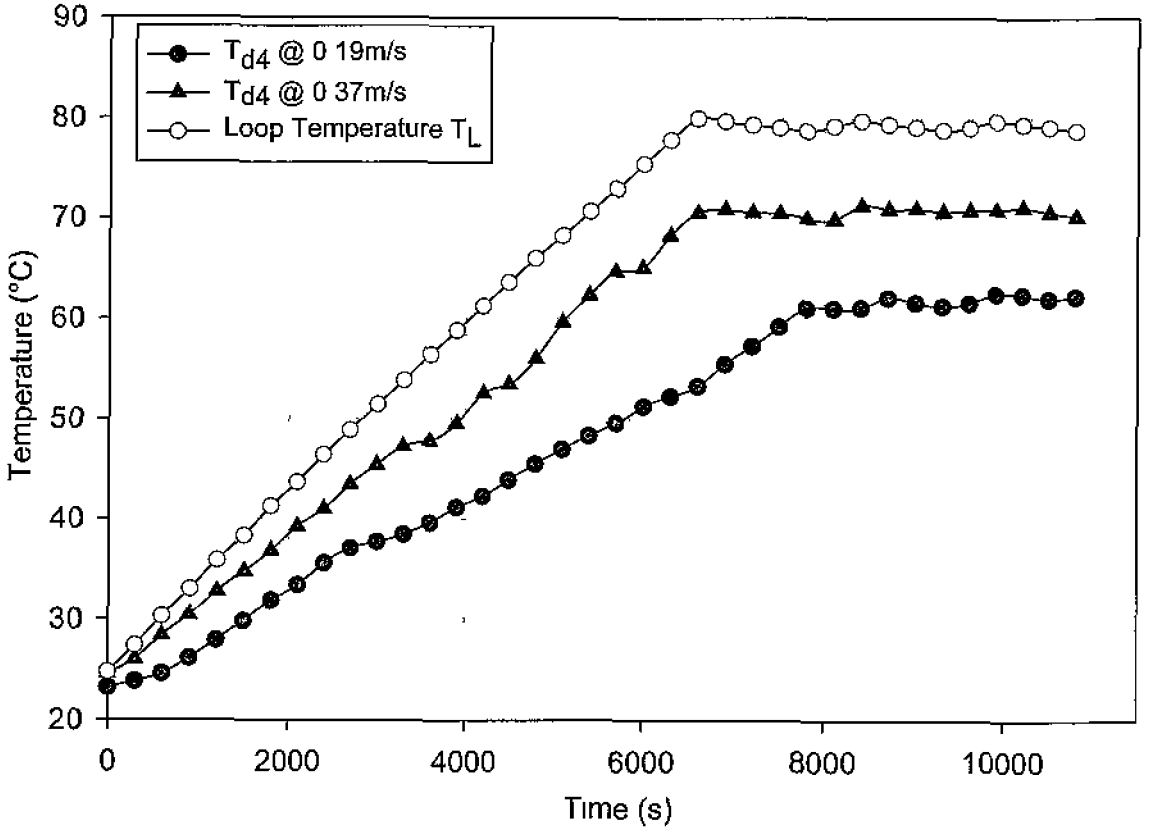

Figure 3 18 - Profiles of T_{d4} for $U_b = 0.19$ and 0.37m/s

With respect to loop velocity 0.19m/s, T_{d4} displays a quasi-linear heating phase prior to reaching steady-state temperature. From initial temperature T_{d4} increases by 39.03°C over the experiment Fluctuations in temperature increase during the heating phase of the profile are noted. Decreases in T_{d4} are recorded at 3000s and 6600s Such intermittent changes in temperature suggest the presence of pulsating fluid flow at the base of the branch at this velocity

Further evidence of non-uniform pulsating flow is evident with respect to loop velocity 0 37m/s. At this loop velocity T_{d4} follows relatively linear temperature increase during the initial stages of experiment, however notable fluctuations in

temperature are evident for 3600 < t > 6600s before a steady-state is maintained As with the previous loop velocity, such temperature response is indicative of dynamic fluid flow at the base of the branch

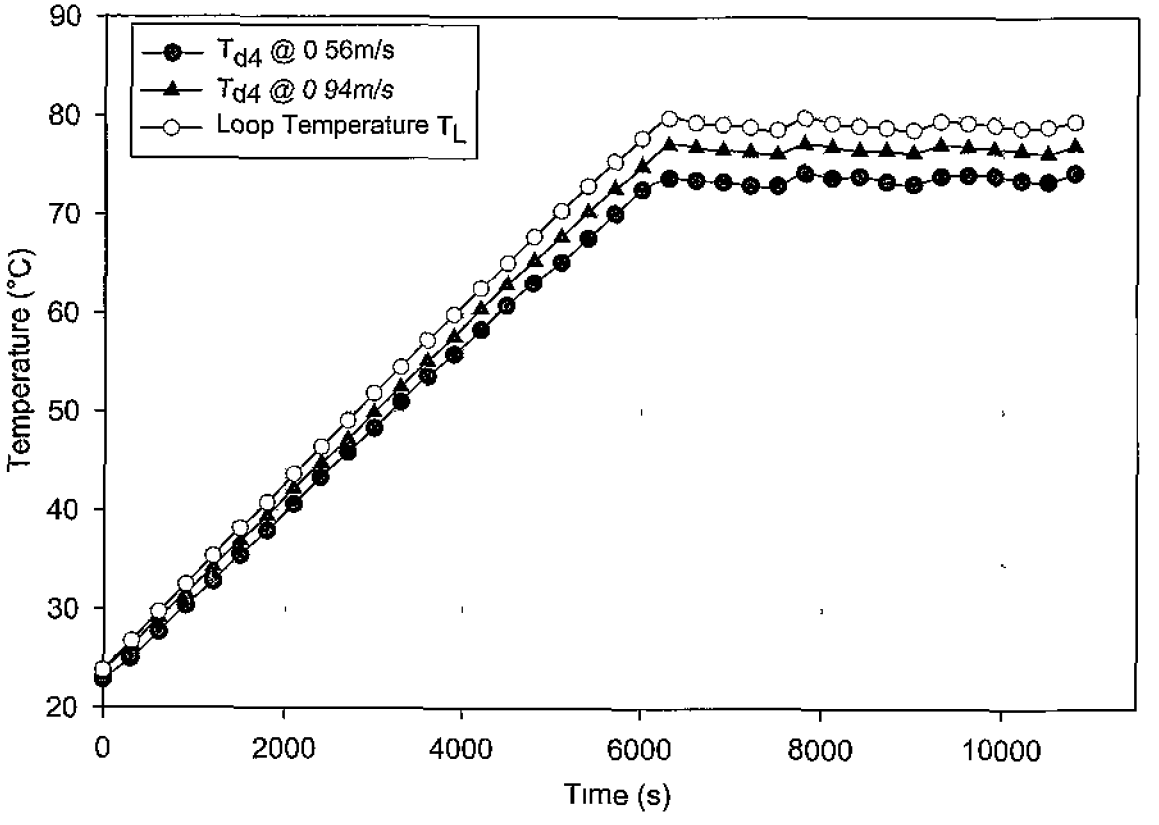

Figure 3.19 - Profiles of T_{d4} for U_b = 0 56 and 0.94m/s

Figure 3.19 presents profiles of T_{d4} for loop velocities 0 56 and 0 94m/s. Profiles exhibit similar patterns, T_{d4} follows the characteristic curve of main loop temperature. Similar temperature increase is also noted, T_{d4} increases by 51 39 and 52.85°C from initial temperatures for velocities 0 56 and 0 94m/s respectively.

Times taken to reach steady-state temperature (6300s) recorded for T_{d4} at both loop velocities confirms the similarity of temperature response. Fluctuations in T_L at steady-state and the subsequent changes in T_{d4} indicate the significant transfer of fluid between main loop and branch base with respect to both velocities

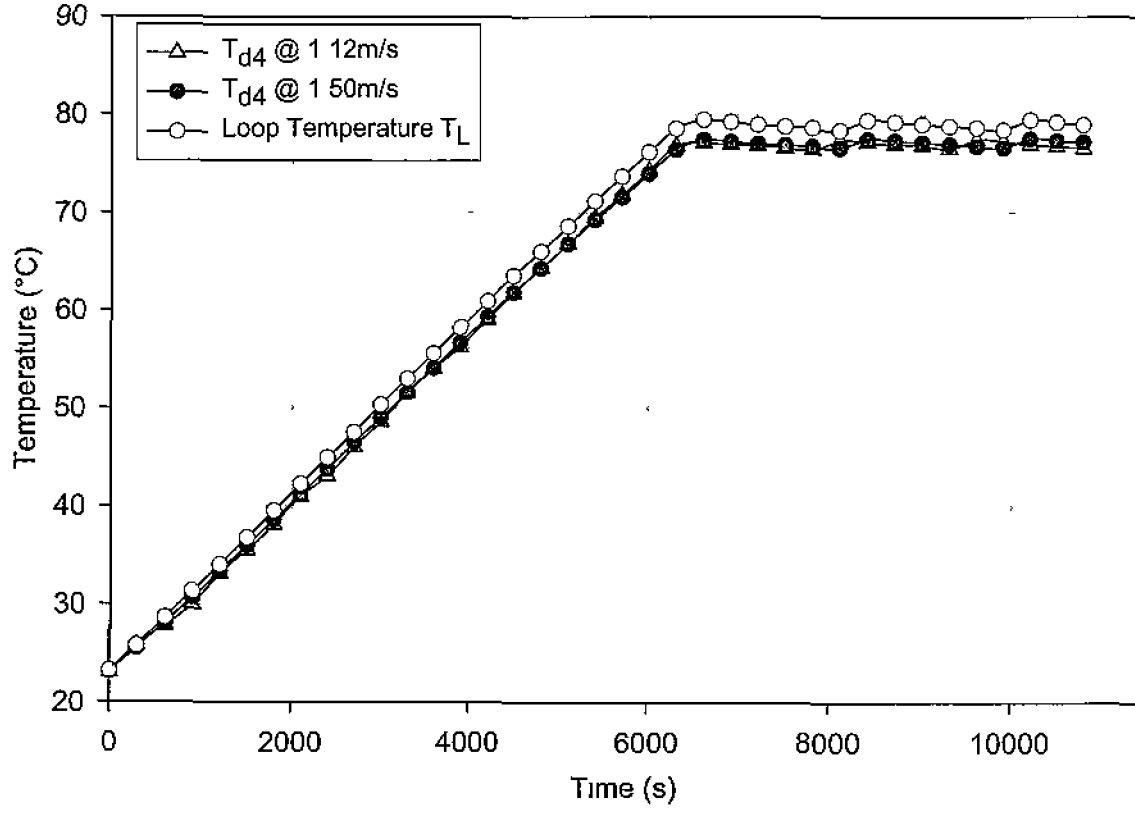

Figure 3.20 - Profiles of T_{d4} for U_b = 1.12 and 1.50m/s

Profiles of T_{d4} for loop velocities 1 12 and 1 50m/s are shown in Figure 3 20 T_{d4} exhibits linear heating phases prior to achieving steady-state temperature in both profiles. The similarity between profile patterns for T_L and T_{d4} indicates the presence of significant fluid mixing between dead-leg base and loop flow T_{d4} temperature increases of 54 17 and 54 06°C are recorded for loop velocities 1.12m/s and 1.50m/s respectively.

A temperature difference remains however at steady state between loop and dead-leg fluid reaching minimums of 1.7°C and 1.6°C for 1.12 and 1.50m/s respectively The overall length of the dead-leg may contribute to this temperature variance as fluid at

the base of the 4d branch may be restricted from re-entering main loop flow In effect this fluid becomes trapped at the base of the dead-leg by faster flowing fluid above. Fluid temperature increase at the base of the branch therefore would be regulated solely by heat transfer via free convective and/or diffusive means from main loop fluid.

Profiles of T_{d4} for loop velocities 0.19, 0 37 and 0 94m/s are shown in figure 3 21 All profiles represent dead-leg temperature recorded across a sample range of 4500 to 5500s The profile of T_{d4} at loop velocity 0 19m/s reflects limited mixing at branch base An increase in T_{d4} of 4.9°C is recorded across the sample range Most notably fluid at the base of the dead-leg shows negligible temperature fluctuations (± 0 32°C) based upon moving average calculations indicating primarily stagnant flow conditions

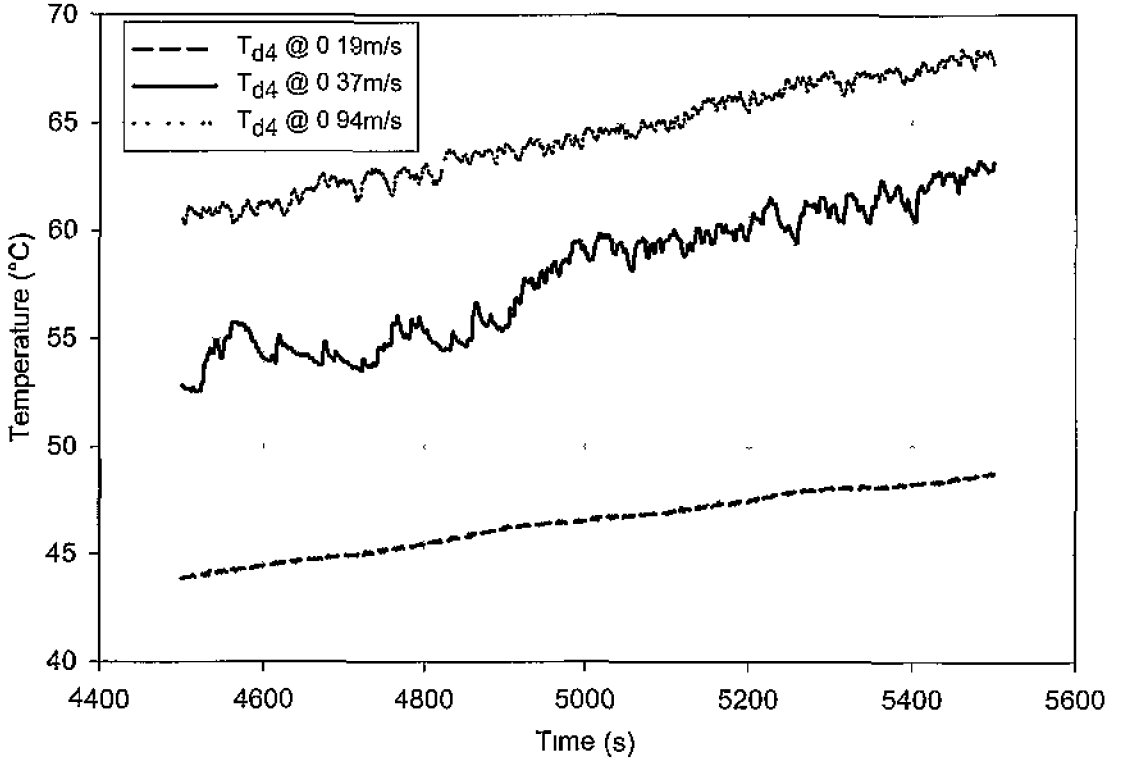

Figure 3.21 - Profiles of T_{d4} over reduced sample period for U_b = 0.19, 0 37, 0 94m/s

However at loop velocity 0 37m/s turbulent mixing is evident Fluctuations in T_{d4} of ± 1 73°C are recorded based upon a moving average Increases and subsequent decreases in temperature indicate the mixing of warmer and cooler fluid at the base of the branch as reflected by the increase in fluid temperature of 10.3°C over the sample period

Further increase of loop velocity to 0.94m/s shows contrasting mixing dynamics at the base of the branch As opposed to significant temperature fluctuations with respect to increased loop velocity, the profile of T_{d4} shows reduced fluctuations of ± 0.88°C based upon moving average calculations Temperature shows an overall increase of 7.2°C across the sample period

The detailed analysis provided by figure 3 21 illustrates a shift from primarily diffusive heat transfer at the base of the branch to increasingly turbulent mixing with dynamic movement between warmer and cooler fluids. Further loop velocity increase results in fully turbulent mixing; forced convection sweeping fluid into the base of the branch Significant fluid transport to and fro the branch base prevails

Table 3 9 displays maximum temperatures recorded at the base of the 4d reduced diameter dead-leg across the range of main loop velocities The maximum temperature recorded in the 4d reduced diameter branch is 77 53°C for a loop velocity 1.50m/s. However the desired dead-leg temperature set-point 79 15 ± 1°C was not achieved across the velocity range

Velocity, U_b (m/s)	**Maximum T_{d4} (°C)**
0 19	62.48
0 37	71 31
0 56	74 29
0.94	77 24
1.12	77.45
1.50	77 53

Table 3 9 - Maximum temperatures recorded for 4d reduced diameter dead-leg

Significant increase in T_{d4} is evident for $U_b > 0.19$m/s. However, maximum recorded temperatures varied little across the remaining velocity range. Previous results (see table 3.8) illustrated increases in dead-leg temperature with respect to increasing Reynolds Number flow Contrary to this, results shown in table 3 9 indicate a thermal threshold is achieved with respect to Reynolds Number variance

The occurrence of a thermal threshold may be attributable to reduced magnitudes of fluid entering the branch under flow conditions Research [45 & 46] has confirmed that loop fluid flow anticipates the entrance of a dead-leg branch under similar flow conditions. In fact recent research [45] has described the presence of a "ripple" flow effect as fast flowing fluid passes over a dead-leg branch entrance.

This "ripple" effect serves to maneuver fluid flow in the main loop into the dead-leg branch, primarily along the upstream wall in equal diameter sections [45] Increased loop velocity however coupled with a reduction in branch diameter would reduce the magnitude of loop fluid entering the dead-leg branch This scenario would effectively restrict mixing at the base of the branch and thus lessen the ability of the dead-leg to reach main loop temperatures. As such, further increase of loop velocity has little positive overall effect upon dead-leg temperatures

3 3.1.6 2d Reduced Diameter Dead-leg

Figure 3 22 presents profiles of T_L and T_{d2} over time for loop velocities 0 19 and 1 50m/s Profiles of T_{d2} represent temperature response to high and low distribution loop velocities recorded at the base of the 2d dead-leg

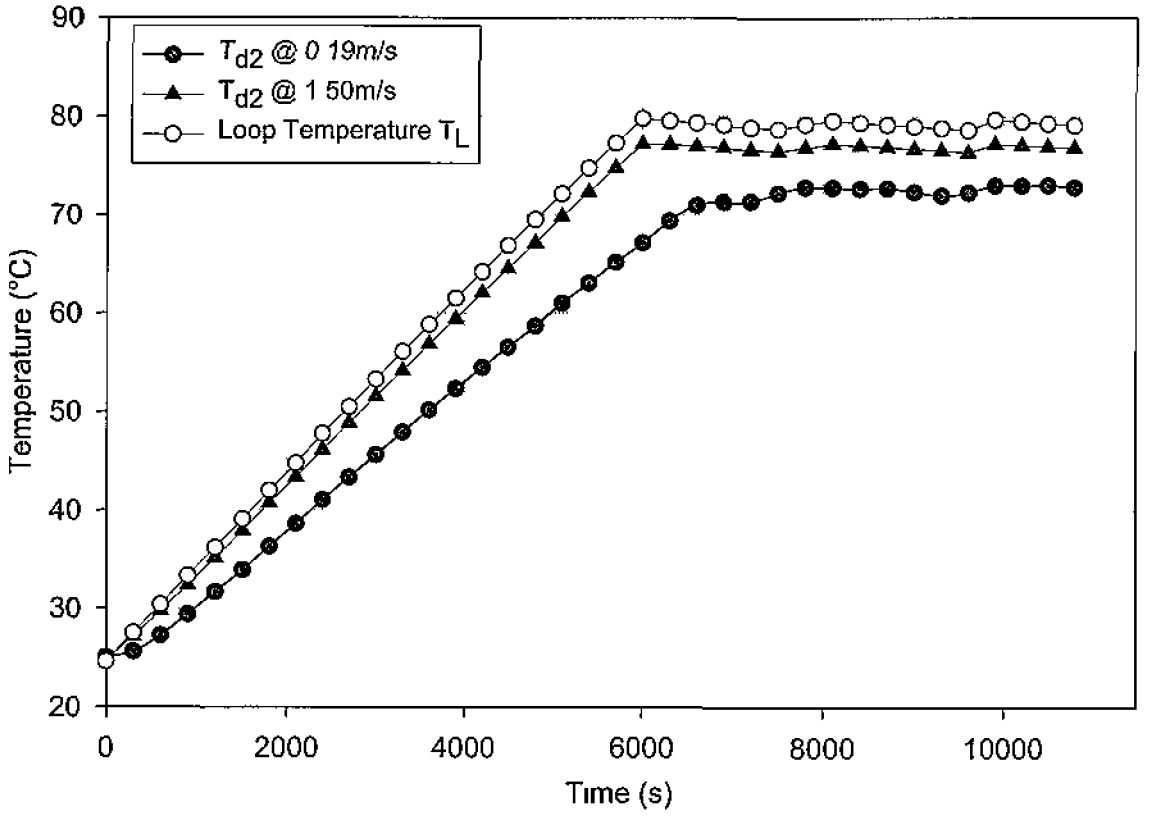

Figure 3.22 - Profiles of T_{d2} for U_b = 0 19 and 1 50m/s

Profiles of both main loop and dead-leg temperature follow similar patterns. The similarity of profiles indicates a strong T_{d2} response to changes in main loop fluid temperature. A minimum temperature difference of 6.56°C is recorded between T_{d2} and loop temperature for velocity 0.19m/s The difference in temperature between loop and dead-leg base is reduced with respect to increased loop velocity, reaching a minimum of 2.21°C for 1 50m/s

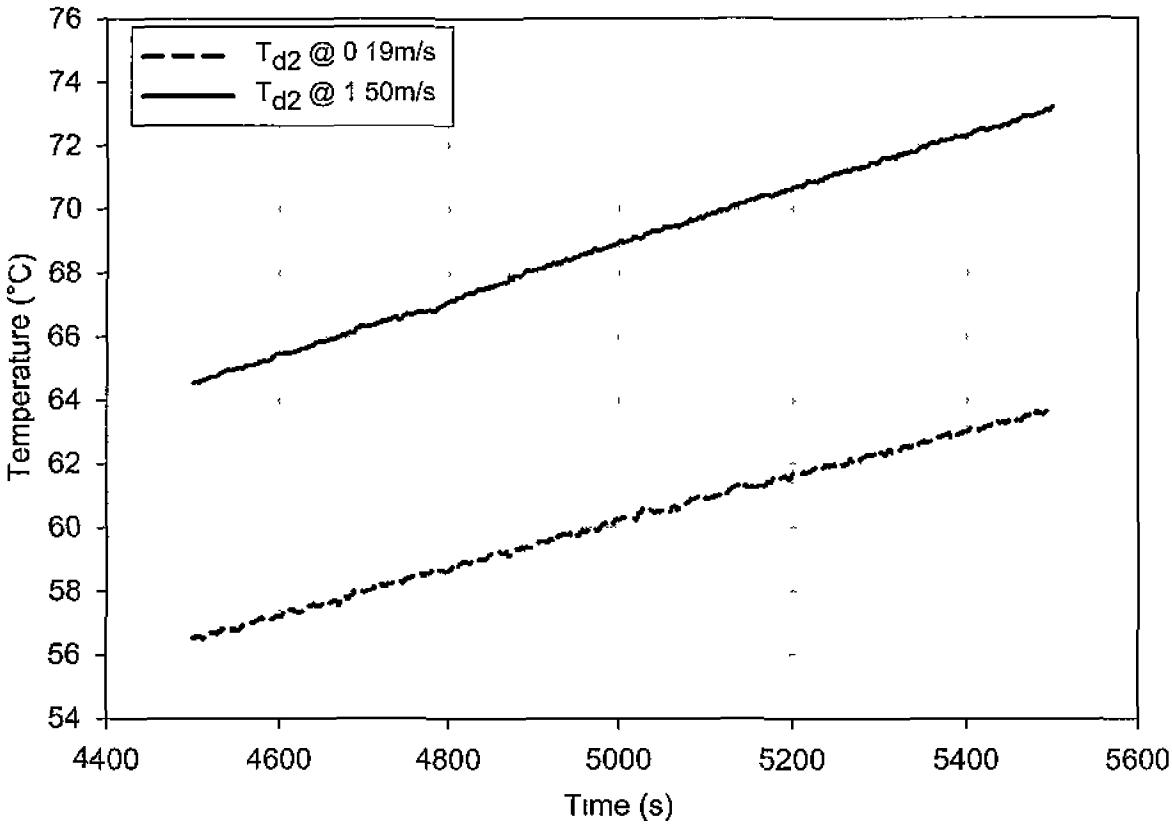

Figure 3.23 - Profiles of T_{d2} over reduced sample period for U_b = 0.19 and 1.50m/s

Figure 3 23 illustrates profiles recorded of T_{d2} for loop velocities 0 19 and 1 50m/s across a sample period between 4500 and 5500s. The linear patterns of T_{d2} are reflected in temperature fluctuations based upon a moving average recorded across the sample range Temperature fluctuations of ± 0 47°C and ± 0 42°C for loop velocities of 0 19 and 1 50m/s are recorded respectively. Both profiles of T_{d2} indicate similar heating magnitudes, 8 65°C and 7 22°C for 1 50 and 0 19m/s velocities respectively

Table 3.10 displays maximum temperature recorded at the base of the 2d reduced diameter dead-leg for both loop velocities. An increase in T_{d2} is recorded with respect to increased Reynolds Number flow. Neither velocity however produced the required temperature set-point 79 15 ± 1°C at the base of the dead-leg

Velocity, U_b (m/s)	Maximum T_{d2} (°C)
0 19	73 01
1 50	77 22

Table 3.10 - Maximum temperatures recorded for 2d reduced diameter dead-leg

Part C: Branch Diameter Comparison

Dead-leg thermal conditions are compared between equal and reduced branch diameter configurations based upon l/d ratio. The ratio is calculated using l, the length of the dead-leg measured from the centre axis of the main loop over d, branch diameter This ratio serves to offer a comparable study between branch temperatures for similar dead-leg configurations

Table 3 11 displays maximum temperatures recorded at the base of a dead-leg l/d = 6. ΔT represents the temperature difference between recorded maxima for bulk loop velocities Across the velocity range $U_b \leq 1$ 12m/s, greater temperatures are recorded in the reduced diameter branch compared with the equal diameter section. Greater dead-leg temperature is recorded in the equal diameter branch for U_b = 1 50m/s. Values of ΔT offer no linear relationship between temperature difference and loop velocity.

Velocity, U_b (m/s)	Maximum Temperature (°C)		ΔT (°C)
	Equal	Reduced	
0 19	22.72	29.08	6.36
0 37	31 26	34.33	3.07
0 56	33 08	36 28	3.20
0.94	41.64	48 97	7 33
1 12	57 60	62.46	4 86
1 50	75 14	72.77	2 37

Table 3.11 - Maximum recorded temperatures for l/d = 6

Figure 3.24 *presents the relationship* between maximum dead-leg temperature and loop velocity for l/d = 6. As illustrated, the relationship between maximum temperature and velocity is similar for both sections; increasing dead-leg temperature

with respect to increased loop velocity The greatest temperature difference (7.33°C) between dead-leg configurations is recorded with respect to loop velocity 0 94m/s.

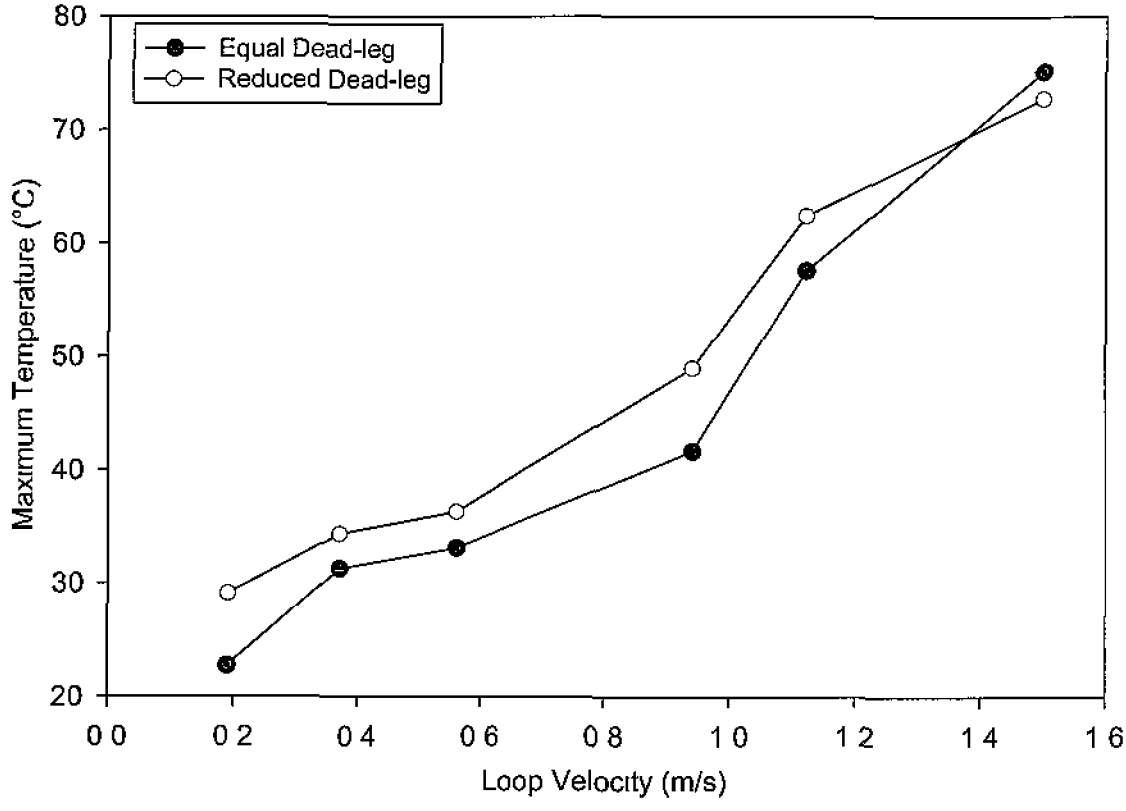

Figure 3 24 - Relationship of T_d and U_b for l/d = 6

With respect to dead-legs of l/d = 6, reduced diameter branch length (l = 150mm) ensures significant fluid transfer to the dead-leg base due to the closer proximity to main loop pipework. At lower velocity ranges (U_b < 1 50m/s) such reduced branch volume ensures improved main loop flow penetration, achieving greater fluid mixing at the base of the section. At increased loop velocities (U_b > 1.50m/s) the beneficial effect of branch length may become less of a factor. The increased branch volume of the equal diameter section contributes to improve mixing within the entire section

Research [45 & 46] has illustrated that fluid flow in the main loop anticipates the entrance of the tee-section branch under normal flow conditions. At increased loop velocities, fast moving fluid in the main loop may glide over the entrance of the reduced dead-leg branch effectively limiting the quantity of fluid entering the

branch. Reduction in fluid transfer into the branch would serve to reduce the *magnitude of* re-circulating flow within the section Research indicates a reduction in size of re-circulating zones in dead-leg branches with respect to decreasing branch diameter [47]. Such recirculating zones are considered to be directly related to heat-transfer within dead-leg branches

Additionally slower moving fluid in the branch would have less opportunity to re-enter main flow, effectively being held by faster moving fluid passing over the branch entrance [49] With reduced opportunity to mix with warmer loop fluids, heat-transfer within the branch would be restricted.

Maximum dead-leg temperatures for l/d = 4 are presented in table 3.12. A considerable temperature difference exists between maxima recorded in equal and reduced diameter branches for $U_b < 0.56$m/s. For increased loop velocity however, similar temperatures are recorded for both branch diameters.

Velocity, U_b (m/s)	Maximum Temperature (°C)		ΔT (°C)
	Equal	Reduced	
0.19	40.98	62 48	21.50
0 37	59 55	71 31	11 76
0.56	75 22	74.29	0.93
0 94	75 08	77.24	2 16
1 12	75 22	77.45	2 23
1 50	76 74	77.53	0 79

Table 3.12 - Maximum recorded temperatures for l/d = 4

The relationship between maximum temperature and velocity in equal and reduced branches for l/d = 4 is shown in figure 3 25 Both equal and reduced diameter profiles indicate the existence of a thermal threshold with respect to loop velocity. Minimal increase in T_{d4} is reported for $U_b > 0.56$m/s for both branch diameters after initial increases at lower velocities.

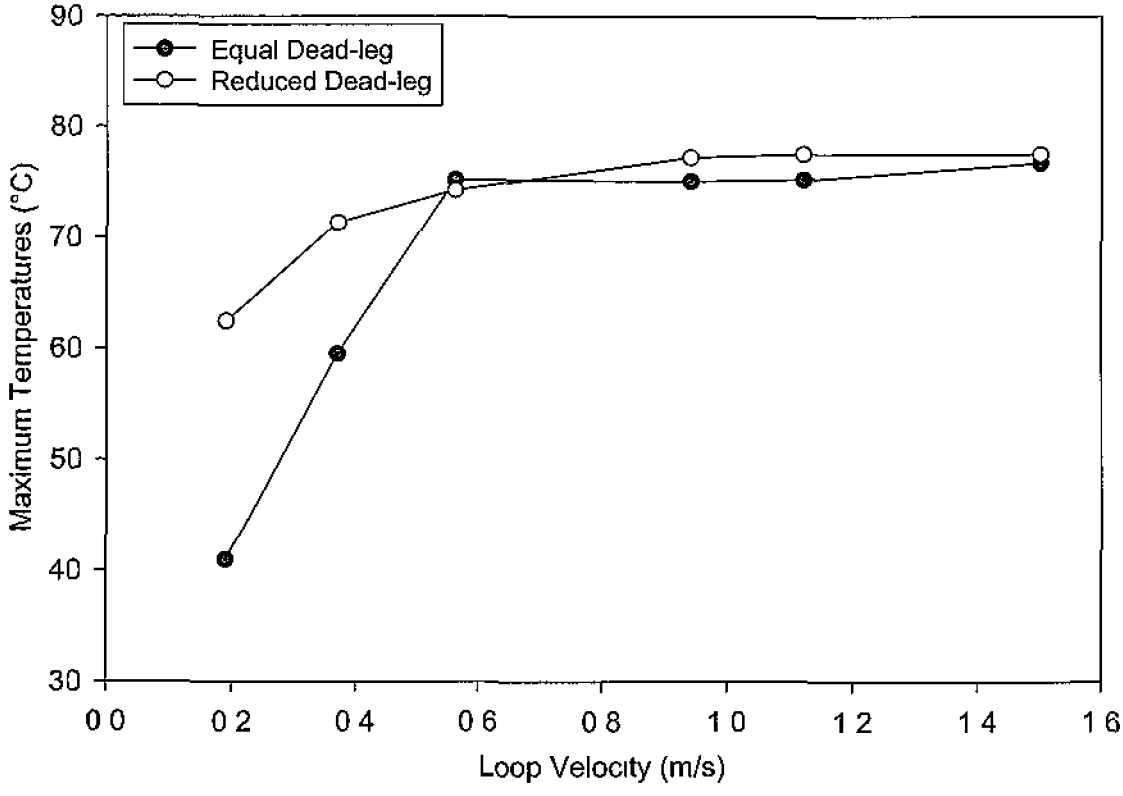

Figure 3 25 - Relationship of T_d and U_b for l/d = 4

As with the previous dead-leg configuration (l/d = 6), at lower velocities reduced branch volume contributes to favourable temperatures at the base of the dead-leg For greater loop velocities, increased branch diameter contributes to improve turbulent mixing ensuring similar dead-leg temperatures attainable in both diameter configurations

Table 3.13 shows recorded maxima for equal and reduced diameter dead-legs for l/d = 2. Data indicates greater temperatures at the base of the equal diameter compared to reduced diameter branch section. However as with the l/d = 4 configuration, the positive effect of larger branch diameter lessened with respect to increased distribution loop velocity.

Velocity, U_b (m/s)	Maximum Temperature (°C)		ΔT (°C)
	Equal	Reduced	
0 19	77.40	73 01	4.39
1 50	79 45	77 22	2 23

Table 3 13 - Maximum recorded temperatures for l/d = 2

Within the confines of the 6d-rule a reduction in branch diameter has the effect of reducing the overall length of the dead-leg branch The distance from dead-leg base to main loop pipe plays a significant role in overall dead-leg temperatures Results indicate improved temperatures are evident for both dead-leg branch diameter configurations with respect to reduced branch lengths

The scale-up of branch diameter contributes to improved mass transfer within equal diameter dead-legs [26]. This phenomenon was recognised as a direct result of a decrease of viscous forces with increasing branch diameter resulting in greater fluid velocities in larger diameter dead-legs [28] Improved turbulence as a result of increased Reynolds Number would contribute to improved mass transfer within the branch aiding CIP cleaning operations. One could agree that diffusive heat transfer would be of no aid to sanitization procedures as the sufficient disruption of fluid at the base of the branch could not be guaranteed

Regarding the sterilization of *Pseudomonas aeruginosa* bacteria; accepted D-value at 70°C is 1.3mins. Temperatures presented previous (tables 3 11-3 13) represent maxima recorded, and may not reflect the transient thermo-fluid conditions occurring at the base of the dead-leg branch. Acceptable sterilization at this destruction limit therefore is evaluated in terms of maintaining temperature T_d > 70°C. As such the destruction of *Pseudomonas aeruginosa* over sustained time periods is considered achievable in 6d dead-legs at U_b > 1 50m/s, 4d dead-legs at U_b > 0 56m/s and in 2d dead-legs across the velocity range.

However considering reduced sample analysis (see figures 3 6, 3.17); turbulent mixing may not be of sufficient magnitudes in 6d dead-legs to support rigorous

cleaning procedures Endotoxins shed by destroyed bacterium would not be fully removed from the branch under CIP flow conditions

HPWS designers should attempt to reduce the overall length of a dead-leg as means of limiting the possibility of stagnant flow conditions occurring at their base Data indicates 6d dead-legs are not capable of sanitization at their base regardless of branch diameter Temperatures close to required sanitization limits were attained in 4d and 2d, equal and reduced diameter sections However loop velocity magnitude played an integral role in the temperatures achieved.

Results detailed in this section provide a comparison between the effective use of large and smaller diameter tee-sections in HPWS design Instrumentation connections or point-of-use requirements are some reasons why tee-section branch diameters vary in system design. However in situations where designers are not restricted to the size of branch diameter installed, the above discussion would provide guidance to ensure installed sections are sanitizable.

One industry expert argues that the initial expenditure of installing larger tubing should be offset against the cost of installing and maintaining flushing mechanisms [28]. Alternatively the distribution loop may be operated at elevated temperatures to overcompensate for the presence of dead-leg stagnation zones However consideration must be taken into seal life and system durability at excessive temperatures. All-in-all dead-legs should be evaluated for cleanability not only by l/d ratio, but also with consideration of operating distribution velocities [10]

3.3.2 Non-intrusive Analysis

As previously discussed the design of HPWS are such that the consistency of water quality is of the utmost importance. A decrease in water purity can ultimately lead to the suspension of manufacturing operations The exposure of purified waters to external non-sterile sampling conditions can compromise this quality. The FDA state in their 'Guide to Inspections of HPWS' [5];

"Regarding microbiological results, for Water for Injection, it is expected that they are essentially sterile. Since sampling frequently is performed in non-sterile areas and is not truly aseptic, occasional low levels counts due to sampling errors may occur "

Non-intrusive analysis includes testing methods used to examine a system without impairing its future usefulness Non-intrusive sampling methods may provide analysis of pharmaceutical water temperature without exposing HPWS to non-sterile externals. Experimentation thus far utilised shafted thermocouples inserted into the branch of a dead-leg to monitor temperature at various positions. With regard systems operating purified waters in industry, such methods of thermal analysis would not be tolerated as thermocouples may be exposed to non-sterile conditions and subsequent insertion into pipework may contaminate waters

The aim of analysis is to develop a method/s of calculating fluid temperature in a dead-leg based upon non-intrusive surface temperature measurement

3.3.2.1 Infrared Thermography

Infrared (IR) thermography is a non-contact data acquisition technique for two-dimensional mapping of surface temperature distributions [50]. An IR device measures and images emitted radiation from an object As radiation is a function of object surface temperature, the device can calculate and display the resultant temperature distribution

Applying thermographic principles, data was generated detailing surface temperature distribution over an operational dead-leg branch. Thermal images were captured

using a ThermoVision™ A20M infrared camera supplied by FLIR Systems Image processing was performed using accompanying ThermaCAM™ QuickView software

Analysis focused upon surface temperatures of a 6d equal diameter dead-leg branch, geometry as per table 3.3. This dead-leg configuration was selected as it remained within the confines of the 6d rule; yet thermal profile analysis demonstrated fluid temperature reduction along the branch base (see section 3 3.1 Part A)

Loop fluid temperature T_L, was increased from ambient to 80°C set-point with consequent changes in branch surface temperature recorded at set time intervals Time zero represents the instance heating was activated in the system. Loop fluid velocity was fixed at 1 50m/s. All experiments were performed in laboratory conditions with no induced air flow, with ambient temperature between 21 ± 1°C. Object parameter values assigned to imaging hardware are detailed in table 3 14, default values taken from accompanying software.

Emissivity (-)	0.16 (default polished stainless steel)
Distance from camera (m)	0 6
Temperature Reflected (°C)	22
Temperature Atmosphere (°C)	21
Relative Humidity (%)	50 (default)
External Optics	OFF

Table 3.14 - Object parameter settings

Thermal images (see figures 3.26–3 29) display colored contours based upon surface temperature distribution. Spot recordings provide point temperature magnitudes at branch mid-point (spot 1) and at its base (spot 2) Spot temperature values are displayed in the top right corner along with a temperature scale on the right-hand side of the image Temperature scales illustrate colors assigned to various

temperatures on the image, high and low temperatures at the upper and lower ends of the color spectrum respectively Spot temperatures and loop temperature are displayed with respect to time in table 3 15 ΔT represents temperature difference between spot positions for time t

Time, t (s)	Loop temperature, T_L (°C)	Surface Temperature (°C)		
		Spot 1	Spot 2	ΔT
0	21 0	18.9	18 3	0.6
2700	49 3	28 2	27 4	0.8
3600	58.5	32 6	31 4	1 2
4500	67.3	35 7	34.4	1 3
5400	75.8	38 8	37.1	1 7
6300	79 6	41 0	39.6	1 4
7200	79 0	40.8	38.7	2 1
8100	79 2	40.2	38.2	2
9000	79 7	40.5	38.4	2 1
9900	79.9	41.1	39.2	1 9
10800	79.3	41.9	39.9	2

Table 3 15 - Infrared thermography temperatures

Transient heat increase at spot positions with respect to increasing loop temperature is evident. This indicates radial heat transfer from the dead-leg fluid through the pipe walls Greater surface temperatures are recorded along the mid-point of the branch section in comparison with the dead-leg base Magnitudes of ΔT are shown to increase over time, reaching a maximum of 2 1°C towards the run end

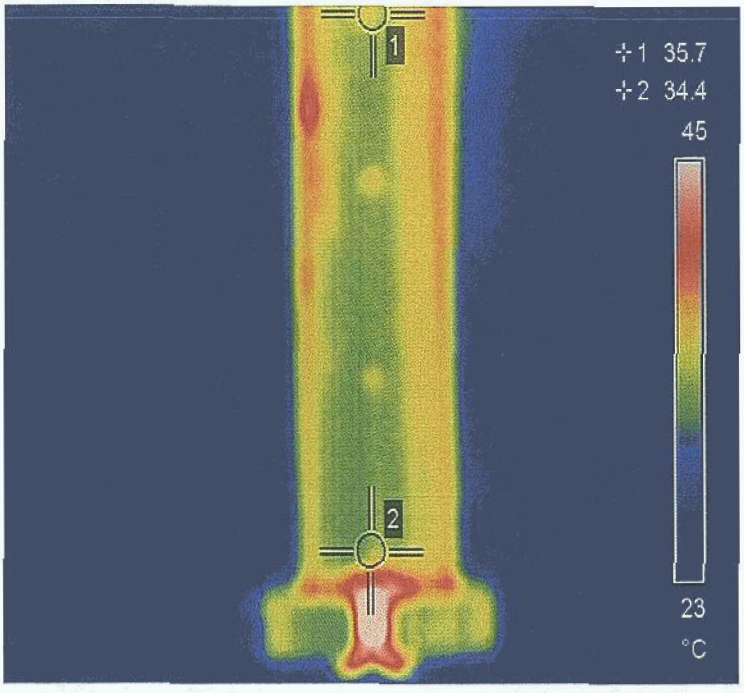

Figure 3.26 - Thermal contour image at t = 4500s, T_L = 67.3°C

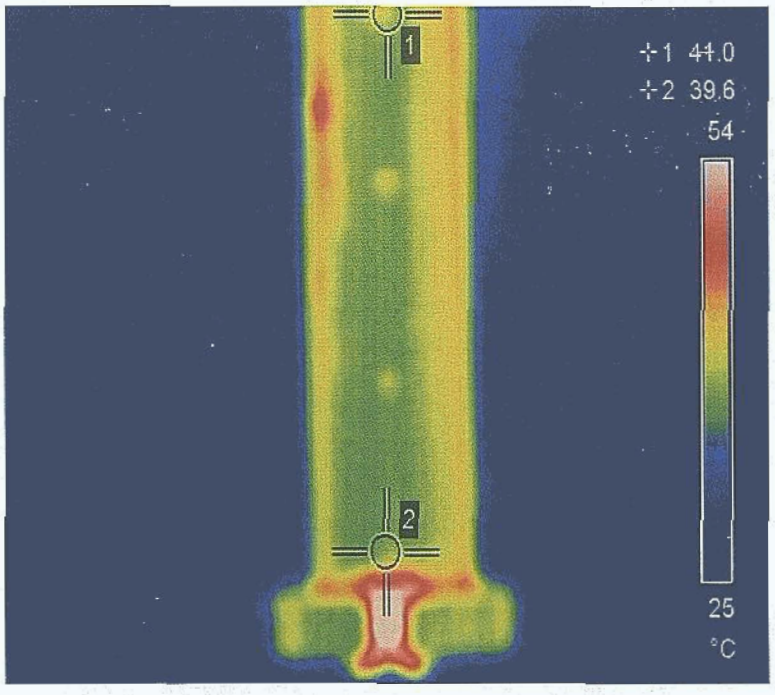

Figure 3.27 - Thermal contour image at t = 6300s, T_L = 79.6°C

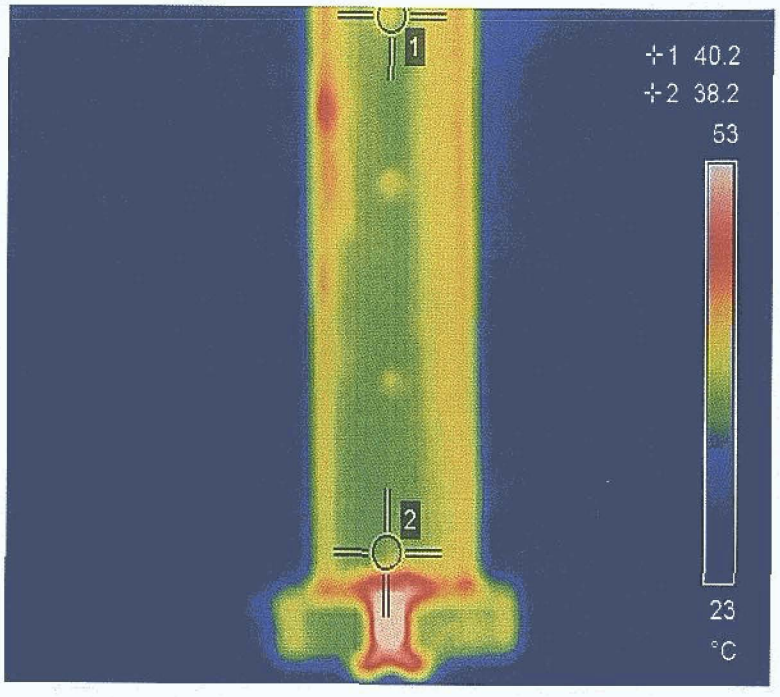

Figure 3.28 - Thermal contour image at t = 8100s, T_L = 79.2°C

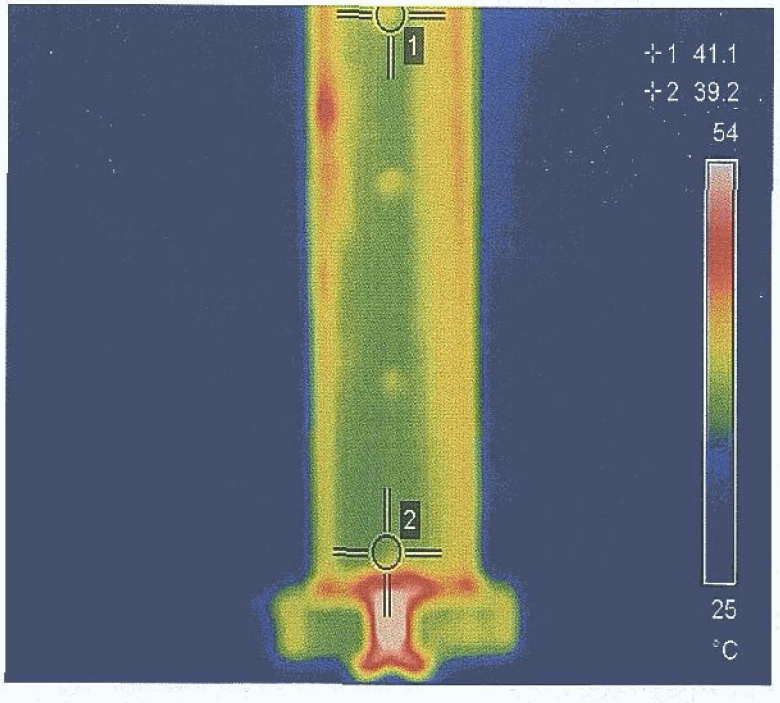

Figure 3.29 - Thermal contour image at t = 9900s, T_L = 79.9°C

3.3.2.2 Surface Thermocouple Analysis

In conjunction with infrared thermography, surface temperature measurements at varying dead-leg branch positions using mounted thermocouples were performed Bead T-type thermocouples were attached to the exterior surface of the dead-leg branch using PVC tape. Fluid temperature at the corresponding positions was recorded using T-type shafted thermocouples as before

Fluid temperature was recorded along the centre axis of the dead-leg branch representing fluid furthest from pipe walls. Results provide comparative data of surface and fluid temperatures within a dead-leg branch at particular points Figure 3 30 illustrates surface and fluid temperature measurement techniques

Experimentation was performed over 10800s (3 hour) sample periods. Temperature was recorded in 300 second intervals, time zero representing the instance heating was activated in the system (see Appendix E). Ambient temperatures and loop set-point temperature remained as before

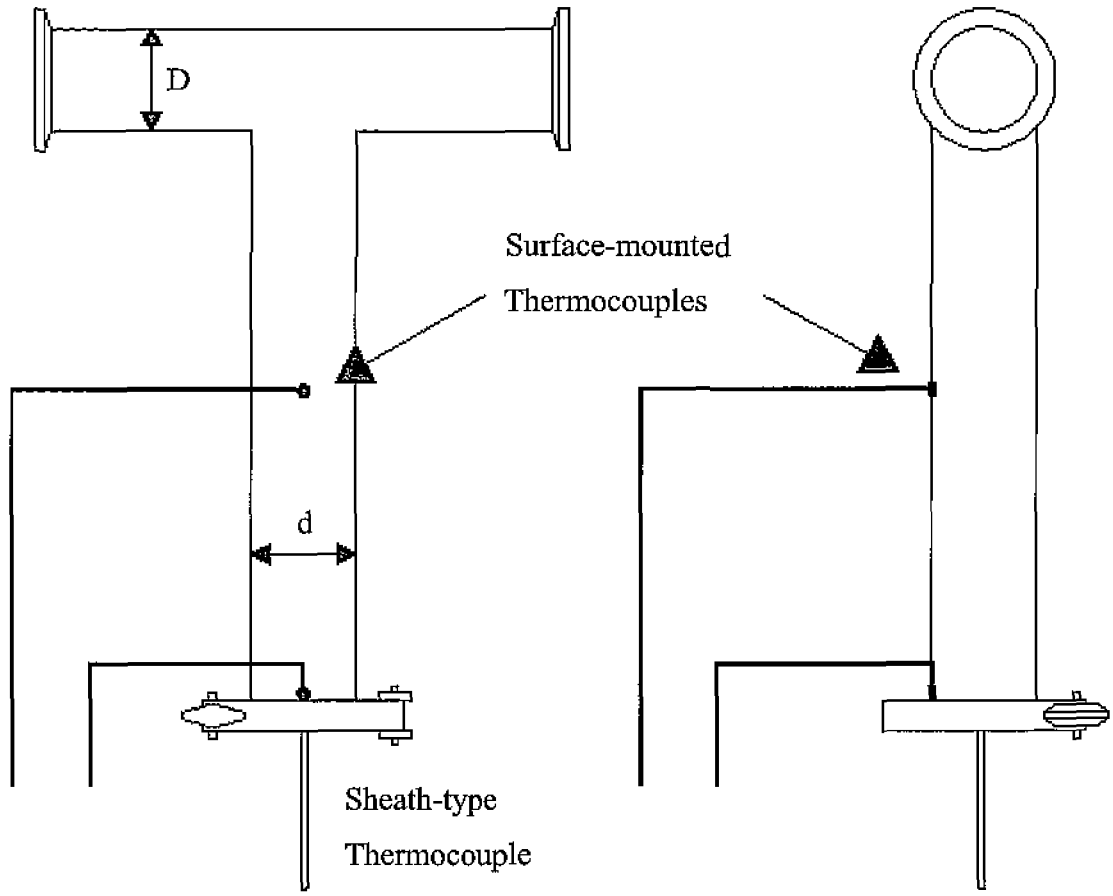

Figure 3 30 - Schematic of surface and fluid thermocouple recording methods

Figure 3 31 represents thermal profiles recorded for surface and dead-leg temperature with respect to time for the 6d equal diameter dead-leg Profiles represent thermal responses at branch base and mid-point positions for loop velocity 1.50m/s. Profile patterns indicate a relationship between fluid and surface thermal responses. Both surface and dead-leg mid-point profiles exhibit similar linear patterns during system ramp-up, achieving and maintaining steady-state temperature at 5520s

Considering temperature response at the branch base, surface and dead-leg profiles also display similar controlled increasing patterns However times recorded to achieve steady-state temperature vary, 5520s for branch surface compared with 6000s for dead-leg fluid.

Excess time taken for fluid to reach thermal equilibrium at the base of the dead-leg is a result of diffusive heat transfer mechanisms as described in thermal profile analysis results (see section 3.3.1).

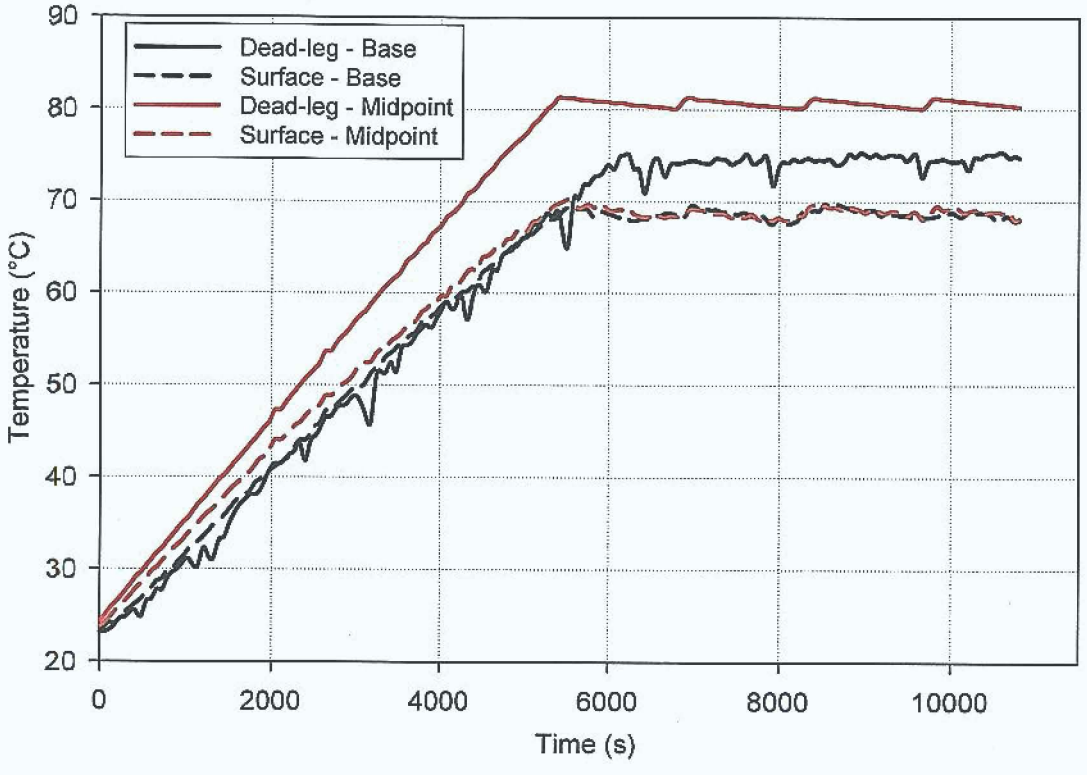

Figure 3.31 - Fluid and surface temperature profiles for $U_b = 1.50$m/s

Considering figure 3.31, the presence of axial wall conduction is evident with respect to profiles of surface temperature. Greater surface temperatures are noted at branch mid-point compared with base measurements during loop ramp-up. Yet after time thermal equilibrium occurs throughout the branch length with similar surface temperatures recorded at mid-point and base for the duration of the experiment.

Further evidence of axial wall heat flow is evident as branch base surface temperatures are shown to reach steady-state before fluid at the dead-leg base reaches thermal equilibrium. This suggests surface temperatures may be influenced by axial conduction of heat along the branch wall as well as radial heat flow from the dead-leg fluid.

With respect to pipes or tubing manufactured from stainless steels, wall conduction can play a significant role in heat transport. Research indicates that axial wall conduction is a primary mechanism of heat transfer in the diffusional transport zone of capped branches [26]. Thermal profile analysis has identified the presence of diffusional zones of heat transport at the base of 6d equal diameter dead-legs.

Figure 3.32 presents surface and dead-leg thermal profiles recorded for a 4d equal diameter dead-leg at loop velocity 0.56m/s, geometry as per table 3.3. Based upon thermal profile analysis results (section 3.3.1 Part A), convective heat transfer is assumed the primary transport mechanism at this dead-leg configuration and loop velocity.

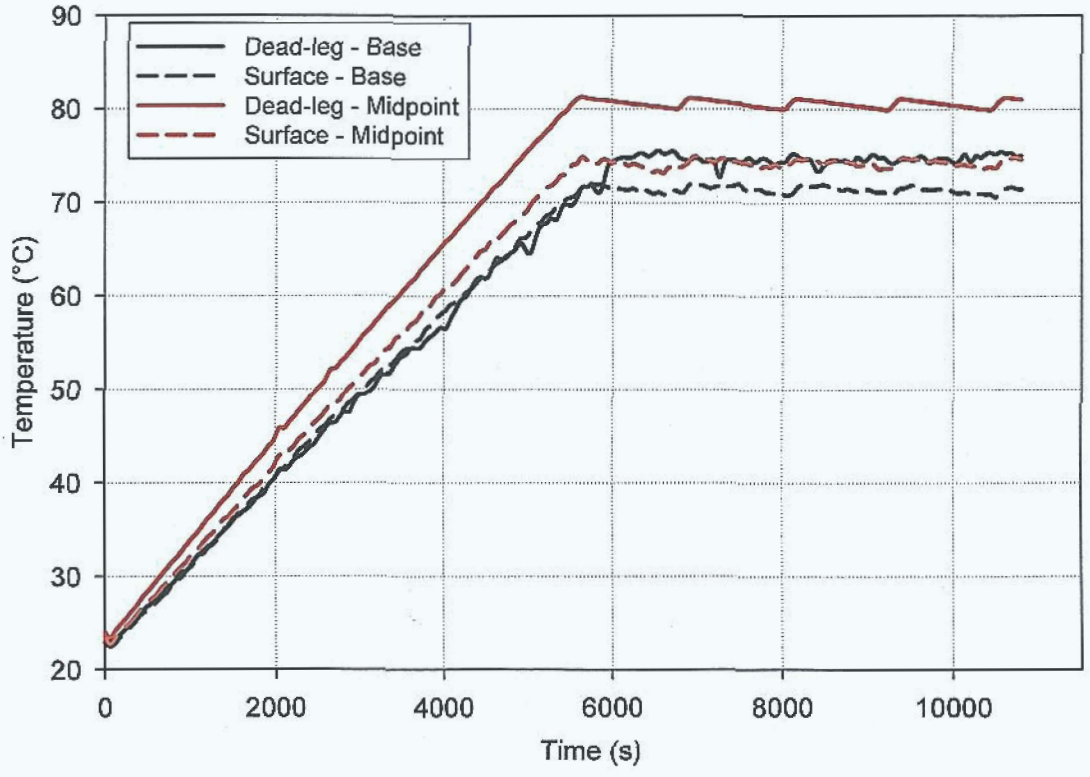

Figure 3.32 - Fluid and surface temperature profiles for U_b = 0.56m/s

Considering surface temperature responses; both mid-point and base profiles exhibit steady-state conditions for t > 5700s. Examination of surface profiles at steady-state reveals little evidence of increasing surface temperatures over time. However the time recorded achieving steady-state dead-leg temperature at the base of the branch

was 6000s The difference in time between thermal equilibrium at surface and fluid instances suggests surface temperatures at the base of the branch remain affected by axial wall conduction, and not solely upon radial heat conduction from fluid within.

3.3.2.3 Comparison of Results

The application of surface thermocouple analysis is limited to dead-leg configurations where fluid temperature throughout the branch is governed by convective heat transfer only and axial heat transfer is assumed negligible along branch walls. With respect to regions where diffusion is the primary mechanism of heat transfer, axial thermal conduction plays a significant role upon surface temperature distribution As such surface temperatures will not truly reflect thermo-fluid conditions within a dead-leg

Yet surface temperature responses for dead-legs experiencing primarily forced convective heat transfer also reveal the presence of axial conduction at branch walls. The author assumes therefore that the effect of axial heat flow along pipe walls cannot be considered negligible and surface temperatures will not accurately reflect temperatures within a dead-leg As such further experimentation is required to establish the magnitudes of radial and axial heat flow along dead-leg surfaces for a branch of finite length l, with fixed loop temperature T_L at constant loop velocity U_b

Axial heat flow overlaps radial heat flow and local surface temperature was shown to vary across the length of the dead-leg. With respect to both infrared thermography and surface thermocouple results; greater temperatures were recorded at branch mid-points compared with at the base of the section

This surface temperature distribution is reflected by the thermal profiles recorded for mid-point and base dead-leg fluid. These profiles highlighted the presence of warmer fluid in the dead-leg branches for regions close to turbulent loop flow. Lower surface temperatures recorded at branch base are related to cooler stagnant fluid within the dead-leg unaffected by turbulent conditions Results support the evidence [10, 26 & 44] of separate regions of turbulent and stagnant flow for positions close to main loop flow and at the base of dead-legs respectively

Time, t (s)	Thermography Temperature (°C)		Surface Thermocouple Temperature (°C)	
	Mid-point	Base	Mid-point	Base
2700	28 20	27 40	48 88	47 19
3600	32 60	31 40	56 29	55 01
4500	35 70	34 40	63 82	62.20
5400	38 80	37.10	69 77	68.37
6300	41.00	39 60	68.64	67.94
7200	40.80	38 70	68.76	69.10
8100	40 20	38 20	68.00	67.60
9000	40.50	38 40	68 79	69 13
9900	41.10	39.20	69 08	68 68
10800	41 90	39 90	68.11	69.08

Table 3 16 - Comparison of surface temperatures for 6d dead-leg, U_b = 1 50m/s

Comparison of thermography and surface thermocouple data for a 6d equal diameter dead-leg are presented in table 3.16. Variances in recorded temperatures at mid-point and base positions are noted with respect to time. The author deemed errors in the thermographical testing procedure as the possible source of such discrepancies. Upon further investigation it was determined that the parameters contributing to the inaccuracy of thermographical results may include,

- Radiation measured by the IR camera is also a function of the objects emissivity. The curved surface of the branch perimeter was not conducive of accurate emissivity detection (see figure 3 33) The face of the dead-leg branch when observed from an elevation view generated radiation concentrations along the leading edge and at the perimeter edges of the pipe. This resulted in the inaccurate detection of elevated surface temperatures at these regions by the IR device

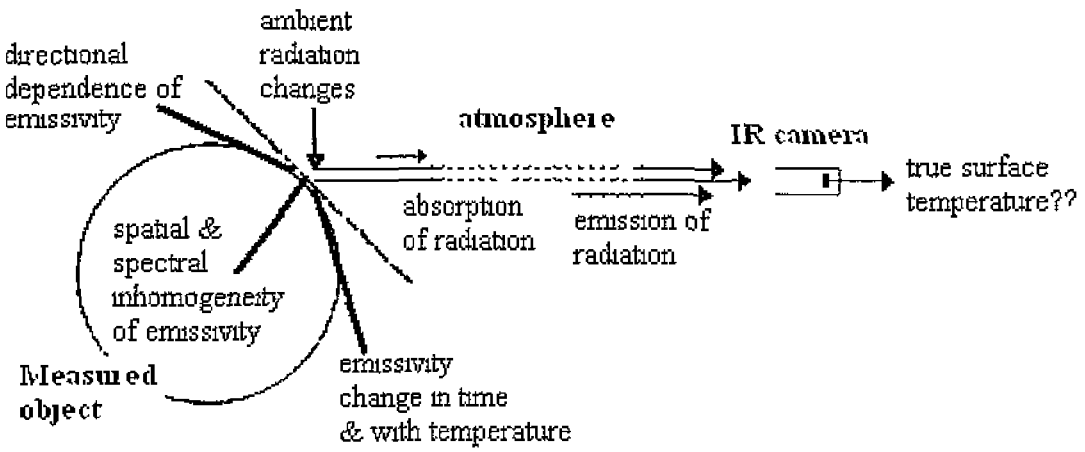

Figure 3.33 - Error sources in non-contact temperature measurement [50]

- Radiation emits from the surroundings and in turn is reflected by the measured object [51]. Highly polished, mirror-like materials will therefore be prone to the reflection of external radiation Difficulty arises when accurately recording temperature distribution for high-polished stainless steel materials due to exterior radiation emissions

- Radiation from the measured object and reflected radiation will also be affected by absorption from atmosphere (see figure 3.33) [51]. In the absence of controlled testing surroundings, variances in atmospheric humidity may contribute to radiation detection errors A default relative humidity value was applied for infrared analysis; however initial humidity testing may be required to develop a true representation of actual testing conditions.

- The transmission of external optics around the measured object can cause imaging errors. Efforts to produce controlled surroundings were attempted however the presence of external optics (sunlight, shadows etc) remained an issue.

The resolution of thermography testing issues was considered beyond the scope of this research The application of thermography techniques for non-intrusive analysis has been explored and with consideration and resolution of aforementioned issues this technique may be applied to non-intrusive analysis

Chapter 4 Conclusions and Recommendations

An analysis of the thermal sanitization characteristics of equal and reduced diameter dead-legs for various branch lengths has been presented Results have illustrated the thermo-fluid scenarios at the base of piping dead-legs with respect to varying distribution loop velocities

4.1 Conclusions

Analysis of results indicates increases in maximum dead-leg temperature with respect to increasing loop velocity for dead-legs in general For dead-leg configurations l/d = 6, greater temperatures are recorded at the base of reduced diameter branches at lower loop velocities ($U_b \leq 1.12$m/s). However with increased loop velocity ($U_b = 1.50$m/s), a greater dead-leg temperature is recorded in the equal branch diameter geometry.

At l/d = 4 considerably greater temperatures are recorded in reduced diameter branches at lower loop velocities ($U_b < 0.56$m/s) However at increased loop velocity ($U_b = 1.50$m/s) similar dead-leg temperatures are recorded for both branch geometries. A maximum temperature threshold is achieved in both equal and reduced diameter dead-legs with respect to increasing loop velocity For l/d = 2, greater temperatures are recorded at the base of the equal diameter dead-leg branches

At lower loop velocities, reduced branch volume contributes to the thermal penetration of loop fluid generating favourable mixing conditions resulting in higher dead-leg temperatures. However with respect to increased loop velocity, scale-up of branch diameter contributes to increased mass transfer generating significant turbulent fluid mixing within the dead-leg

6d and 4d dead-legs regardless of branch diameter were not capable of achieving desired loop temperatures Loop temperature set-point 79.15 ± 1°C was achieved and maintained at the base of a 2d equal diameter dead-leg for loop velocity 1.50m/s However maximum temperatures of sanitizable limits were attained for 4d dead-legs

at $U_b > 0$ 94m/s, 2d reduced diameter dead-leg at 1 50m/s and 2d equal diameter dead-legs across the velocity range

With consideration to the application of the 6d-rule, results have indicated the law is ultimately flawed Acceptable sanitization temperatures were not achievable in 6d dead-legs Additionally fluid dynamics at the base of a branch l/d = 6 suggest contaminants would be neither thermally destroyed nor removed under flow conditions.

High purity water system designers should aim to limit the length of dead-leg branches to < 4d and operate distribution loop velocity > 1.50m/s to eliminate the presence of diffusive heat transfer at the base of operational dead-legs With consideration of industrial cleaning procedures, the rigorous turbulent mixing of loop fluid throughout the branch is required to completely remove free-floating and attached contaminants

An investigation of the application of non-intrusive temperature measurement techniques was presented Infrared thermography highlighted surface temperature distribution across an operational piping dead-leg In conjunction with surface thermocouple analysis, greater temperatures were recorded at mid-point branch positions compared with at the base of the dead-leg. Surface temperature distribution supported thermo-fluid dynamics highlighted by previous results The application of non-intrusive techniques is limited however, due to the presence of axial heat conduction along pipe walls which inhibits the accurate detection of dead-leg fluid temperature within.

4.2 Recommendations

Analysis performed during experimentation has highlighted areas for possible continued research on this topic Author recommendations include;

- Evaluation of dead-leg thermal responses over increased loop velocity ranges

- An investigation of the application of infrared thermography to the detection of fluid temperature deceases in HPWS distribution loops

- The direct measurement of bacterial population and activity prior to and after dead-leg sterilization procedures in an operational system.

- Surface temperature mapping of operational dead-leg branches for the development of heat transfer coefficients

- An investigation of the thermal responses for dead-legs horizontally orientated or at an angle to the vertical.

- An investigation of the effect of branch insulation upon dead-leg temperatures

- A development of standard flushing procedures and intervals per branch configuration and loop velocity

References

[1] Fessenden B , 'A Guide to Water for the Pharmaceutical Industry Part 1', *Journal of Validation Technology*, Vol 1 (4), pp 30-39 (1995)

[2] Mc William A J , 'The Design of High Purity Water Distribution Systems', *Pharmaceutical Engineering*, Vol. Sep/Oct, pp 54-71 (1995).

[3] Carvell J P , 'Sterility and Containment Considerations in Valve Selection', *Pharmaceutical Engineering*, Vol. 12 (1), pp. 31-34 (1992).

[4] Meltzer T H., Pharmaceutical Water Systems, Tall Oaks, Littleton (1997)

[5] U S Food and Drug Administration, 'Guide to Inspections of High Purity Water Systems', Division of field investigations, Office of regional operations, Office of regulatory affairs, Rockville MD (1993)

[6] 'Modular Block Bodies', Pure-Flo® product brochure, Industrial & BioPharm Group (2006).

[7] 'Bioprocessing Equipment', American Society of Mechanical Engineers, Section SD-3.11 (1997)

[8] Bacaoanu A and Jennings T A , 'Steam Sterilization of Freeze-Dryers - Dead Legs', *European Pharmaceutical Review*, Vol. 5 (3), pp. 27-30 (2000).

[9] Seiberling D.A., 'Clean-In-Place & Sterilize-In-Place Applications in the Parenteral Solutions Process', *Pharmaceutical Engineering*, Vol 6 (6), pp 30-35 (1986)

[10] Haga R., Murakami S., Ostrove S. and Weiss S., 'Cleaning Mechanism Study for Bio-Pharmaceutical Plant Design', *Pharmaceutical Engineering*, Vol 17 (5), pp. 8-21 (1997)

[11] Hinks H. and Bosch D , 'Aseptic Pharmaceutical Manufacturing The Design and Validation of Water for Injection Systems', *Pharmaceutical Manufacturing and Packing Sourcer*, Vol. 4 (4), pp 32-35 (2003).

[12] Wood R. T., 'Regulation and Control of Water Quality in the Pharmaceutical Industry', *Annual Technical Meeting - Institute of Environmental Sciences*, pp 57-66 (1985)

[13] Free drinking water [online], www freedrinkingwater com (accessed 30 March 2005).

[14] Canadian Health Board [online], http //www.hc-sc gc ca/hecs-sesc/water/pdf/dwg/hardness pdf (accessed 20 April 2005)

[15] Drinking Water Treatment Water Softening (Ion Exchange), Institute of Agriculture and Natural Resources [online], http //ianrpubs.unl edu/water/g1491 htm (accessed 20 March 2005)

[16] Sanitization of Automated Watering Systems, Edstrom Industries [online], http://www.edstrom com/DocLib/MI4183 pdf (accessed 20 March 2005).

[17] 'Pharmaceutical: A Practical Approach to Controlling Microbial Growth', GE Infrastructure [online], http //www.gewater com/library/tp/822_Pharmaceutical_A jsp (accessed 22 October 2004).

[18] Reverse Osmosis, Maintenance Manual for RODI 500-800 Series equipment, Christ Waterman Group, (2000)

[19] Inspection of water treatment systems in the pharmaceutical industry, World Health Organization [online], www.who int/medecines/organization/qsm/activites/qualityassurance/gmp/gmp-sup (accessed 31 March 2005)

[20] Gray G.C., 'Recirculation Velocities in Water for Injection Distribution Systems', *Pharmaceutical Engineering*, Vol 17 (6), pp. 28-33 (1997)

[21] Forday W.L., 'Clean In Place Technology', *Signapore Microbiologist-Microbiology and Biotechnology News*, July-Sep 5-7 (1995).

[22] Greene D., 'Practical CIP System Design', *Pharmaceutical Engineering*, Vol 23 (2), pp. 1-7 (2003).

[23] Smith E and Vivan B E , 'An Introductory Guide to Valve Selection', Mechanical Engineering Publications Ltd., London (1995)

[24] Kakaç S , Bergles A E. and Mayinger F , 'Heat Exchangers Thermal-Hydraulic Fundamentals and Design', McGraw-Hill Book Company, Washington (1981)

[25] Melo L F and Bott T R , 'Biofouling in Water Systems', *Experimental Thermal and Fluid Science*, Vol. 14, pp 375-381 (1997).

[26] Noble P T , 'Transport Considerations for Microbiological Control in Piping', *Journal of Pharmaceutical Science & Technology*, Vol 48 (2), pp.76-85 (1994)

[27] 'Hot Water Sanitization Recommendations', Technical Information, Filtration and Separations group, Osmonics Inc, Vista, CA (2002)

[28] Young J. H., 'Sterilization of Various Diameter Dead-Ended Tubes', *Biotechnology and Bioengineering*, Vol. 42, pp 125-132 (1993)

[29] Frobisher M. et al, 'Fundamentals of Microbiology', 9th Edition, W B Saunders Company, Philadelphia (1974).
[30] Pseudomonas and Related Bacteria, Online Textbook of Bacteriology [online], http://textbookofbacteriology.net/Pseudomonas.etc.html (accessed August 2006)
[31] Stout J E , Best M.G. and Yu V L , 'Susceptibility of members of the Family Legionellaceae to Thermal Stress Implications for Heat Eradication Methods in Water Distribution Systems', *Applied & Environmental Microbiology*, Vol 52 (2), pp. 396-399 (1986).
[32] Seiberling D.A., 'Alternatives to Conventional Process/ CIP Design – for improved Cleanability', *Pharmaceutical Engineering*, Vol 12 (2), pp 16-26 (1992)
[33] Weitnauer A K , 'Pharmaceutical A Practical Approach to Controlling Microbial Growth' [online], http://www.environmentalexpert.com/articles/article303/article303.htm (accessed August 2006)
[34] van Loosdrecht et al, 'Influence of Interfaces on Microbial Activity', *Microbiological Reviews*, Vol 51 (1), pp 75-87 (1990).
[35] Biobore High Purity tubing systems, Product Catalogue, Stainless Fittings Ltd (2002)
[36] McCoy W.F and Costerton J W., 'Fouling Biofilm Development in Tubular Flow Systems', *Developments in Industrial Microbiology*, Vol. 23, pp. 551-558 (1982)
[37] McCoy W.F., Bryers J D , Robbins J. and Costeron J W., 'Observations of Fouling Biofilm Formation', *Canadian Journal of Microbiology*, Vol 27 (9), pp. 910-917 (1981).
[38] Husted G. and Rutkowski A., 'Control of Micro-organisms in Mixed Bed Resin Polishers by Thermal Sanitization', *Proceedings from Watertech*, San Jose, 20-22 November, pp 43-51 (1991)
[39] 'High Purity Diaphragm Valves', Product Brochure, Aquasyn California LLC (2005)
[40] Bader B., 'Technology Update: Dead-Legs and Dollars', Alfa Laval Biokinetics Inc., June (2002)
[41] Marks D.M , 'An Integrated Approach to CIP/ SIP Design for Bioprocess Equipment', *Pharmaceutical Engineering*, Vol 19 (2), pp 34-40 (1999)

[42] Bates C et al, 'Experimental and numerical comparison of the Flow in a 90° Tee Junction', *Separated and Complex flows, ASME Summer Meeting*, Vol. 217, pp 43-50 (1995)

[43] Sierra-Espinosa F , Bates C and O'Doherty T , 'Reverse and fully developed flow in an equally divided 90° pipe junction', *ASME Summer Meeting*, June 22-26 (1997)

[44] Nakamori N. et al, 'Thermal Stratification in a Branch Pipe', *International Topical Meeting on Nuclear Reactor Thermal Hydraulics*, Tokyo, pp. 782-790 (1997).

[45] Corcoran B G , Esmonde H. and Hashmi M.S J., 'Investigation of Turbulent Flow in Pharmaceutical Pipe Tee-junctions', *International Conference on Heat Transfer, Fluid Mechanics and Thermodynamics*, April 8-10, South Africa (2002)

[46] Habib M.A et al, 'On the Development of Deadleg Criterion', *Journal of Fluids Engineering*, Vol. 127 (1), pp. 124-135 (2005)

[47] El-Shaboury A M.F., Soliman H M and Ormiston S.J., 'Laminar Forced Convection in Two-Dimensional Equal-Sided and Reduced Branching Ducts', *Numerical Heat Transfer*, Vol 42 (5), pp 487-512 (2002)

[48] Çengal Y.A and Turner R.H., 'Fundamentals of Thermal-Fluid Sciences', McGraw Hill International Edition, Mechanical Engineering series, Singapore (2001)

[49] Corcoran B.G., 'Pharmaceutical water systems and the 6D rule· a computational fluid dynamics analysis', Thesis, Dublin City University, Dublin (2003)

[50] Litos P , Honner M and Kunes J , 'Thermography Applications in Technology Research', *Proc InfraMation*, 27th July, Las Vegas (2004)

[51] Thermographic measurement techniques, ThermoVision™ A20M Operator's Manual, FLIR Systems (2004)

Appendix A

- Drawings not to scale
- All dimensions shown in mm

2d Equal Diameter Dead-leg

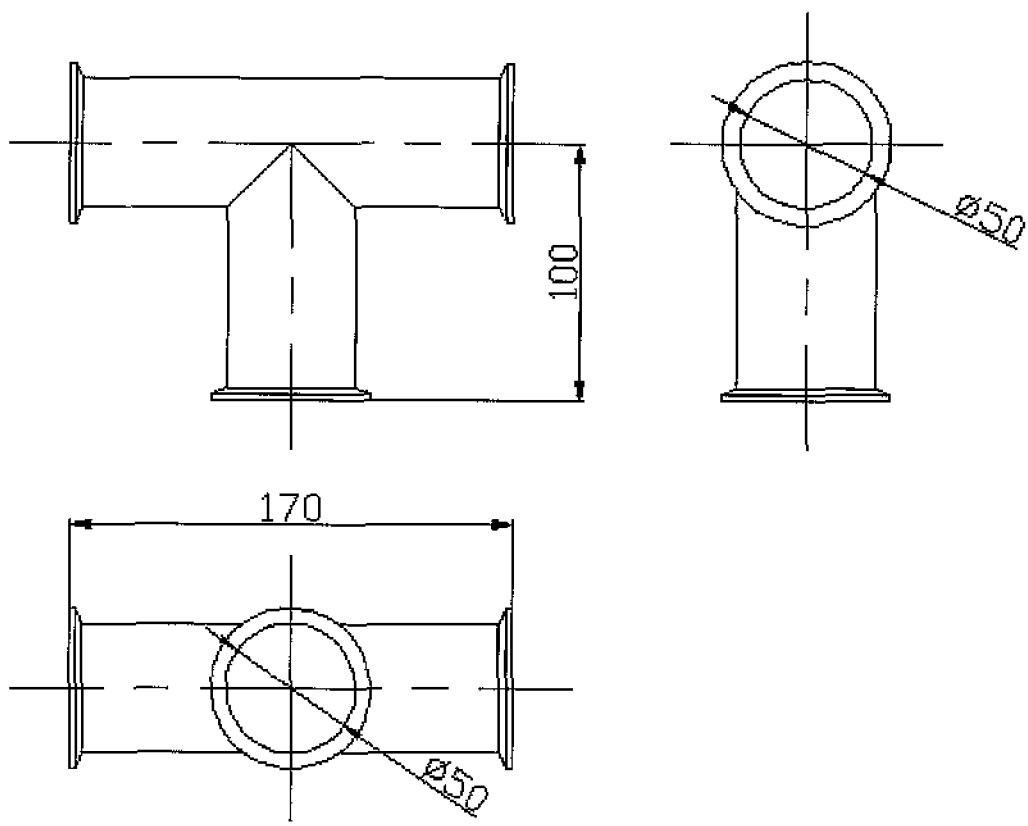

4d Equal Diameter Dead-leg

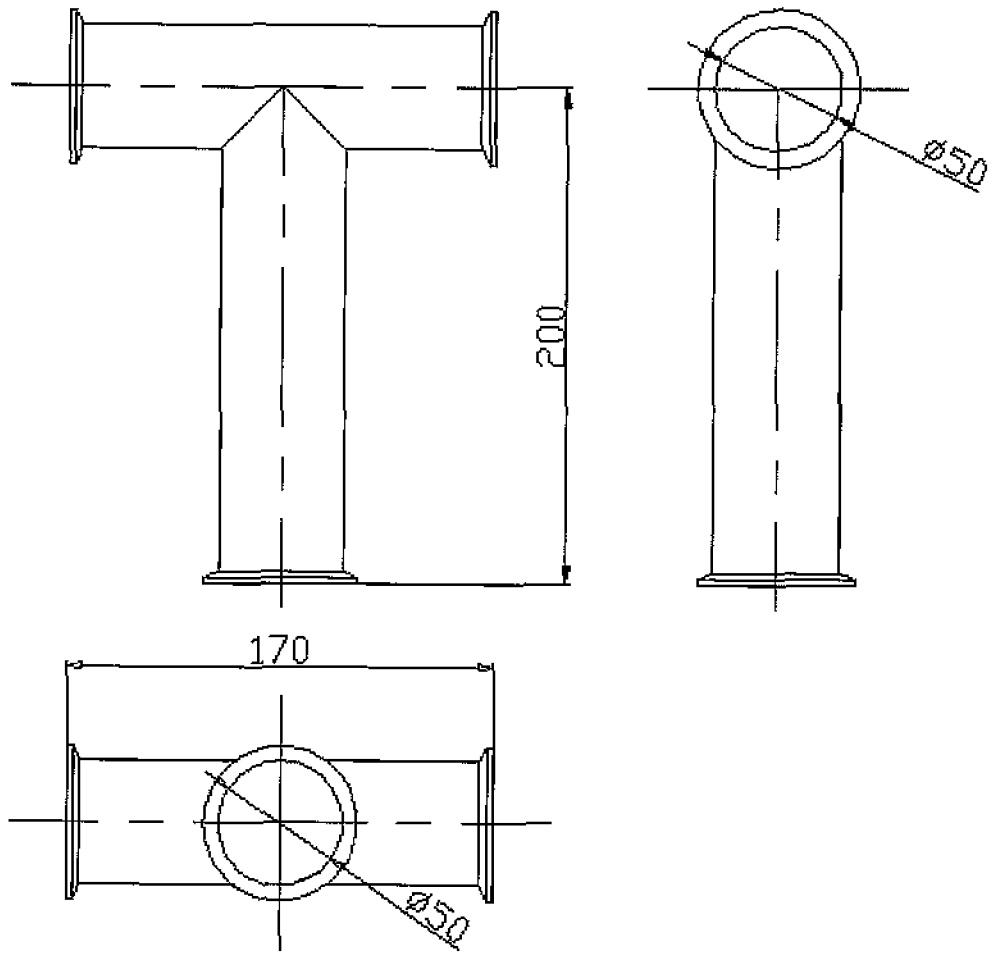

6d Equal Diameter Dead-leg

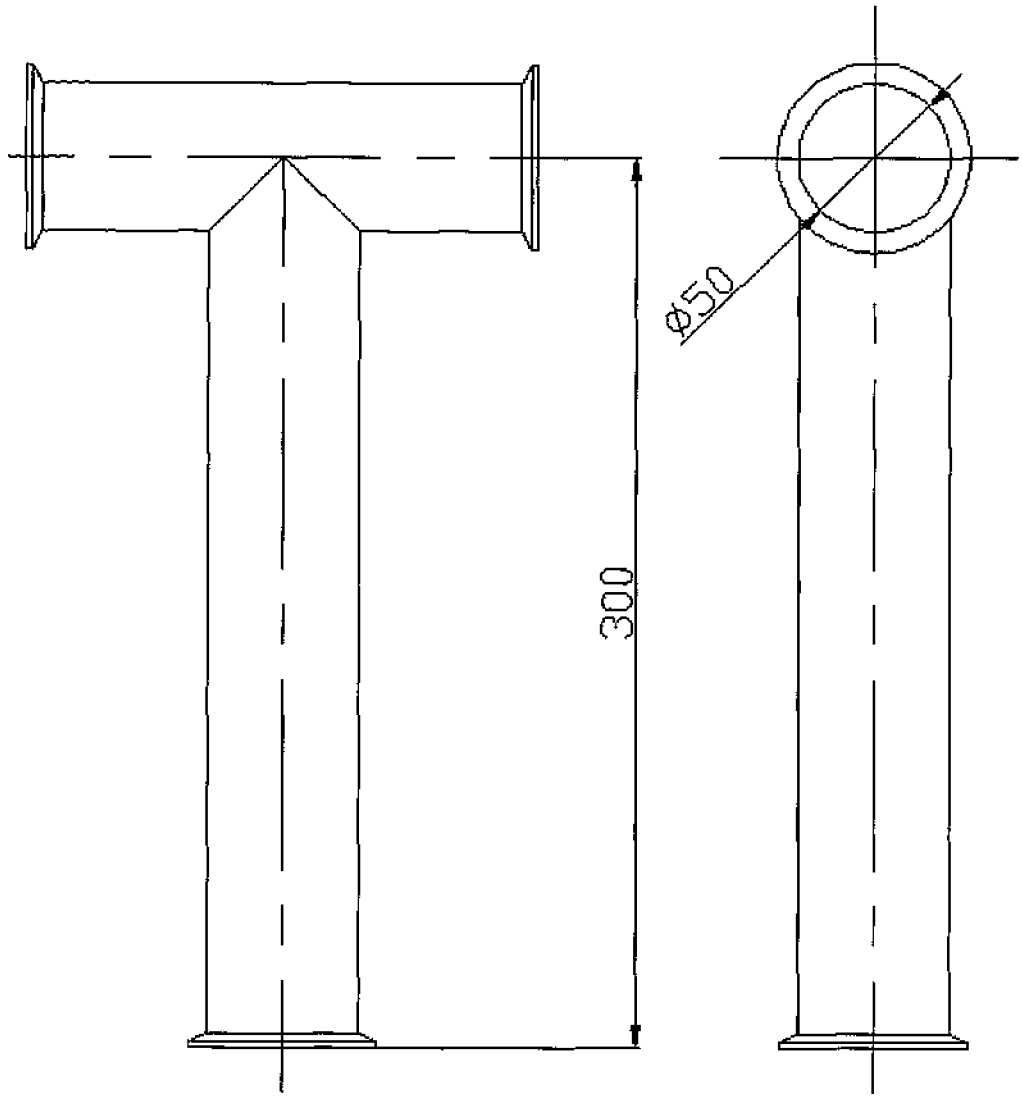

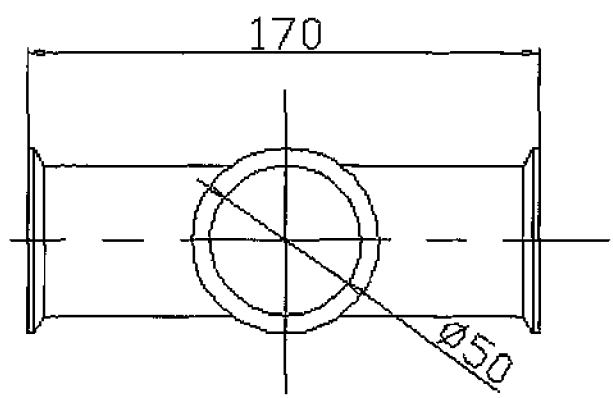

6d Reduced Diameter Dead-leg

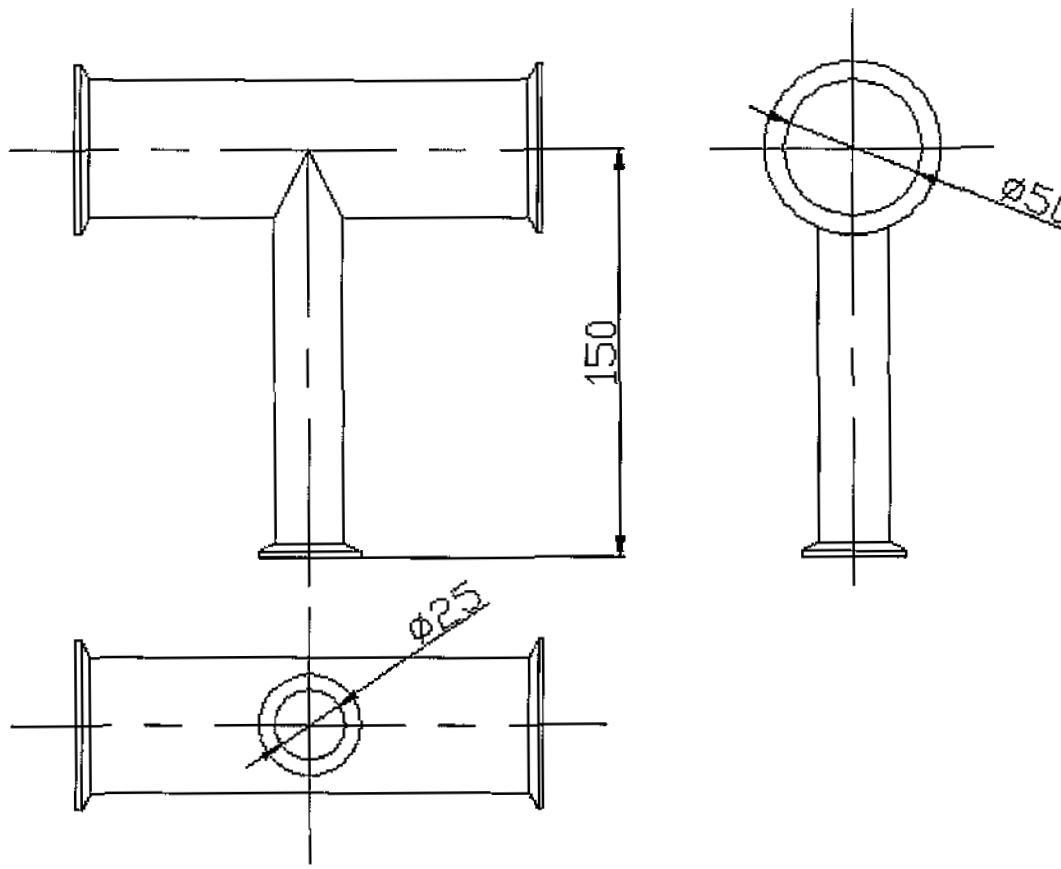

Reduced Dead-leg nylon inserts

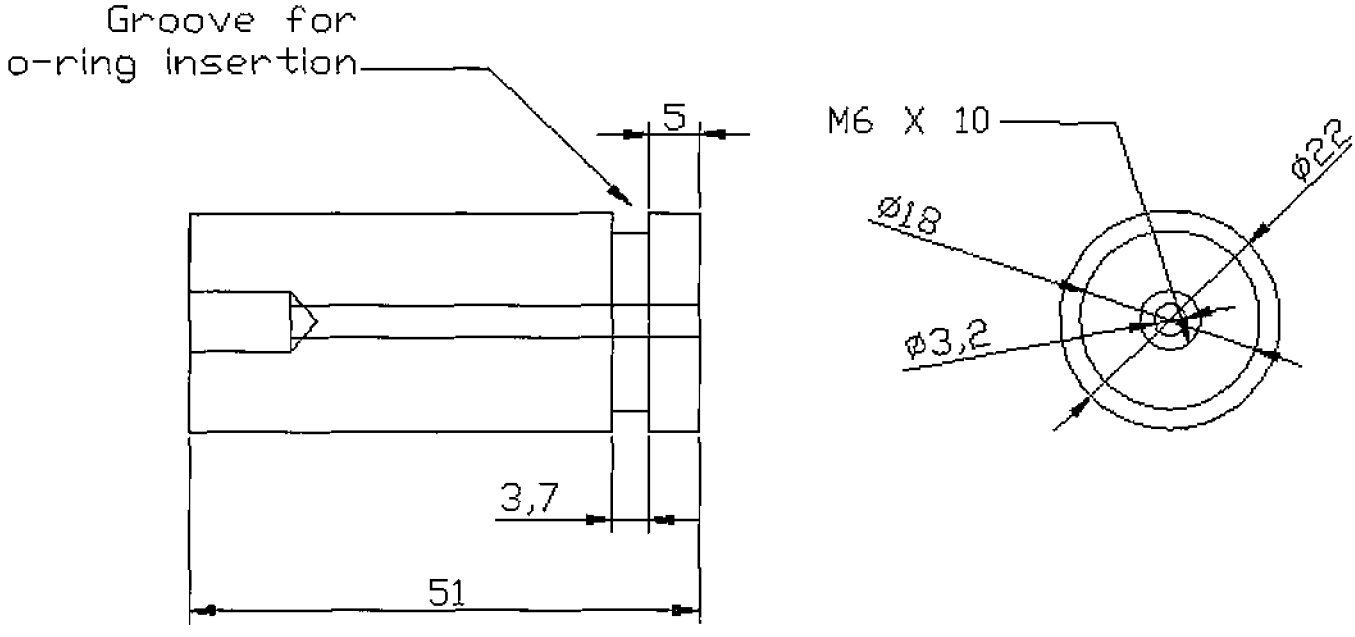

Appendix B

An expression {3} is applied to convert flowrate,

$$1\ (\text{L/min})\ (\frac{10^{-3}}{60}) = 1\ \text{m}^3/\text{s} \qquad \{3\}$$

Bulk fluid velocity calculated based upon flowrate and pipe area {4}.

$$q = A\ U_b \qquad \{4\}$$

A, cross-sectional area of fluid flow given by {5},

$$A = \frac{\pi ID^2}{4} \qquad \{5\}$$

Volumetric flowrate, Q (L/min)	**Volumetric flowrate, q (m^3/s)**	**Loop velocity, U_b (m/s)**
20	$0\ 34 \times 10^{-3}$	0.19
40	$0\ 67 \times 10^{-3}$	0 37
60	1×10^{-3}	0.56
100	1.67×10^{-3}	0.94
120	2×10^{-3}	1.12
160	2.67×10^{-3}	1.50

Reynolds Numbers (*Re*) for experimental fluid flow calculated based upon {6},

$$Re = \frac{\rho v D}{\mu} \qquad \{6\}$$

Loop fluid properties given as below;

Water Temperature (°C)	80
Dynamic viscosity, μ (kg/ms)	0.355×10^{-3}
Fluid density, ρ (kg/m^3)	971.78

Appendix C

Temperature profiles for 6d equal diameter dead-leg @ $U_b = 0$ 19m/s

Time, t (s)	Maximum dead-leg temperature, T_{d6} (°C)	Maximum loop temperature, T_L (°C)
1	21 74	22.52
300	21.33	23.75
600	21 20	26 11
900	21 07	28 61
1200	20.91	31 24
1500	20.89	33.85
1800	20.82	36.43
2100	20 80	39.03
2400	20 78	41.62
2700	20.78	44 11
3000	20 80	46 70
3300	20 80	49.31
3600	20.82	51 74
3900	20.82	54.25
4200	20.82	56 67
4500	20 78	59 17
4800	20.80	61 58
5100	20 84	64.46
5400	20 89	67.05
5700	20.87	69 42
6000	20.91	71.78
6300	20.95	74 04
6600	21 02	76 41
6900	21.11	78 68
7200	21 22	80.15
7500	21 29	80.17
7800	21.38	80.01
8100	21.49	79 79
8400	21.62	79 57
8700	21 71	79.29
9000	21 85	78.96
9300	21 98	79 00
9600	22 09	80.15
9900	22.23	80.07
10200	22 43	79.97
10500	22 61	79 83
10800	22 72	79 55

Temperature profiles for 6d equal diameter dead-leg @ $U_b = 0.37$m/s

Time, t (s)	Maximum dead-leg temperature, T_{d6} (°C)	Maximum loop temperature, T_L (°C)
1	22.52	25.73
300	22.56	28.50
600	22.52	31.11
900	22.52	34.04
1200	22.52	36.82
1500	22.54	39.47
1800	22.63	42.14
2100	22.70	44.77
2400	22.87	47.53
2700	23.08	49.97
3000	23.37	52.69
3300	23.66	55.24
3600	23.95	57.85
3900	24.28	60.41
4200	24.73	62.96
4500	24.97	65.32
4800	25.37	67.77
5100	25.75	70.36
5400	26.11	72.69
5700	26.51	75.04
6000	26.87	77.32
6300	27.27	79.77
6600	27.67	80.11
6900	28.05	79.75
7200	28.43	79.37
7500	28.79	78.98
7800	29.21	80.21
8100	29.50	79.81
8400	29.86	79.45
8700	30.13	79.04
9000	30.41	80.19
9300	30.63	80.00
9600	30.83	79.59
9900	30.98	79.21
10200	31.13	79.31
10500	31.20	80.03
10800	31.26	79.63

Temperature profiles for 6d equal diameter dead-leg @ U_b = 0 56m/s

Time, t (s)	Maximum dead-leg temperature, T_{d6} (°C)	Maximum loop temperature, T_L (°C)
1	22 25	23.57
300	22.16	26.20
600	22.12	28 92
900	22.07	31 75
1200	22.07	34.35
1500	22.09	36.78
1800	22 23	39 54
2100	22 38	42 01
2400	22.58	44 64
2700	22 81	46.91
3000	23.10	49.46
3300	23.39	51 81
3600	23 79	54 27
3900	24 12	56 90
4200	24 50	59 30
4500	24 93	61.76
4800	25 35	64 23
5100	25.84	66 44
5400	26.33	68.80
5700	26.80	71 23
6000	27 29	73.54
6300	27 76	75 64
6600	28 30	77 89
6900	28 77	79 97
7200	29 17	79 71
7500	29.57	79.43
7800	30 02	79.14
8100	30 41	78 90
8400	30 85	80.33
8700	31 33	79.65
9000	31 77	79.43
9300	32.16	79.14
9600	32 45	78.84
9900	32 69	79.73
10200	32 82	79.41
10500	32 93	79 08
10800	33 08	78 80

Temperature profiles for 6d equal diameter dead-leg @ U_b = 0 94m/s

Time, t (s)	Maximum dead-leg temperature, T_{d6} (°C)	Maximum loop temperature, T_L (°C)
1	24.39	26 00
300	24.10	29 17
600	24 17	32 18
900	24 39	35 16
1200	24 73	38.14
1500	25 11	41 00
1800	25.55	43.76
2100	26.09	46 74
2400	26 65	49 5
2700	27 27	52 33
3000	27 96	55.17
3300	28 90	57.95
3600	29.75	60.69
3900	30 43	63.41
4200	31 18	66.17
4500	32 12	68 76
4800	32 91	71.49
5100	33 61	74.06
5400	34.31	76 43
5700	35 12	79 21
6000	36.03	79 85
6300	37.00	79.49
6600	37.94	79.19
6900	38 73	78.86
7200	39 23	79 79
7500	39 49	79 47
7800	39.75	79.19
8100	39 91	78.90
8400	40.10	79 83
8700	40.36	79.47
9000	40.70	79.14
9300	41 09	79 51
9600	41 39	79 75
9900	41 64	79 43
10200	41.58	79.17
10500	41.52	79.49
10800	41.60	79.71

Temperature profiles for 6d equal diameter dead-leg @ U_b = 1.12m/s

Time, t (s)	Maximum dead-leg temperature, T_{d6} (°C)	Maximum loop temperature, T_L (°C)
1	23 25	25.49
300	23 75	28.57
600	24.75	31 57
900	25 06	34 59
1200	26 29	37 41
1500	27 20	40 34
1800	28 99	43.36
2100	30 43	45.97
2400	32 58	48 84
2700	34 07	51.64
3000	35.40	54 48
3300	36 28	57 13
3600	36 58	60.04
3900	36 87	62.59
4200	38 86	65 24
4500	41.00	67.90
4800	43.79	70.54
5100	45.82	73.11
5400	46.35	75.76
5700	47.06	78.25
6000	48 39	79 89
6300	48 77	79 61
6600	49 74	79 27
6900	50 29	79 10
7200	51.24	78.90
7500	51.01	79 83
7800	50 86	79.59
8100	52 14	79.35
8400	53 28	79.12
8700	53 57	79.81
9000	54 42	79.83
9300	55.03	79.61
9600	56.16	79.39
9900	56.12	79 12
10200	55 78	80 25
10500	56 73	79 83
10800	57 60	79 57

Temperature profiles for 6d equal diameter dead-leg @ U_b = 1 50m/s

Time, t (s)	Maximum dead-leg temperature, T_{d6} (°C)	Maximum loop temperature, T_L (°C)
1	23 23	24.26
300	24 84	27.27
600	26 76	30 37
900	30 04	33 23
1200	32 27	36.25
1500	34 87	39.21
1800	38.09	42 14
2100	41 45	44.92
2400	41.79	47.70
2700	46 57	50.50
3000	48 82	53 30
3300	51 45	56 10
3600	54.31	58 84
3900	56.23	61.52
4200	58 96	64 15
4500	60 59	66.83
4800	64.48	69.48
5100	67.34	72.12
5400	69 01	74 65
5700	71 78	77 28
6000	74.00	79 73
6300	73.52	79.59
6600	74 21	79 31
6900	74 33	79 06
7200	74.23	78.78
7500	74.35	79.83
7800	74 75	79.49
8100	74 25	79 25
8400	74 45	78 98
8700	74.04	78 68
9000	75.12	79 73
9300	75 14	79.47
9600	74 95	79.21
9900	74 65	78.96
10200	73.42	79 39
10500	75 08	79 65
10800	74.73	79.43

Temperature profiles for 4d equal diameter dead-leg @ U_b = 0 19m/s

Time, t (s)	Maximum dead-leg temperature, T_{d4} (°C)	Maximum loop temperature, T_L (°C)
1	23 03	24.19
300	22.54	26 11
600	22 54	28.86
900	22 79	31.72
1200	23 14	34 42
1500	23 52	37 22
1800	24 04	40 08
2100	24 59	42 80
2400	25 17	45.65
2700	25 82	48.50
3000	26 49	51 17
3300	27 18	53 93
3600	27.81	56.67
3900	28.52	59.38
4200	29.17	62.07
4500	29 86	64.69
4800	30 80	67 44
5100	31 72	70.10
5400	32 56	72 67
5700	33 34	75.32
6000	34 02	77 79
6300	34 77	80 21
6600	35 55	80.39
6900	36 25	80.27
7200	36 98	80.09
7500	37 65	79.75
7800	38 29	79 43
8100	38 81	79 04
8400	39 23	79 17
8700	39.51	80.27
9000	39.84	80.19
9300	40 08	80 00
9600	40 32	79 65
9900	40 40	79.29
10200	40 66	78 92
10500	40.87	79 85
10800	40 98	80 33

Temperature profiles for 4d equal diameter dead-leg @ $U_b = 0.37$m/s

Time, t (s)	Maximum dead-leg temperature, T_{d4} (°C)	Maximum loop temperature, T_L (°C)
1	22 81	24.86
300	24.50	27 29
600	25 78	29 88
900	27 07	32.66
1200	28 57	35 44
1500	30 10	38 20
1800	31 37	40 74
2100	32.80	43.64
2400	34 33	46.05
2700	36 03	48 69
3000	37.59	51.32
3300	39 51	53 95
3600	41 73	56 54
3900	43.04	58.94
4200	44.00	61.44
4500	45.26	63.88
4800	46 18	66 33
5100	47.49	68.82
5400	48 92	71 25
5700	50 61	73 60
6000	52.21	76 03
6300	53 76	78 29
6600	54.40	80.25
6900	54.96	80.11
7200	56.16	79.81
7500	56 88	79 49
7800	57 55	79 19
8100	58 12	78.92
8400	57 95	80 09
8700	58 71	79 79
9000	59.01	79 51
9300	59.43	79.27
9600	59.47	78 94
9900	59 53	80 15
10200	59 24	79 95
10500	59.22	79.57
10800	59.55	79.29

Temperature profiles for 4d equal diameter dead-leg @ U_b = 0.56m/s

Time, t (s)	Maximum dead-leg temperature, T_{d4} (°C)	Maximum loop temperature, T_L (°C)
1	22.92	23 41
300	24.91	26 49
600	27 67	29.44
900	30 48	32 47
1200	33.21	35 66
1500	36.19	38 49
1800	38.62	41 52
2100	41.41	44.28
2400	43 81	47 28
2700	46 48	50.12
3000	49 42	53.01
3300	51.57	55.89
3600	54.42	58 69
3900	56 18	61 41
4200	59.60	64 13
4500	61.91	66.85
4800	64.62	69 54
5100	66 37	72 40
5400	69.44	74.87
5700	71.68	77.30
6000	74 39	79.97
6300	75.16	79 83
6600	75.22	79.51
6900	74 49	79 19
7200	74 31	78 84
7500	74 25	79 97
7800	74.73	79.67
8100	75.12	79.37
8400	73 46	79.04
8700	74 51	80.19
9000	74.73	79 91
9300	74 21	79.59
9600	74 95	79.27
9900	74 75	78.98
10200	74.39	80.13
10500	75 18	79.77
10800	75 04	79.45

Temperature profiles for 4d equal diameter dead-leg @ U_b = 0 94m/s

Time, t (s)	Maximum dead-leg temperature, T_{d4} (°C)	Maximum loop temperature, T_L (°C)
1	24 39	24.97
300	26.49	28 10
600	29.39	31 29
900	32 27	34 17
1200	35 07	37.41
1500	37 98	40.38
1800	40 74	43 29
2100	43 21	46 31
2400	45 78	49.20
2700	48.37	52 02
3000	51 01	54.92
3300	54.27	57.95
3600	56 92	60 72
3900	59 49	63.39
4200	61.99	66 27
4500	64.60	68 99
4800	66.89	71 68
5100	69 36	74 29
5400	71 37	77.02
5700	74 19	79 73
6000	75 08	79.75
6300	74 79	79 45
6600	74 59	79 17
6900	74 21	78 88
7200	74 89	79.73
7500	74.57	79 51
7800	74.23	79 23
8100	73.84	78.92
8400	74 29	79.83
8700	74 14	79 49
9000	74.02	79.23
9300	73.92	78 94
9600	74 55	79.91
9900	74 57	79.65
10200	74 31	79.37
10500	74 14	79 12
10800	73 78	79.71

Temperature profiles for 4d equal diameter dead-leg @ U_b = 1.12m/s

Time, t (s)	Maximum dead-leg temperature, T_{d4} (°C)	Maximum loop temperature, T_l (°C)
1	23 00	26.91
300	25 99	29.95
600	27 99	32.84
900	30.01	35.75
1200	33 33	38 53
1500	36 02	41 43
1800	38 50	44.28
2100	40 50	47.06
2400	42 03	49 87
2700	46 54	52.69
3000	49 03	55 55
3300	52 03	58 23
3600	54 54	61 00
3900	57 02	63 51
4200	59 05	66 15
4500	62.59	68.74
4800	64.58	71.21
5100	67.46	73.92
5400	70 33	76 39
5700	72 45	78 88
6000	75 17	79.89
6300	75.04	79 55
6600	74.73	79.29
6900	74 37	78.96
7200	75.14	80.27
7500	75.22	79.73
7800	74.81	79 37
8100	74.57	79.12
8400	74 29	79.08
8700	75.02	79 85
9000	74 83	79 51
9300	74 39	79 23
9600	74.27	78 94
9900	74.95	80 00
10200	75 08	79 67
10500	74 79	79 37
10800	74.29	78 98

Temperature profiles for 4d equal diameter dead-leg @ U_b = 1 50m/s

Time, t (s)	Maximum dead-leg temperature, T_{d4} (°C)	Maximum loop temperature, T_L (°C)
1	25 75	26 22
300	27 87	29 21
600	30 56	32 01
900	33 21	34 87
1200	35 99	37.72
1500	38 62	40 62
1800	41.30	43 29
2100	43 96	46.12
2400	46 44	48.99
2700	49 14	51 68
3000	51 68	54 48
3300	54 31	57.11
3600	56.75	59 78
3900	59.36	62.34
4200	61 70	65 02
4500	64 46	67.59
4800	66 81	70.12
5100	69 25	72.61
5400	71 78	75 08
5700	74 27	77 63
6000	76.45	80 09
6300	76.55	79 77
6600	76 27	79 49
6900	76.13	79 23
7200	75.99	78.94
7500	76 72	80.05
7800	76 59	79 67
8100	76 35	79 37
8400	76.15	79 14
8700	75 89	78.88
9000	76.68	79 87
9300	76 63	79.71
9600	76 35	79 41
9900	76.15	79 10
10200	75 80	79 25
10500	76 74	79 85
10800	76.45	79 61

Temperature profiles for 2d equal diameter dead-leg @ $U_b = 0.19$m/s

Time, t (s)	Maximum dead-leg temperature, T_{d2} (°C)	Maximum loop temperature, T_L (°C)
1	25 20	25.60
300	26 76	28 01
600	29 66	30 96
900	32 53	34.07
1200	35 44	37 13
1500	38 38	40 17
1800	41.17	43 21
2100	43 98	46 20
2400	46 89	49 01
2700	49 89	52 00
3000	52 54	54.96
3300	55 41	57.83
3600	58.06	60 69
3900	60 74	63.53
4200	63 31	66 35
4500	65 67	69 07
4800	68 35	71.84
5100	70 91	74 61
5400	73 52	77.34
5700	76 13	80.03
6000	77 40	80.47
6300	77.26	80 33
6600	77.00	80 00
6900	76 61	79 57
7200	76 35	79 25
7500	75.97	78 92
7800	76 65	80 25
8100	77.12	80.39
8400	77 12	80 17
8700	76 65	79 81
9000	76.31	79 45
9300	76 01	79.10
9600	75 85	79.41
9900	76.90	80 33
10200	77 08	80.25
10500	76.78	79 87
10800	76 43	79 51

Temperature profiles for 2d equal diameter dead-leg @ U_b = 1.50m/s

Time, t (s)	Maximum dead-leg temperature, T_{d2} (°C)	Maximum loop temperature, T_L (°C)
1	26 02	26 09
300	28.90	29.06
600	31 72	31 90
900	34 52	34 77
1200	37 37	37 61
1500	40 19	40.47
1800	42 89	43 23
2100	45.52	45.93
2400	48.28	48 69
2700	51 07	51.51
3000	53 81	54 12
3300	56 44	56 82
3600	59 09	59 51
3900	61.66	62.16
4200	64.21	64 69
4500	66.79	67 32
4800	69 23	69 79
5100	71.80	72 34
5400	74 23	74 85
5700	76.68	77.32
6000	79 06	79.73
6300	79.02	79 65
6600	78.84	79 39
6900	78.58	79 17
7200	78 31	78 92
7500	79.33	80 03
7800	79 04	79 65
8100	78.82	79 45
8400	78.54	79.23
8700	78.27	78 92
9000	79.45	80 11
9300	79 08	79 77
9600	78 86	79 55
9900	78 60	79 27
10200	78 34	79.00
10500	78 66	79.41
10800	79 14	79.79

Appendix D

Temperature profiles for 6d reduced diameter dead-leg @ $U_b = 0.19$m/s

Time, t (s)	Maximum dead-leg temperature, T_{d6} (°C)	Maximum loop temperature, T_L (°C)
1	22.27	24.44
300	20.84	27.32
600	20.44	30.50
900	20.17	33.69
1200	20.04	37.15
1500	20.04	40.49
1800	20.06	44.06
2100	20.15	47.28
2400	20.40	50.54
2700	20.66	53.81
3000	20.98	56.94
3300	21.31	60.14
3600	21.71	63.27
3900	22.20	66.33
4200	22.70	69.44
4500	23.12	72.53
4800	23.54	75.50
5100	23.99	78.60
5400	24.35	80.59
5700	24.79	80.61
6000	25.24	80.23
6300	25.75	79.89
6600	26.18	79.49
6900	26.60	79.14
7200	27.00	78.72
7500	27.29	79.93
7800	27.56	80.17
8100	27.81	79.89
8400	28.03	79.51
8700	28.23	79.14
9000	28.41	78.82
9300	28.54	79.69
9600	28.70	80.23
9900	28.79	79.97
10200	28.90	79.63
10500	28.97	79.33
10800	29.08	78.94

Temperature profiles for 6d reduced diameter dead-leg @ U_b = 0 37m/s

Time, t (s)	Maximum dead-leg temperature, T_{d6} (°C)	Maximum loop temperature, T_L (°C)
1	24.44	22 27
300	23 90	27.92
600	23 79	30.78
900	23 79	33 41
1200	23.95	36 17
1500	24 28	38 90
1800	24.66	41.71
2100	25.00	44 26
2400	25.33	46 78
2700	25.75	49 48
3000	26 16	52.12
3300	26 60	54.52
3600	27.09	57 05
3900	27.54	59 57
4200	27.96	61.83
4500	28.39	64 34
4800	28 79	66 64
5100	29 19	68 95
5400	29 64	71 01
5700	30 15	73.38
6000	30.59	75 36
6300	31 05	77 53
6600	31 46	79.53
6900	31.9	79 61
7200	32 34	78 98
7500	32 64	79 55
7800	32 95	79.39
8100	33 17	78 78
8400	33 34	79.77
8700	33.52	79 23
9000	33 69	78.60
9300	33.82	79.77
9600	33 96	79 12
9900	34 07	78 88
10200	34 22	79.67
10500	34.31	79.00
10800	34.33	79 33

Temperature profiles for 6d reduced diameter dead-leg @ U_b = 0 56m/s

Time, t (s)	Maximum dead-leg temperature, T_{d6} (°C)	Maximum loop temperature, T_L (°C)
1	24.75	25 15
300	23.32	27.81
600	23.03	30 70
900	23.05	33.61
1200	23 23	36 47
1500	23 63	39 16
1800	24 17	42.16
2100	24.77	44 98
2400	25 42	47 66
2700	26 13	50 33
3000	26 78	53 13
3300	27 47	55.66
3600	28 08	58.44
3900	28 63	61 09
4200	29 28	63 55
4500	29.93	66 19
4800	30.37	68 78
5100	30 80	71 39
5400	31 53	73.82
5700	32 12	76.39
6000	32 80	78.90
6300	33.47	79 63
6600	34 11	79 37
6900	34.63	79 12
7200	35 12	78 82
7500	35.38	78 56
7800	35.62	79 69
8100	35.79	79 51
8400	36 06	79 25
8700	36.12	78.94
9000	36 17	78 68
9300	36 21	78 46
9600	36 17	79 57
9900	36 17	79 33
10200	36 17	79.04
10500	36 28	78 78
10800	36 28	78 52

Temperature profiles for 6d reduced diameter dead-leg @ U_b = 0 94m/s

Time, t (s)	Maximum dead-leg temperature, T_{d6} (°C)	Maximum loop temperature, T_L (°C)
1	23 59	23 86
300	23 54	26 85
600	23.99	30.00
900	24 86	32 80
1200	25 62	35 62
1500	26 62	38 51
1800	27 58	41 43
2100	28 43	44 13
2400	29 39	46 87
2700	30 35	49.61
3000	31 22	52.35
3300	32.40	55 05
3600	33 85	57 78
3900	35 03	60 45
4200	36 54	63.12
4500	37.50	65.72
4800	38.88	68.23
5100	40.14	70.74
5400	41.02	73.29
5700	42 07	75 74
6000	43 12	78 19
6300	44 36	79 59
6600	45 22	79 33
6900	46.27	79.04
7200	47 47	78.78
7500	47 68	78.52
7800	48 62	79.53
8100	48 77	79.25
8400	48.80	78 98
8700	48.60	78 72
9000	48.97	79 55
9300	48 73	79.41
9600	48 60	79 10
9900	48 32	78 92
10200	48 11	78 60
10500	48 02	79.43
10800	47 96	79 19

Temperature profiles for 6d reduced diameter dead-leg @ U_b = 1 12m/s

Time, t (s)	Maximum dead-leg temperature, T_{d6} (°C)	Maximum loop temperature, T_L (°C)
1	22.92	24 28
300	22.47	27 45
600	23.08	30 56
900	24.12	33 58
1200	25.26	36 45
1500	26.47	39 47
1800	27 87	42.37
2100	29 21	45 33
2400	30 74	48.24
2700	32 25	51 03
3000	33.54	53 89
3300	34 63	56 77
3600	35 97	59.64
3900	37 33	62 44
4200	39 36	65 16
4500	41 62	67 81
4800	44 79	70 40
5100	47.00	73 11
5400	49 31	75 78
5700	50 31	78 34
6000	53 20	79 63
6300	55 62	79 35
6600	59 03	79 04
6900	59 05	78.74
7200	58 29	79 67
7500	57.20	79 53
7800	61.91	79.23
8100	59.87	78 96
8400	58 00	78 68
8700	57 38	79 91
9000	61 68	79 39
9300	58.71	79 06
9600	59 36	78.78
9900	58 88	78.56
10200	58 88	79.53
10500	62 20	79 27
10800	62 46	79 00

Temperature profiles for 6d reduced diameter dead-leg @ U_b = 1 50m/s

Time, t (s)	Maximum dead-leg temperature, T_{d6} (°C)	Maximum loop temperature, T_L (°C)
1	23.52	24 68
300	24 41	27.92
600	26 83	30.98
900	27 45	34 02
1200	29 59	37 00
1500	31.31	40 04
1800	33.45	42.97
2100	38 24	46.03
2400	40 17	48 95
2700	43 89	51 78
3000	45 28	54 65
3300	50 27	57.57
3600	53.53	60.41
3900	56 73	63 18
4200	59.68	65.96
4500	61 76	68 72
4800	64 25	71.47
5100	66 17	74 12
5400	68 86	76 84
5700	69 81	79 43
6000	71 15	79.53
6300	71.49	79.25
6600	72 06	78.94
6900	71 57	78 84
7200	72 77	80.11
7500	71 29	79 73
7800	71 37	79 27
8100	72 02	78 90
8400	71.29	78 64
8700	72 06	79 69
9000	72 36	79 39
9300	72 48	79 14
9600	71 55	78 88
9900	71 45	78.62
10200	71.90	79 61
10500	71.21	79 33
10800	71.76	79.06

Temperature profiles for 4d reduced diameter dead-leg @ U_b = 0 19m/s

Time, t (s)	Maximum dead-leg temperature, T_{d4} (°C)	Maximum loop temperature, T_L (°C)
1	23.21	23 88
300	23.83	25.64
600	24 57	28 26
900	26 11	30 79
1200	27 90	33 39
1500	29 84	36 12
1800	31 85	38 81
2100	33 39	41 19
2400	35 55	43 88
2700	37 04	46 40
3000	37 68	48 67
3300	38 40	51 14
3600	39 60	53.43
3900	41 13	55.93
4200	42.24	58.46
4500	43 89	60 84
4800	45 48	63.23
5100	46 95	65 67
5400	48 32	68.04
5700	49 57	70 40
6000	51 26	72 79
6300	52.26	75.04
6600	53.30	77.33
6900	55 51	79.57
7200	57.30	80.17
7500	59.25	80 09
7800	61 09	79 95
8100	61 06	79 80
8400	61 13	79 49
8700	62.11	79.23
9000	61 62	78 94
9300	61 25	78.70
9600	61 56	80 00
9900	62.48	80 01
10200	62 38	79 86
10500	61 97	79.49
10800	62 24	79.23

Temperature profiles for 4d reduced diameter dead-leg @ U_b = 0 37m/s

Time, t (s)	Maximum dead-leg temperature, T_{d4} (°C)	Maximum loop temperature, T_L (°C)
1	24 57	24.77
300	26 04	27 38
600	28 37	30.28
900	30 39	32 95
1200	32 73	35 82
1500	34.77	38 31
1800	36 82	41 24
2100	39 25	43 64
2400	40 96	46 38
2700	43 44	48.84
3000	45 37	51 41
3300	47 19	53.81
3600	47.79	56 42
3900	49 52	58.82
4200	52 54	61 25
4500	53 47	63.60
4800	56 02	66 00
5100	59 66	68.25
5400	62 34	70 68
5700	64 67	72 95
6000	65 10	75 46
6300	68.31	77 85
6600	70 58	80.00
6900	70 91	79 73
7200	70.62	79 39
7500	70 52	79 10
7800	70.02	78.80
8100	69 95	79 29
8400	71 31	79 79
8700	70.95	79 43
9000	70.97	79.14
9300	70.66	78.82
9600	70 78	79 04
9900	70 85	79 73
10200	71.07	79 41
10500	70 60	79.12
10800	70 20	78.78

Temperature profiles for 4d reduced diameter dead-leg @ U_b = 0 56m/s

Time, t (s)	Maximum dead-leg temperature, T_{d4} (°C)	Maximum loop temperature, T_L (°C)
1	22 90	23.32
300	25.02	26.33
600	27 72	29.28
900	30 35	32 29
1200	32 8	35 22
1500	35 49	37.96
1800	37 94	40 89
2100	40 64	43 72
2400	43 31	46 53
2700	45 88	49 37
3000	48 30	52.14
3300	50 98	54 83
3600	53.60	57.64
3900	55.83	60 43
4200	58.33	63 10
4500	60.82	65.80
4800	63 06	68 49
5100	65 14	71 21
5400	67 57	73 82
5700	70 08	76 33
6000	72 59	78.96
6300	73.74	79 51
6600	73 54	79.21
6900	73 38	78 94
7200	73 03	78 66
7500	73 03	78 88
7800	74 29	79 59
8100	73.84	79 31
8400	74 00	79.00
8700	73.44	78 74
9000	73.17	78 48
9300	73 98	79 57
9600	74.06	79.27
9900	73 98	78.98
10200	73 56	78.72
10500	73.42	78 46
10800	74 29	79.65

Temperature profiles for 4d reduced diameter dead-leg @ U_b = 0 94m/s

Time, t (s)	Maximum dead-leg temperature, T_{d4} (°C)	Maximum loop temperature, T_L (°C)
1	23.83	23 83
300	26.27	26.76
600	29 12	29 73
900	31.58	32 49
1200	34.24	35 36
1500	36.93	38 2
1800	39 43	40.77
2100	42 20	43.66
2400	44 77	46.40
2700	47.17	49 06
3000	49.88	51 83
3300	52.48	54 50
3600	55 13	57.25
3900	57 64	59 87
4200	60 45	62.55
4500	62 90	65 08
4800	65 31	67 77
5100	67.73	70.38
5400	70 24	72 87
5700	72 65	75.36
6000	74 91	77.78
6300	77 10	79 81
6600	76 86	79.37
6900	76 59	79 17
7200	76 43	78 92
7500	76 21	78 66
7800	77.24	79 87
8100	76.96	79.37
8400	76.63	79.08
8700	76 59	78 9
9000	76.35	78 64
9300	77 10	79 51
9600	76.88	79 31
9900	76.72	79.10
10200	76 53	78.82
10500	76.27	78 94
10800	77 04	79 48

Temperature profiles for 4d reduced diameter dead-leg @ U_b = 1 12m/s

Time, t (s)	Maximum dead-leg temperature, T_{d4} (°C)	Maximum loop temperature, T_L (°C)
1	23 28	23.48
300	26 08	26 79
600	28 75	29.59
900	31 64	32.58
1200	34 45	35 51
1500	37 11	38 42
1800	40 02	41 39
2100	42 69	44 21
2400	45 54	47.08
2700	48 22	49.89
3000	50 98	52 67
3300	53 51	55 36
3600	56 25	58 32
3900	59 01	61 06
4200	61 74	63.84
4500	64 34	66 44
4800	66 79	69.11
5100	69 48	71 82
5400	71 82	74.45
5700	74 33	76.94
6000	76.86	79.59
6300	77 18	79 59
6600	77 03	79 33
6900	76 92	79.08
7200	76 65	78.86
7500	76 47	78.62
7800	77.38	79 61
8100	77 20	79.39
8400	76 98	79 15
8700	76 88	78 88
9000	76 53	78.66
9300	77.42	79.77
9600	77 27	79 41
9900	76 94	79.10
10200	76.78	78 88
10500	76 57	78.70
10800	77.45	79 79

Temperature profiles for 4d reduced diameter dead-leg @ U_b = 1 50m/s

Time, t (s)	Maximum dead-leg temperature, T_{d4} (°C)	Maximum loop temperature, T_L (°C)
1	23 16	23 23
300	25 53	25 80
600	28 08	28 63
900	30 67	31 33
1200	33 35	34.04
1500	35 99	36.79
1800	38.59	39.51
2100	41 16	42 24
2400	43 74	44 92
2700	46 44	47 51
3000	48 97	50.34
3300	51 57	52.98
3600	54.06	55 57
3900	56 65	58.23
4200	59 28	60 90
4500	61 84	63.55
4800	64 30	66.04
5100	66 81	68.62
5400	69 26	71 19
5700	71.59	73.72
6000	74 02	76 21
6300	76.45	78.61
6600	77 48	79 51
6900	77 30	79.31
7200	77 10	79 04
7500	76 96	78 84
7800	76 78	78 66
8100	76 65	78.45
8400	77.51	79 45
8700	77 36	79 25
9000	77 18	79 02
9300	76 96	78 82
9600	76 76	78 66
9900	76.61	78 43
10200	77 53	79.45
10500	77 36	79.23
10800	77 22	78.98

Temperature profiles for 2d reduced diameter dead-leg @ $U_b = 0$ 19m/s

Time, t (s)	Maximum dead-leg temperature, T_{d2} (°C)	Maximum loop temperature, T_L (°C)
1	25 06	25 24
300	25 64	26 60
600	27 27	29.06
900	29 41	31.88
1200	31.66	34.55
1500	33 91	37 15
1800	36 30	39.89
2100	38.64	42 56
2400	41 04	45 28
2700	43.34	47 94
3000	45 61	50.58
3300	47 90	53 13
3600	50.14	55 64
3900	52 31	58 23
4200	54 46	60 74
4500	56.52	63.18
4800	58.67	65.65
5100	60.98	68.27
5400	63.02	70.70
5700	65 16	73 11
6000	67 13	75 50
6300	69 36	77 87
6600	70 93	78 76
6900	71.27	78.72
7200	71.39	79.19
7500	72.24	80.00
7800	72.83	79 91
8100	72.79	79 77
8400	72 69	79 57
8700	72 71	79 35
9000	72 34	79 10
9300	71.98	78.76
9600	72.28	79 81
9900	73 01	80 19
10200	72.99	80.01
10500	73 01	79.85
10800	72.79	79.63

Temperature profiles for 2d reduced diameter dead-leg @ $U_b = 1.50$m/s

Time, t (s)	Maximum dead-leg temperature, T_{d2} (°C)	Maximum loop temperature, T_L (°C)
1	24 79	24.62
300	27 14	27.54
600	29 75	30.39
900	32 38	33.34
1200	35 12	36.17
1500	37 92	39.08
1800	40 74	41 99
2100	43.36	44.77
2400	46.14	47.77
2700	48 86	50 46
3000	51 53	53 26
3300	54 16	56 08
3600	56 86	58 82
3900	59.41	61 50
4200	62.05	64.19
4500	64.54	66.87
4800	67 11	69.50
5100	69 81	72.12
5400	72 28	74 73
5700	74 79	77 28
6000	77 18	79.77
6300	77 16	79 53
6600	76 94	79 31
6900	76.80	79 10
7200	76.63	78 9
7500	76.49	78.74
7800	76.84	79.23
8100	77 22	79 59
8400	77 06	79 37
8700	76.90	79.19
9000	76.72	79.00
9300	76.57	78.82
9600	76.35	78.62
9900	77.22	79 67
10200	77 08	79 47
10500	76 94	79.29
10800	76 78	79 10

Appendix E

6d equal diameter dead-leg for base positions @ U_b = 1 50m/s

Time, t (s)	Maximum dead-leg base temperature (°C)	Maximum surface base temperature (°C)
1	23 23	23.21
300	24.84	25 35
600	26 76	27 92
900	30 04	30 72
1200	32 27	33 54
1500	34 87	36 47
1800	38 09	39 29
2100	41.45	41.49
2400	41 79	44 02
2700	46 57	47 19
3000	48 82	49.80
3300	51 45	52.31
3600	54 31	55 01
3900	56 23	57 51
4200	58 96	59 64
4500	60 59	62 20
4800	64 48	64 50
5100	67.34	66 48
5400	69 01	68 37
5700	71.78	69.17
6000	74 00	68 64
6300	73.52	67.94
6600	74 21	68 46
6900	74 33	68 44
7200	74 23	69.10
7500	74 35	68 59
7800	74 75	68.48
8100	74 25	67.60
8400	74 45	69.11
8700	74 04	69 69
9000	75 12	69 13
9300	75 14	68.64
9600	74 95	68.54
9900	74 65	68.68
10200	73.42	68.85
10500	75 08	68.17
10800	74 73	69 08

6d equal diameter dead-leg for mid-point positions @ U_b = 1.50m/s

Time, t (s)	Maximum dead-leg mid-point temperature (°C)	Maximum surface mid-point temperature (°C)
1	24 41	23 77
300	27 70	26 62
600	31 05	29.75
900	34 37	32 66
1200	37 63	35.66
1500	40 83	38 51
1800	44.11	41.26
2100	47 28	44 04
2400	50 65	46 61
2700	53 68	48 88
3000	57 05	51 53
3300	60 20	53 85
3600	63 37	56 29
3900	66.39	58.86
4200	69.21	61.02
4500	72 42	63 82
4800	75 38	65.84
5100	78 31	67 73
5400	81 29	69 77
5700	81.05	69.44
6000	80 83	69 05
6300	80 49	68 64
6600	80 29	68 41
6900	81 19	68 76
7200	81 03	68 76
7500	80 77	68.43
7800	80 49	68.06
8100	80.25	68.00
8400	81.29	69 62
8700	80 97	69 18
9000	80 69	68 79
9300	80 43	68 96
9600	80 17	68 79
9900	81 13	69.08
10200	80.83	68.90
10500	80.61	68 86
10800	80 31	68 11

4d equal diameter dead-leg for base positions @ U_b = 0 56m/s

Time, t (s)	Maximum dead-leg base temperature (°C)	Maximum surface base temperature (°C)
1	22 87	23 03
300	24.91	24 55
600	27.67	27 16
900	30 48	29 97
1200	33.21	33.01
1500	36.19	36.03
1800	38 62	38.57
2100	41.41	41 58
2400	43 81	44.38
2700	46.48	47 13
3000	49 42	49 74
3300	51.57	52.12
3600	54.42	54.71
3900	56.18	57 55
4200	59.60	59 95
4500	61.91	62 34
4800	64 62	64 69
5100	66 37	67 55
5400	69 44	69 93
5700	71 68	71 92
6000	74.39	71 65
6300	75 16	71 27
6600	75 22	70 87
6900	74 49	71 84
7200	74 31	71.65
7500	74 25	71 90
7800	74.73	71 13
8100	75 12	70.91
8400	73.46	71.78
8700	74 51	71.31
9000	74 73	71 43
9300	74 21	70 93
9600	74 95	71.47
9900	74 75	71.33
10200	74 39	70.93
10500	75 18	70 62
10800	75 04	71 43

4d equal diameter dead-leg for mid-point positions @ U_b = 0 56m/s

Time, t (s)	Maximum dead-leg mid-point temperature (°C)	Maximum surface mid-point temperature (°C)
1	24 01	23 63
300	26 11	25 08
600	29 48	27.96
900	32 77	31 13
1200	36.19	34 20
1500	39 49	37 06
1800	42.63	39 86
2100	45 88	42.93
2400	49 07	45.84
2700	52 27	48 65
3000	55 45	51.45
3300	58 54	54 21
3600	61.52	56 98
3900	64.58	59.91
4200	67 59	62 28
4500	70 52	65.10
4800	73 42	67 65
5100	76 51	70 48
5400	79.43	72 95
5700	81.21	74 57
6000	80.87	74 29
6300	80.53	74 02
6600	80 19	73.19
6900	81.15	74 39
7200	80 89	74 35
7500	80 57	74.29
7800	80.21	73 96
8100	80 71	74.27
8400	80 89	74 59
8700	80 59	74.41
9000	80 23	73.90
9300	80 45	73 90
9600	80 89	74 63
9900	80.57	74 35
10200	80 21	73.96
10500	80 39	73.74
10800	81 05	74 63